Theses and Dissertations

8-2017

Peptoid-Based Microsphere Coatings for use as Tunable Biocompatible Interfaces

German Raul Perez Bakovic
University of Arkansas, Fayetteville

Peptoid-Based Microsphere Coatings for use as Tunable Biocompatible Interfaces

A dissertation submitted in partial fulfillment
of the requirements for the degree of
Doctor of Philosophy in Engineering

by

German Raul Perez Bakovic
University of Arkansas
Bachelor of Science in Chemistry, 2012

August 2017
University of Arkansas

This thesis is approved for recommendation to the Graduate Council.

_____
Dr. Shannon Servoss
Thesis Director

_____   _____
Dr. Kartik Balachandran   Dr. Robert Beitle
Committee Member   Committee Member

_____   _____
Dr. Colin Heyes   Dr. Ranil Wickramasinghe
Committee Member   Committee Member

Abstract

The pursuit of sensitive, non-invasive, and cost efficient diagnostic tools for early stage disease detection have led to the development of sophisticated biosensor technologies for proteomic studies. As these markers increase in complexity, the role of support substrates grows increasingly important. Limitations in existing support substrates include the potential for increased sensitivity, binding specificity, and bio-stability. Ideal support substrates need to provide biocompatible and bioresistant surfaces, that offer high surface areas for binding, and enables the incorporation of diverse chemistries. The use of peptoids as the basis for the deposition of uniform microsphere coatings offers a mean to the attainment of such characteristics. Specifically, it enables for the utilization of its unique characteristics, namely, ease of synthesis and highly customizable side chain chemistries, in order to create a robust, biocompatible surface.

Table of Contents

1. Introduction

Although knowledge of different types of cancer and their progression has grown remarkably in the last decades, progress in the efforts has in large been hampered by the technology to detect them at an early stage. This difficulty stems from the fact that the diagnosis of a disease cannot be considered analogous to its detection. Diagnosis predominantly follows the recognition of symptoms, and many of those initial symptoms are often indicative of a number of diseases with similar features, rather than specific to the one responsible. Most importantly however, cancer diagnosis often occurs too late, as symptoms manifest themselves once tumors are considerably large and the disease consequently widespread.

Mortality rates in cancer increase with disease progression. For this reason, it is at its incipient stages of development that the therapeutic treatment of cancer presents its greatest potential. However, these early stages are often asymptomatic, resulting in delayed diagnoses of more advanced stages for which treatment is found often ineffective [1]. Data from the Surveillance Epidemiology and End Results (SEER) Program of the National Cancer Institute demonstrates the sharp contrast that exists in areas where tumor growth can be more easily observed, and hence detected, as compared to internal organs where it is much more difficult [2]. While the 5 year survival rate in skin cancer (91.5%) and breast cancer (89.4%) paints a much more optimistic outlook, lung cancer (17.4%) and pancreatic cancer (7.2%) drop a sobering dose of reality (http://seer.cancer.gov) [3]. The identification of cancer by pathological techniques is reliant on the morphologic assessment of tumor tissue. While this method is suitable for the identification of tumors

that occur at certain accessible areas (cervix), this same type of assessment is not feasible at other less accessible regions (ovaries), which hence hold much higher rates of mortality [4]. While crucial for the current prognosis of cancer, these techniques unfortunately fall short in providing the basis for the development of a technology that would allow for early detection [5].

Early detection decreases the economic costs, extensiveness of the treatment, and mortality associated with the disease [6]. The value of diagnostic technologies is intrinsically related to accuracy and stage at which they are able to identify a disease. Disease identification needs the existence of sensitive assays that can detect molecular changes associated with the onset of the disease with high specificity. Early detection requires the screening of asymptomatic populations in a minimally invasive manner and with small sample volumes. Biomarker-based technologies offer promising means for the attainment of these goals [4].

1.1. Biomarkers

Over the last decades, there has been an enormous effort to develop sensitive disease-specific assays that can assist in therapeutic decision [1]. Biomarkers are molecular indicators of a physiological status, and as a result can be assayed to provide information on the state of a biological process [7]. The use of biomarkers is integral to cancer research because of the unique association genomic changes in cancer cells have with the progression of the disease [1]. Cancer biomarkers reflect genotoxicity, hyperproliferation, hyperplasia, inflammation, mutations, altered patterns of gene and protein expression, promoter methylation, and enzymatic changes produced by the disease or the host system

in response to the disease [5] [7]. Understanding these changes as natural identifiers of disease progression will allow for the discovery of new biomarkers for (i) early detection, (ii) diagnosis, (iii) prognosis of high-risk individuals, (iv) response to treatment and/or (v) recurrence of the disease [8].

Progress in proteomic technologies have led to the discovery of novel biomarkers through the assessment of proteome profiles in disease states [9]. In contrast to the genome, which is rather more of a constant entity, the proteome represents a dynamic compilation of diverse proteins that vary among different individuals, cell types, and pathophysiological conditions [10]. While the genome comprises the genetic makeup of each cell, it provides little information about their structure, interactions, modifications, cellular localization, activities, biological function, and, potential involvement in the carcinogenic process [11]. In fact, gene activity and protein abundance show no reliable correlation [12]. The biological roles of proteins are determined by post-translation modifications and interactions such as glycosylation, phosphorylation, cleavage, crosslinking, oxidation or reduction, and lipid attachment [13]. The complexity of these modifications has lead to the realization that protein dynamics cannot be probed using genetics and DNA-based methods [14]. Protein-based approaches provide a natural platform for these studies. They are based on the identification of altered protein expression levels in disease states [15] [16]. Antibody-based arrays are also often utilized for diagnosis. Antibodies, being natural binders of proteins, provide a means to compare and quantify protein levels in health and disease [17]. Antibody platforms have been developed on monoclonal, polyclonal and recombinant antibodies [13] [18] [19] [20] [21] [22] [23] [24] [25]. Antibodies are widely utilized in protein detection because of the high specificity that is required in order to

identify a target [26]. Additionally, the relative structural uniformity of antibodies allows for the utilization of single support surfaces.

Changes in post-translational modifications of protein structures have important roles in disease progression, and thus if profiled correctly offer valuable information associated to the disease. Glycosylation is one of many post-translational modifications, prevalent in over 50% of proteins [27]. Glycans are involved in recognition, adherence, motility, and signaling processes [28] [29]. The potential as biomarkers is reflected by the occurrence of cancer-associated glycans resultant from oncogenic altered glycosylation. Cancer-associated glycans are predominantly located on the surface of cells, and therefore ideal targets for detection [30]. Glycans have been screening in human serum for diagnostic purposes [31] [32] [33] [34] [35] and utilized for malignancy-identification for breast cancer [35] and Hodgkin's lymphoma [36].

1.2. Microarrays

While advances in technology continue to accelerate the discovery of potential biomarkers [37] [38] [39], assessment of their true value for the screening of complex disease lags behind. In fact, the approval rate of new clinical biomarkers is in decline [37]. A major obstacle hampering biomarker validation is the intrinsic molecular heterogeneity that exists across diverse populations and tumor tissues. To overcome this large variability, validation technologies need to reproducibly analyze thousands of samples to effectively assess assay performance [40]. Enzyme-linked immunosorbent assay (ELISA) microarray technology can analyze a profile of biomarkers in parallel and, thus, has the sensitivity and specificity necessary to accelerate the validation of clinical biomarkers [41] [42].

The concept of the 'microspot' assay was introduced by Ekins under the fundamental premise that miniaturization would allow for the detection of analytes with higher sensitivity than those of conventional macroscopic immunoassays [43] [44]. ELISA microarray technology was developed in early 2000 [17] by combining protocols and instrumentation for DNA microarrays and 96-well plate ELISA [45], yielding a robust and automated platform of unmatched high-throughput sensitivity and reproducibility [46]. Antibody microarray technology has been utilized for the non-invasive detection of disease-specific analytes in bodily fluids (serum, plasma, urine, tears) and tissues extracts [47] for leukemia [48], breast cancer [49] [50] [51] [52], prostate cancer [53], pancreatic cancer [54] [55], lung cancer [56] [57] [58], bladder cancer [47], colorectal cancer [59] [60], cystic fibrosis [61], primary Sjogren's syndrome [62], psoriatic arthritis [63], as well as congestive heart failure [64].

1.2.1. Enzyme-Linked Immunosorbent Assay (ELISA) Microarray

Enzyme-linked immunosorbent assay (ELISA) microarray technology has emerged as a strong platform for the analysis of biomarkers. Advantages of this platform are associated to the miniature nature of its design, which allows for the cost-effective and efficient parallel screening of small volumes of precious clinical samples and expensive antibodies in a high-throughput manner, thus enabling the study of large populations of samples necessary for the identification and validation of biomarkers [45]. In addition, the assays allow for the quantitative measurement of multiple proteins in complex biological fluids over a large concentration range with high sensitivity and specificity [65]. Furthermore, its similarity to ELISA protocols used routinely in clinical laboratories facilitates assay transfer

from the laboratory to clinical settings [66].

The capability to analyze multiple proteins in parallel offers many benefits. Aside from practical benefits (time, cost, reagent consumption), parallel measurements are of great scientific interest [13]. Multiplex studies allow for the screening of biomarkers to reveal associations in proteins and disease states. Proteins interact in complex networks and often have overlapping or complementary functions. Multiplex studies thus provide experimental conditions that can portray a much more meaningful picture of a biological state [13]. Furthermore, multiplex studies can increase the sensitivity and specificity of disease diagnostics, and thus result in fewer false positives and false negatives as compared to single markers [67].

The miniaturized design of these antibody microarrays (<1 cm^2) is based on the immobilization of minute amounts of antibodies ($\sim$ 400 pL) onto a solid support in an ordered pattern, a microarray (Figure 1.1.) [18]. These antibodies serve to bind protein analytes onto the surface. The microarrays are incubated with small amounts of sample ($\sim$ 20 µL) and then generally tagged for fluorescent detection. An enzyme-dependent signal amplification step, such as biotin tyramide, is often used to reach sensitivities in the fM range, and allow for the detection of low-abundant (pg/ml) protein analytes [18] [51] [68] [69].
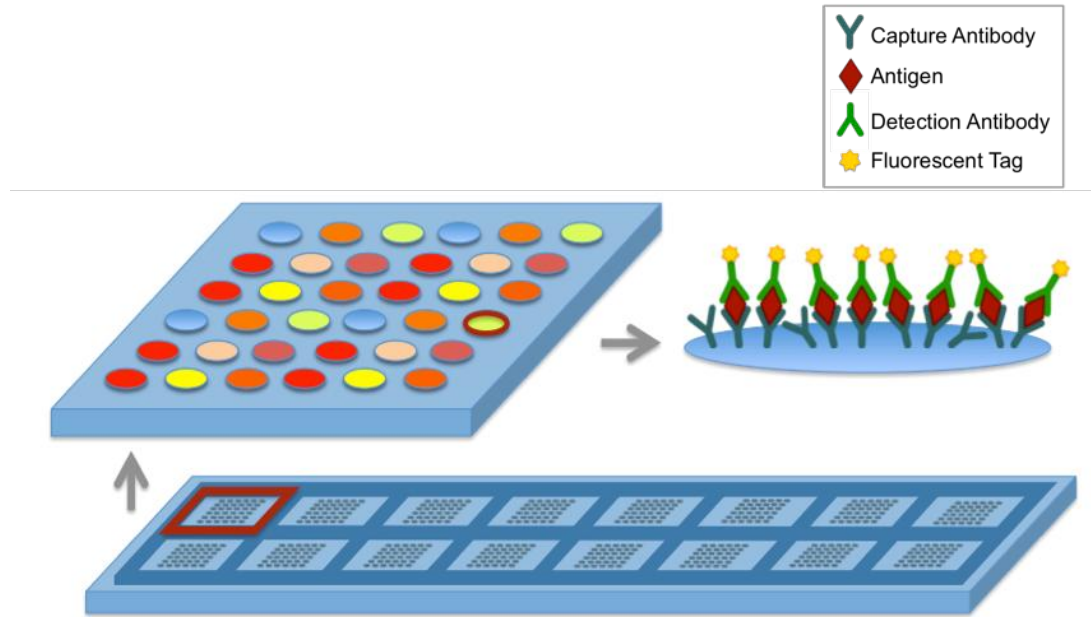
Figure 1.1. Schematic diagram of sandwich ELISA microarray. Antibody microarrays are often performed based on two distinct experimental constructs: label-based assays or sandwich assays [67]. Label-based assays rely on the capture of tagged protein analytes for detection. This format allows the co-incubation of different tagged protein analytes. Co-incubation makes analytes compete for binding. Competitive assays have some advantages over non-competitive assays in terms of linearity of response and dynamic range [70]

Sandwich assays rely on the presence of a second 'detection' antibody that binds to the

same antigen as the immobilized 'capture' antibody, but with affinity for a different site

(Figure 1.2.). This detection antibody is typically biotinylated for subsequent measured

using streptavidin labeled with a fluorophore or enzyme [13]. The use of matched antibody

pairs to target each antigen increases assay sensitivity and specificity [45]. Sandwich

assays are non-competitive as they permit the incubation of only one sample. Non-

competitive assays have sigmoidal binding responses of narrower dynamic ranges [67].
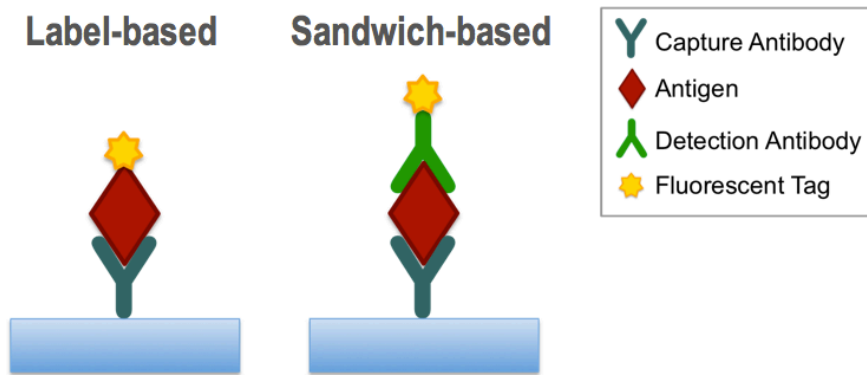
Figure 1.2. Schematic demonstrating the difference between labeled based assays and sandwich based assays.

1.2.2. Specificity and Cross-Reactivity

Sensitivity refers to the percentage of individuals with a disease who test positive for a marker in question, while specificity refers to the percentage of individuals without disease who test negative for the same marker [8]. The lower the sensitivity, the more often individuals with the disease will pass undetected, and the lower the specificity, the more often individuals without the disease will test positive [71]. A major challenge in the validation of cancer biomarkers is high variability and low incidence of specific cancers across populations [45]. As a result, assays of very high sensitivity and specificity are required. Otherwise, biomarkers are unable to distinguish individuals both with and without the disease [45]. A number of potential biomarkers do not progress beyond this point for this very reason [60]. Similarly, even many of the best biomarkers presently available, often fall short in meeting those expectations, as is the case with prostate specific antigen (PSA). As a biomarker for prostrate cancer PSA exhibits sensitivities greater than 90%, however has specificities of only 25%. This high incidence of false positives results in a large number of unnecessary and often invasive biopsies that take a toll in the lives of

people that extends far the financial one [72] [73] [74] [75]. In a similar manner, the biomarker for breast cancer CA15.3 only reaches sensitivities of 23% and specificities of 69% and as a result is limited to monitoring advanced stage breast cancer responses to treatment or recurrence [8]. The analysis of multiple protein profiles rather than reliance on single biomarkers offer the potential to achieve the sensitivity and specificity that is required the early detection [7].

Although sandwich assays are known for their high sensitive and specificity, in multiplex studies great care needs to be taken in order to ensure no cross-reactivity or interference exists. While often negligible in arrays of limited complexity, large-scale studies screening libraries of antibodies against a number of potential targets increase the prevalence of cross-reactive binding. Cross-reactivity often occurs due to sequence and/or structure similarity of binding sites. Monoclonal antibodies tend to be more susceptible to cross-reactions than polyclonal antibodies, for which effects are dissipated by the heterogeneity of the antibody population [4]. In addition, non-specific interactions can render proteins inactive, often just by making binding sites inaccessible through steric hindrance. Efforts to further develop the microarray technology as a result are directed toward the reduction of cross-reactivity between assays [76].

1.2.3 Surface and Attachment

One of the main challenges in the development of protein and antibody microarrays is the immobilization of molecules of diverse structures and characteristics onto a solid support in a manner that also maintains their innate binding properties. Surface chemistries and immobilization procedures are crucial for the optimal performance of microarray

platforms, as is evident by the large number of slide surfaces commercially available [77].

Ideal surfaces for ELISA microarray need to provide not only strong attachment of the

immobilized antibodies, but also retain their inherent activity and display high binding

capacities, signal-to-noise ratios, and reproducibility across all chips, slides, and

experiments [78]. Additionally, the high-throughput nature of the platform requires

supports to be robust and retain high levels of specificity and sensitivity through rigorous

processing conditions and prolonged storage periods.

Globular proteins usually consist of a hydrophobic core and hydrophilic surface.

Immobilization onto hydrophobic surfaces destabilizes protein structure, in essence

turning its inside out, and as a result rendering it inactive [79]. Antibodies in particular

need to maintain their native confirmation upon immobilization in order to retain binding

specificity [80]. In addition, unlike DNA, which have a uniform negatively charged

phosphate backbone exterior that allows for its relatively facile immobilization onto

oppositely charged surfaces, protein surface charges are very diverse, and consequently

often require complex surface chemistries and immobilization procedures [77]. The

challenge lies in designing a microarray support that accommodates proteins of varying

characteristics in a way that provides a non-denaturing environment that preserves the

active form of the protein.

There are a number of immobilization strategies and solid supports currently in existence

[81] [82] [83] [84] [85] [86]. However, microarray surfaces can in general be broadly

categorized into two main types: two-dimensional surfaces and three-dimensional

surfaces. While two-dimensional surfaces allow for the direct attachment of proteins to the

surface, three-dimensional surfaces retain proteins within a matrix (Figure 1.2.). Glass

slides are widely preferred as two-dimensional solid support platforms because of their

inherent low fluorescence [65] [87] [88] [89] [90] [91]. However, in order to facilitate

attachment, glass slides have been functionalized with a variety of different chemical

modifications. Two-dimensional surfaces include aldehyde [89] [92], aminosilane [77] [93]

[94], epoxysilane [93] [94], mercaptosilane [94], polystyrene [77], and poly-L-lysine coated

slides [65]. These surfaces immobilize proteins through electrostatic and covalent

interactions. Covalent attachment is often achieved through cross-linking, via amine or

thiol groups. While these surfaces offer a number of advantages, due predominantly to the

unique combination of both strong attachment and low coefficients of variation, they also

present distinct disadvantages, including, high rates of evaporation and close contact with

the surface, which can affect protein structure [24].
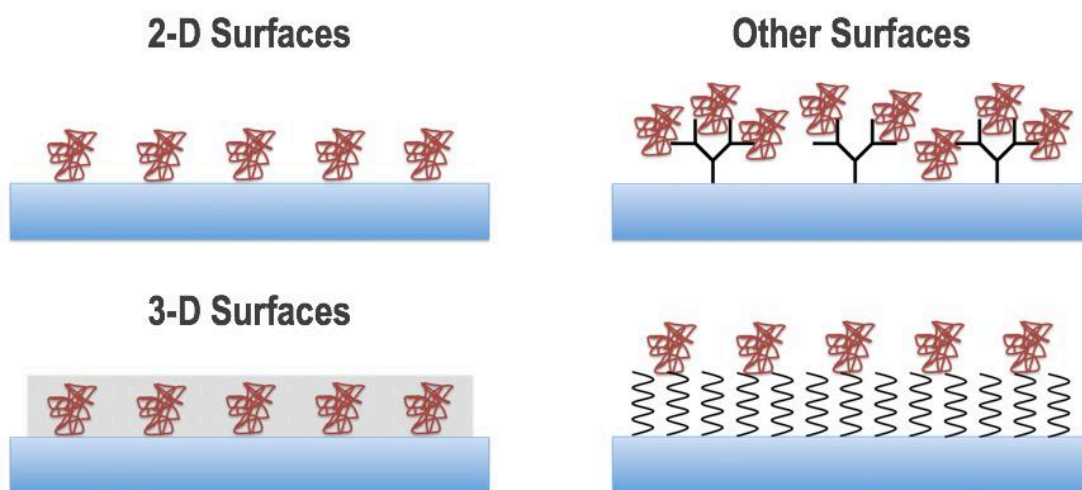
Figure 1.3. Schematic demonstrating the three-dimensional surfaces, two-dimensional
surfaces, and other more specialized microarray surfaces.

Three-dimensional surfaces include polyacrylamide [89] [95], agarose [90] and

nitrocellulose gels [96] [97] [98] [99] [100] [101], as well as poly(vinylidene fluoride)

(PVDF) membranes [102] [103]. These surfaces immobilize proteins through physical adsorption, retaining them within its structure via hydrophobic interactions. These matrices provide a more protein friendly environment that preserves their native conformation, allowing for a more optimal surface for binding, and hence higher binding capacities and signal intensities [104]. However, while these surfaces perform well in terms of limits of detection, as a whole, they display much higher coefficients of variation [77]. Background fluorescence can also be matter of concern, and surfaces often require much more involved pretreatment and blocking procedures. Additionally, because of the more complex nature of their three-dimensional structure, permeability can also considerably complicate the kinetics of the protein interactions, due primarily to the slow rates of protein diffusion [98].
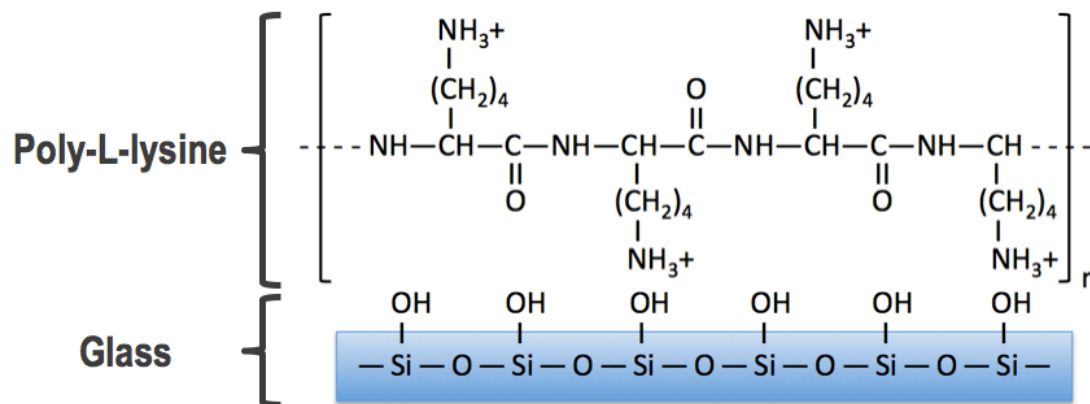
Figure 1.4. Schematic representation poly-L-lysine coated microarray slides.

There exist other more specialized surface chemistries that are more difficult to categorize as they combine characteristics of the two. While they do not provide a three-dimensional structure within which proteins could be retained, these surfaces cannot be considered to

be two-dimensional either as the do incorporate some sort of supra-molecular surface

assembly for attachment [24]. Surfaces which these characteristics include avidin [105],

streptavidin [84], nickel [92] dendrimer [106] [107], or polyethylene glycol (PEG) slides

[108]. These surfaces immobilize proteins through the covalent attachment of epoxy and

specialized affinity groups. Affinity binding improves coupling and lessens direct surface

contact destabilization. Avidin and streptavidin-coated surfaces are for these reasons

widely used for the immobilization of biotinylated capture molecules. In a similar manner,

histidine tags facilitate attachment on nickel-coated surfaces. Dendrimers increase the

density of functional surface groups to optimize protein immobilization. PEG layers prevent

direct surface contact and reduce background binding lessening the need of blocking

reagents.

High-throughput demands in protein microarrays require the selection and development of

optimized support surfaces that allow for more generally applicable and direct

immobilization procedures. While high binding affinities are imperative in preventing

antibody loss and ensuring surface attachment withstands processing conditions, which

involve rather extensive wash procedures. The reality of antibody immobilizations is that

functional loss can occur as a result of relatively passive interactions, as well as more

structurally intrusive chemical linkages. Angenendt *et al.* [77] compared the limits of

detection, coefficients of inter- and intra-chip variation, and storage characteristics for

different commercially available slide variations. While no particular slide took all areas, in

terms of overall array performance, poly-L-lysine and aldehyde slides displayed the best

signal uniformity and signal-to-noise ratios. Kusznezow *et al.* [94] studied a number of

variables affecting antibody microarrays, including surface modifications, cross-linking

strategies, spotting buffer compositions, blocking reagents, antibody concentrations, and storage conditions. For surfaces where antibodies were not covalently attached, poly-L-lysine slides displayed superior signal-to-noise ratios, despite having rather relative low signal intensities. Nitrocellulose surfaces on the other hand exhibited the highest signal intensities, however as with other three-dimensional surfaces, also produced high background signals. For surfaces where antibodies were covalently attached, cross-linked silane surfaces performed best, displaying good sensitivity and signal-to-noise ratios. Evaluating similar surfaces, Servoss *et al.* [78] found that as a whole, three-dimensional slide surfaces have higher background fluorescence than two-dimensional slide surfaces, due predominantly to the increased difficulty these more complex surfaces present to efficiently block and wash the surface. Additionally, no significant drop off was observed when assessing antibodies immobilized on non-covalent surfaces as compared to those attached covalently.

1.3. Poly-N-Substituted Glycines (Peptoids)

Inspired by natural polymers, the work of chemists and chemical engineers has focused in the development of synthetic polymeric materials that are able to mimic some of the fundamental molecular features that allow for the diverse array of functional structures nature so elegantly creates with just a set of monomeric sequences and interactions [109]. Polypeptides confer proteins a myriad of unique functional properties, providing for example, binding and catalytic sites that together hence enable molecular recognition. However, as biocompatible materials peptides present a major drawback, they are susceptible to *in vivo* proteolitic degradation, and as a result are limited in their potential

for biomedical and therapeutic applications [110]. Efforts to overcome these limitations have led to the design and development of innovative peptidomimetic oligomers [111] [112] [113] [114] [115] [116]. Synthetic polymer analogs exploit structural similarities in order to allow for the mimicry of bioactive functionalities. These bioactive roles are often determined by the unique ability of peptides to self-assemble into complex, sequence-specific three-dimensional secondary structures [117]. Specific peptidomimetic oligomers, commonly referred to as foldamers [118], which in addition to the mimicry of primary structure display well-defined secondary structures, are therefore of great interest.

Oligomeric *N*-substituted glycines (peptoids) are a form of bioinspired peptidomimetic polymers whose backbone structure closely resembles that of peptides, but have side chains appended to the amide groups rather than the α-carbons (Figure 1.5.). This structural modification prevents proteolytic degradation, making peptoids a promising alternative as biocompatible materials for therapeutic applications. However, this modification also removes the presence of backbone amide hydrogens, critical for secondary structure, at least in terms of allowing for the formation of the same type of hydrogen bond linkages that stabilize beta sheets and helices in peptides. Despite these limitations, secondary structures such as turns, loops, and helices that in turn allow for the formation of supramolecular assemblies can be induced in peptoids upon the addition and proper placement of specific side chains [119]. The inclusion of chiral aromatic side chains has been demonstrated to incite the formation of helical secondary structures reminiscent of polyproline type I helix [120], stabilized primarily through steric and electrostatic interactions [117]. Circular dichroism (CD) spectra of these peptoids closely resemble the spectra of peptide α-helices [121].

Peptide
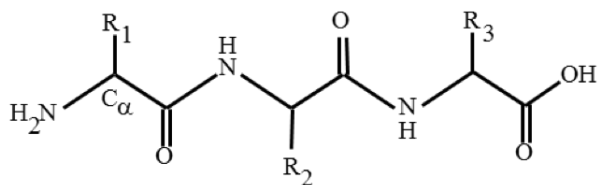
Peptoid
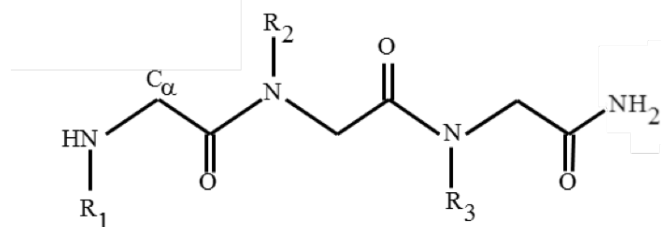
Figure 1.5. Structural comparison of peptide and peptoid molecules.

Like peptides, peptoids can be constructed via an automated, solid-phase synthesis [122].
The submonomer method provides a robust and highly efficient platform for synthesis,
enabling precise control over sequence functionality. Synthesis follows a carboxy to amino
direction, in which each cycle of monomer addition consists of a two-step process: (1)
acylation and (2) nucleophilic substitution (Figure 1.6.) [121]. Functional moieties are
introduced by the incorporation of commercially available primary amines, enabling access
to a wide variety of side chain chemistries (>100 monomers) [109]. High monomer
coupling efficiencies (98%) [123] additionally allow for the precise sequence-specific
synthesis of polymer chains surpassing over 300 monomeric subunits in length [124].
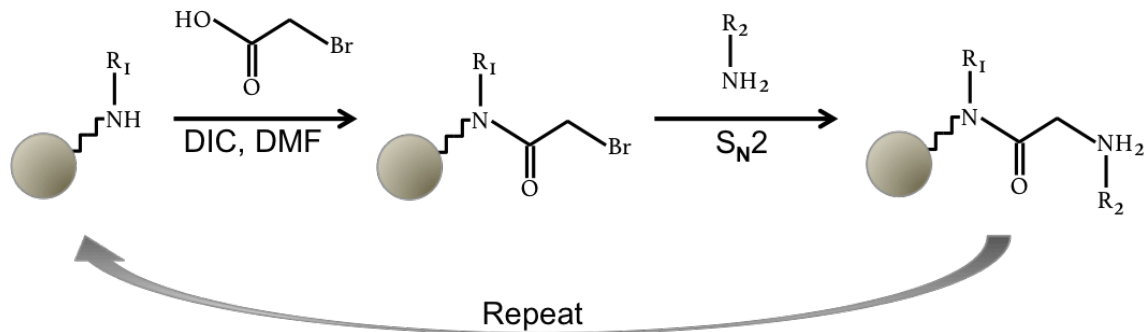
Figure 1.6. Submononer synthesis on Rink-amide resin.

Peptiods allow for the precise spatial positioning of diverse chemical functionalities, enabling the design of novel materials with distinct chemical properties. Peptoids are of great interest as biomimetic materials for therapeutic applications because they display low immunogenicity, are protease-resistant, biocompatible, and soluble in water. They are attractive as polymeric materials as they offer a remarkable ease of assembly, sequence programmability, and relatively low costs. In addition, they enable the incorporation of a variety of highly customizable side chain chemistries, and allow for the precise control of sequence and length specificity, as well as the formation of defined three-dimensional conformational assemblies. Lastly, the mimicry of the natural proteins allows for the study of fundamental sequence, structure, and function relationships, and hence potential sighting in the understanding of the protein structure-function paradigm.

2. Research Rationale

While knowledge of different types of diseases and their progression has grown remarkably in the last decades, the economic costs, extensiveness of treatment, and mortality associated with many of these diseases continue to in large be hampered by our ability to detect when therapeutic treatments present their greatest potential—before the

disease is widespread—the incipient stages of development. Thus, there is a critical need to develop sensitive assays that can detect molecular changes associated with the onset of the disease. Enzyme-linked immunosorbent assay (ELISA) microarray technology offers a promising mean for the attainment of this goal. Surface chemistries and immobilization procedures are crucial for the optimal performance of microarray platforms. The challenge lies in the immobilization of capture molecules of diverse structures and characteristics onto a solid support in a manner that allows for strong attachment, but also retains their inherent activity. These assays need to display high reproducibility, binding capacities, and signal-to-noise ratios. Additionally, the high-throughput nature of the platform requires supports to be robust and retain high levels of specificity and sensitivity through rigorous processing conditions and prolonged storage periods.
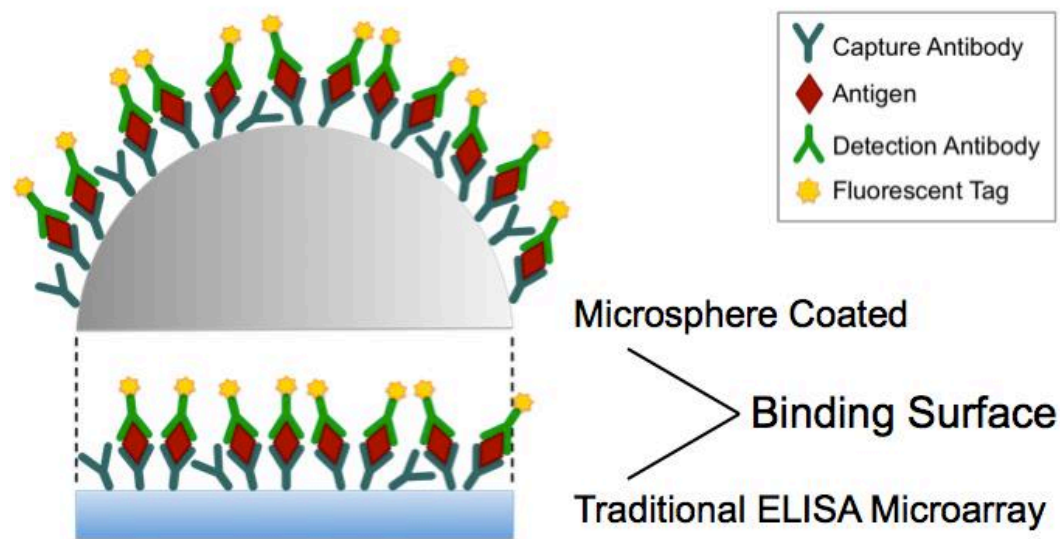

Figure 2.1. Representative schematic for the increased antibodies binding.

The comprehensive goal of this project is to develop a biocompatible surface coating that increases the available surface area. The surface area difference between the microsphere

coated three-dimensional surface and the uncoated two-dimensional surface given the average microsphere diameter of 1.59 um is of 157% assuming that antibody immobilization occurs only in the projected top half of each microsphere. We hypothesize that the proposed peptoid-based microsphere coatings will enhance the binding efficiency of capture reagents, increasing the dynamic range and sensitivity of biosensor technologies. Peptoids are bio-inspired sequence-specific polymers based on a polyglycine backbone with side chains appended to the amide groups. Peptoids are attractive as biocompatible materials for therapeutic applications because of their relative low costs, ease of synthesis, highly customizable side-chain chemistry, biostability, biocompatibility, and low cytotoxicity. The Servoss lab has demonstrated that helical peptoids with partial water solubility self-assemble into microspheres.

The hypothesis will be confirmed by completing the following aims:

1. **Compare the ELISA microarray performance of the peptoid microsphere-coated slides with commercially available slides.** We hypothesize that the increase in surface area provided by the microsphere coatings will enhance the dynamic range and sensitivity of assays performed in surfaces providing similar chemistries for attachment. The proposed peptoid-based coating will be assessed in reference to glass and poly-L-lysine coated surfaces in order to evaluate non-covalent and covalent immobilization strategies. The binding efficacy of the peptoid microsphere-coated glass substrates will be analyzed by ELISA microarray with known antibody assays.
2. **Investigate the factors affecting microsphere morphology following deposition on a solid surface.** We hypothesize that the ionic properties of the solvent, including ionic

strength, pH, and Hofmeister solubility, play a crucial role in determining the ultimate stability of the microspheres. It is believed that pi-pi stacking of the chiral aromatic groups along with hydrophobic effects lead to self-assembly of the peptoids into microspheres. Preliminary robustness studies have demonstrated that the microsphere coatings are able to withstand all processing conditions associated with ELISA microarray, but prolonged exposure to water leads to degradation of the peptoid microspheres. CD will be used in order to determine any effect on helicity, while SEM will be used in order to study the robustness of the spheres in the diverse conditions.

3. **Investigate the effect helicity plays on microsphere size formations.** We hypothesize that peptoid sequences exhibiting stronger helical secondary structure will form smaller microspheres as compared to those peptoids exhibiting less structured helices. Preliminary findings demonstrate that the inclusion of positively and negatively charged groups in the third face of the helix formed microspheres nearly 10 times smaller than those obtained with the sequence being currently used. It is believed that these opposite charges interact to form tighter helices which result in the smaller supramolecular assemblies observed [125]. CD studies will be performed in order to quantify peptoid helicity, while SEM will be used for the visual assessment of microsphere size.

3. Deposition of Uniform Peptoid Microspheres Coatings

3.1. Materials

Amine sub-monomers: 4-methoxybenzylamine and (S)-methylbenzylamine were purchased from Acros Organics (Pittsburgh, PA). *tert*-butyl N-(4-aminobutyl)carbamate

was purchased from CNH Technologies Inc. (Woburn, MA). MBHA rink amide resin was purchased from NovaBiochem (Gibbstown, NJ). Piperidine was purchased from Sigma-Aldrich (St. Louis, MO). Test grade silicon wafers were purchased from University Wafer (South Boston, MA). Poly-L-lysine and ultra clean glass microarray slides were purchased from Thermo Scientific (Pittsburgh, PA). Disuccinimidyl suberate (DSS) and bis[sulfosuccinimidyl] suberate (BS^3) were purchased from Pierce (Rockford, IL, USA). Purified antibodies and antigens were purchased from R&D Systems (Minneapolis, MN, USA). Blocking solution containing 10 mg/ml casein in phosphate-buffered saline (PBS) was purchased from Bio Rad Laboratories (Hercules, CA, USA). Tyramide Signal Amplification (TSA) system, including streptavidin-conjugated horseradish peroxidase, amplification diluent, and biotinyl tyramide, was purchased from Perkin Elmer (Wellesley, MA, USA). All other reagents for synthesis, purification and sample preparation were purchased from VWR (Radnor, PA). All chemicals were used without further modification unless otherwise specified.

3.2. Methods

3.2.1 Peptoid Synthesis

Peptoids were synthesized via the submonomer solid-phase method on rink amide resin [122]. The resin was initially swelled with dimethylformamide (DMF), and the Fmoc protecting group on the resin was removed using a 20% solution of piperidine in DMF. The resin-bound secondary amine was acylated with 0.4 M bromoacetic acid (BAA) in DMF, in the presence of N,N'-diisopropyl carbodiimide (DIC), mixing for 1 minute. Amine sub-

monomers were incorporated via an S_N2 nucleophilic substitution reaction with 0.5M

primary amine in DMF, mixing for 2 minutes. The two-step bromoacetylation and

nucleophilic substitution cycle were repeated until all desired side chains has been

incorporated (Figure 3.1.). Once the synthesis was complete, the peptoid was cleaved from

the resin using a mixture of 95% trifluoroacetic acid (TFA), 2.5% water, and 2.5%

triisopropylsilane (TIS), mixing for 5 minutes. The acid was removed using a Heidolph

A   Laborota 4001 rotating evaporator (Elk Grove Village, IL) and peptoids were diluted to a

concentration of ~3 mg/mL in a 50:50 acetonitrile-water solution.

B
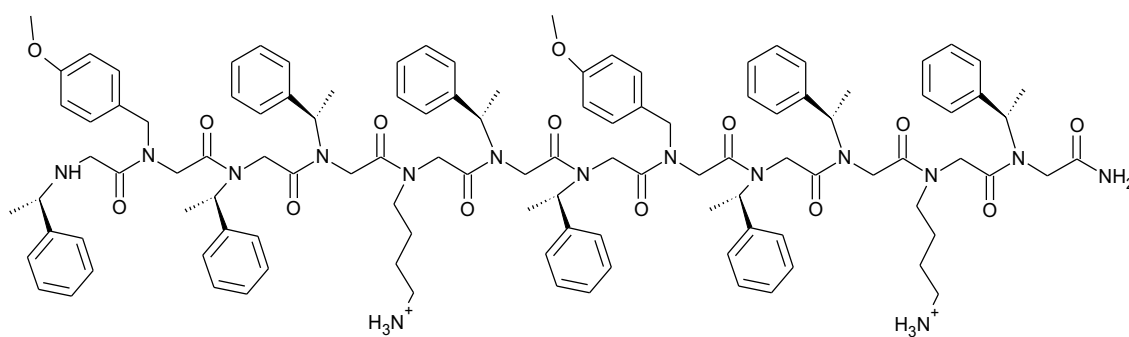
Figure 3.1. Peptoid structure for the P3 sequence.

3.2.2 Purification

Peptoids were purified using a Waters Delta 600 preparative high-performance liquid

chromatography (HPLC) instrument (Milford, MA) with a Duragel G C18 150 × 20 mm

column (Peeke Scientific, Novato, CA) using a linear gradient of 35-95% solvent B

(acetonitrile, 5% water, 0.1% TFA) in A (water, 5% acetonitrile, 0.1% TFA), over 60

minutes. Peptoids were confirmed to be >98% pure via analytical HPLC (Waters Alliance,

Milford, MA) with a Duragel G C18 150 × 2.1 mm column (Peeke Scientific, Novato, CA)

22

using a linear gradient of 35 to 95% solvent D (acetonitrile, 0.1% TFA) in C (water, 0.1%
TFA), over 30 minutes. Purified peptoid fractions were lyophilized using a Labconco
lyophilizer (Kansas City, MO) and stored for use as a powder at -20 °C.

3.2.3 Characterization

Matrix Assisted Laser Desorption/ionization Time of Flight (MALDI-TOF). Proper
synthesis was confirmed via MALDI (Bruker, Billerica, MA) mass spectrometry. The mass
of the purified peptoid samples (Figure 3.2.) matches the expected theoretical molecular
weight (1917 Da).
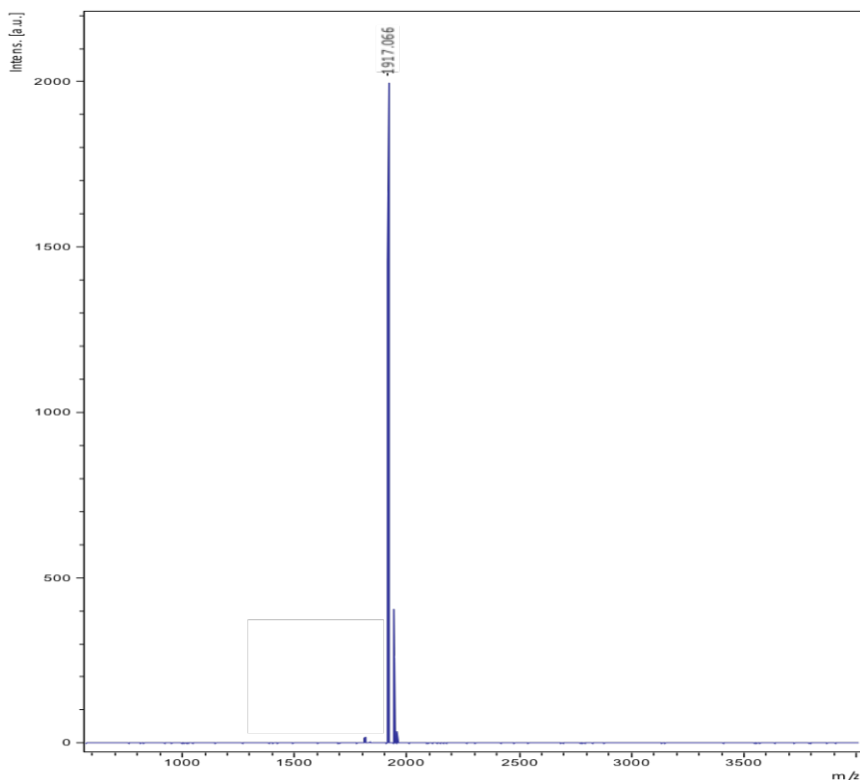
Figure 3.2. MALDI-TOF spectrum of peptoid, MW: 1917 Da.

Circular dichroism (CD). Secondary structure was confirmed via CD spectrometry using a

Jasco J-715 instrument (Easton, MD) at room temperature with a scanning speed of 20 nm/min and a path length of 0.1 mm. The spectra (Figure 3.3.) exhibits the characteristic maxima near 190 nm and two minima near 205 and 220 nm commonly associated to polyproline type I helices [121]. The peptoid was dissolved in methanol at a concentration of 120 μM because protic solvents have been demonstrated to help induce helical secondary structure in peptoids. Each spectrum was the average of twenty accumulations.
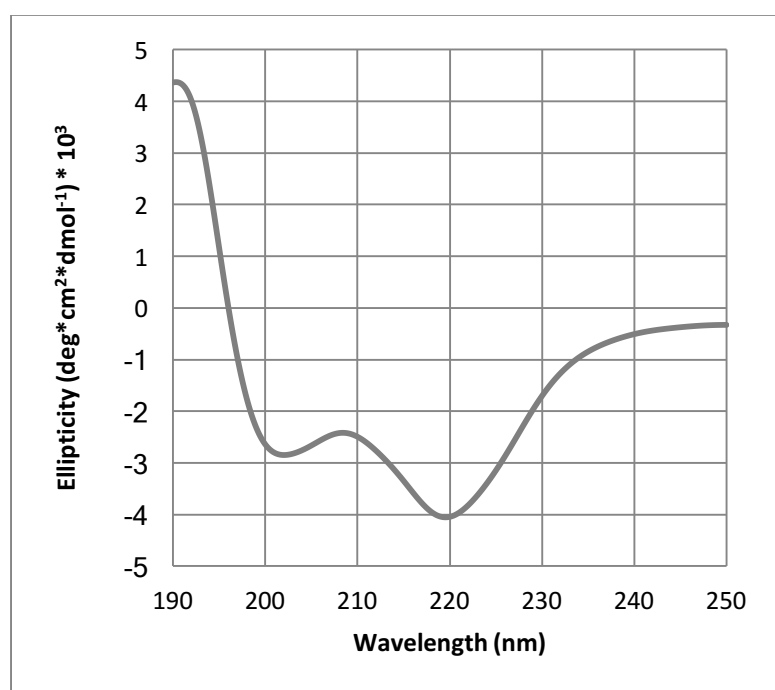
Figure 3.3. Circular dichroism spectra of peptoid showing a poly-proline type-1-like helical secondary structure. CD spectra were taken at room temperature with a scanning speed of 20 nm/min and a path length of 0.1 mm. The peptoid was dissolved in methanol at a concentration of 120 μM.

3.2.4. Microsphere Formation

Peptoid microspheres were prepared by dissolving the peptoid in a 4:1 (v/v) solution of various organic solvents/water at a range of concentrations. The peptoid solutions were deposited onto various surfaces of approximately 1 cm × 1 cm using a pipette under a

variety of different conditions.

3.3.5 Morphology Studies

Scanning electron microscopy (SEM). Peptoid microsphere coating morphologies were visually assessed at the Material Characterization Facility using a Phillips XL-30 environmental SEM (FEI, Hillsboro, OR) in order to determine effect of a number of optimization conditions on both the ability to form uniform self-assembling peptoid microsphere and consequent coatings with the latter.

3.3. Peptoid Microspheres Coatings

3.3.1. Peptoid Microspheres

Previous work in our lab has shown that helical peptoids that are in addition partially soluble in water are able to self-assemble into microspheres. Helicity in the structure is sterically induced with the inclusion of chiral aromatic side chains in two of the three faces of the helix (Figure 3.1.). Because these microspheres ($\sim$2 μm) (Figure 3.4.) are orders of magnitude larger than the single peptoid helix ($\sim$24 Å), we have proposed that the stacking of the chiral aromatic groups allow for formation of larger peptoid groupings that coupled to hydrophobic effects self-assemble into microspheres (Figure 3.5.) [125]. Similar types of supra-molecular assemblies have been observed by this sort of aromatic stacking in both peptides and peptoids [126] [127] [128] [129] [130].
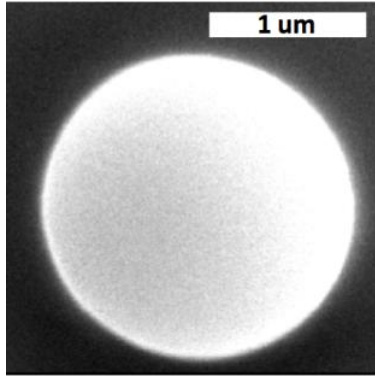
Figure 3.4. SEM image of peptoid microsphere.
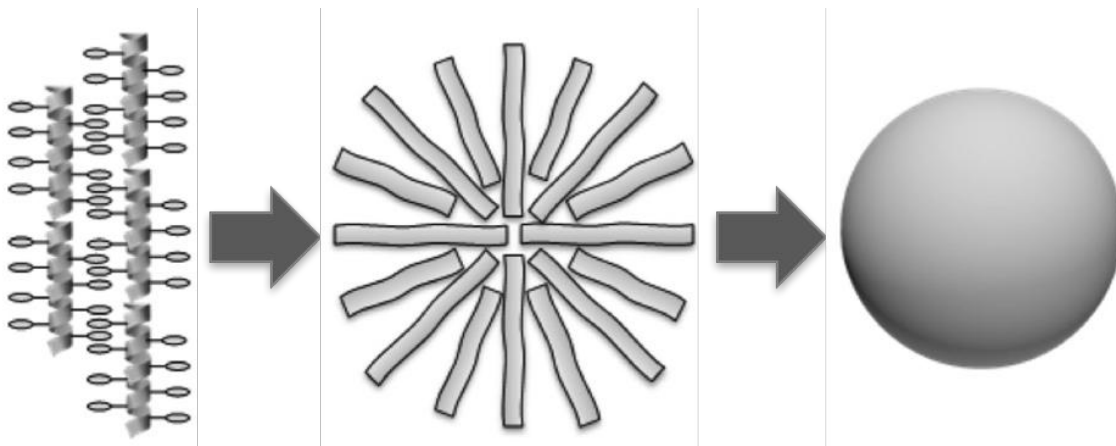
Figure 3.5. Schematic Representation of peptoid microsphere formation [146].

Past work in our lab has focused in the analysis of various parameters (i.e. partial water solubility, helical content, charge placement, and side chain bulk) affecting the self-assembly peptoids microspheres [125], and to an extent even the reproducible formation of these microspheres on silica surfaces [131]. Focus now continues on to the controlled deposition of robust uniform petoid microsphere coatings on glass slides. The peptoid sequence that has been selected for this work is based on these prior studies. SEM studies reveal that the administration technique by which the peptoid solution is applied to a surface greatly affected the uniformity of the coating and suggest that the horizontal full

26

coverage, as compared to some of the more readily utilized high throughput alternatives, such as dip coating, was necessary for best results. In order to ensure reproducibility of results, fixed peptoid volumes were administered with a pipette, covering the entire surface outlined by 1 cm × 1 cm delimiting wax imprints. It has been shown that protic solvents aid in stabilizing helical secondary structure in peptoids through hydrogen bonding [117] [132] [133] [134]. Solvent choice was investigated with the use of three different protic solvents (i) methanol, (ii) isopropanol, and (iii) ethanol (Figure 3.6.). Peptoids were dissolved in 4:1 organic solvent/water solution. While SEM images reveal sphere-like assemblies for all solvents, the most uniform spheres are formed with the use of ethanol as the protic solvent choice.
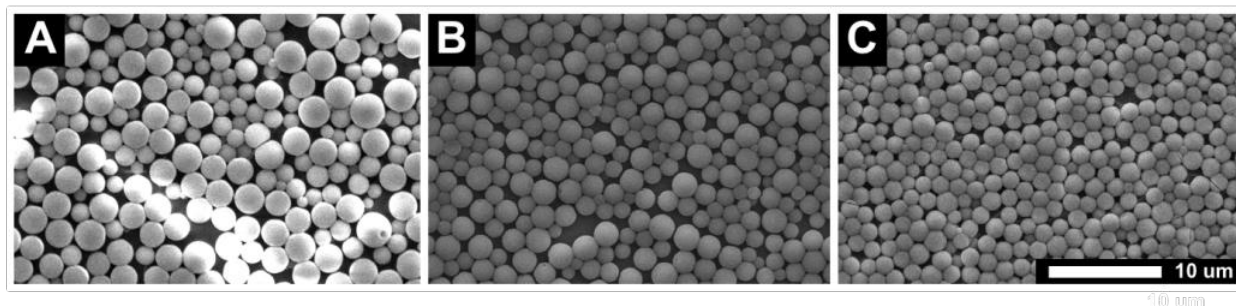
Figure 3.6. SEM images demonstrating the effect of different protic solvents on sphere formation: A) methanol, B) isopropanol, and C) ethanol.

3.3.2. Microsphere Coatings

The effect of drying conditions was similarly investigated by varying the humidity at which the peptoid solution was allowed to evaporate. For this analysis, the peptoid solutions were dried at (i) high humidity (85%) in a humid chamber (~120 minutes), (ii) open air (~30 minutes), and (iii) vacuum chamber (~5 minutes). Drying conditions greatly affected the uniformity of the spheres and coating deposition on the surface. Whether it was the

formation of sparse clusters of non-uniform globular aggregates at vacuum or clumped spheres at high-density regions towards the perimeter and center of the coverage area at a high humidity. Open air-drying, although with its own detriments (i.e. still perimetral intensive and sparse in the inner region) from a coverage standpoint, consistently formed the most uniform microspheres and surface coverage (Figure 3.7.).
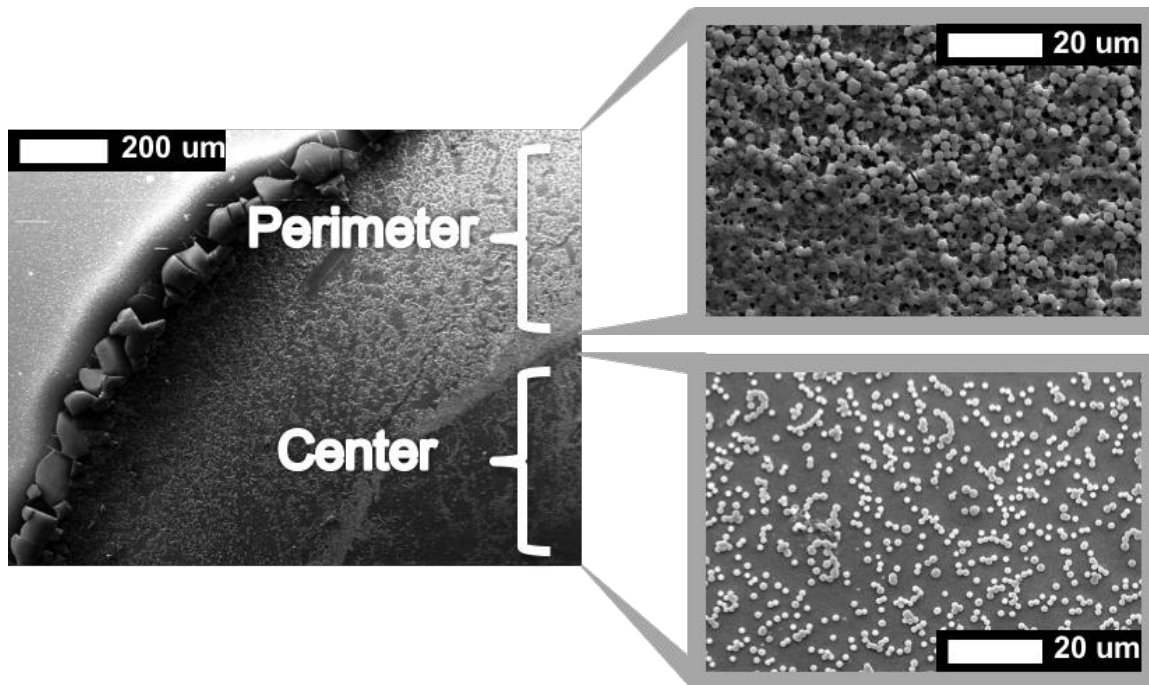
Figure 3.7. SEM images demonstrating the microsphere coatings coverage difference at the perimeter and center.
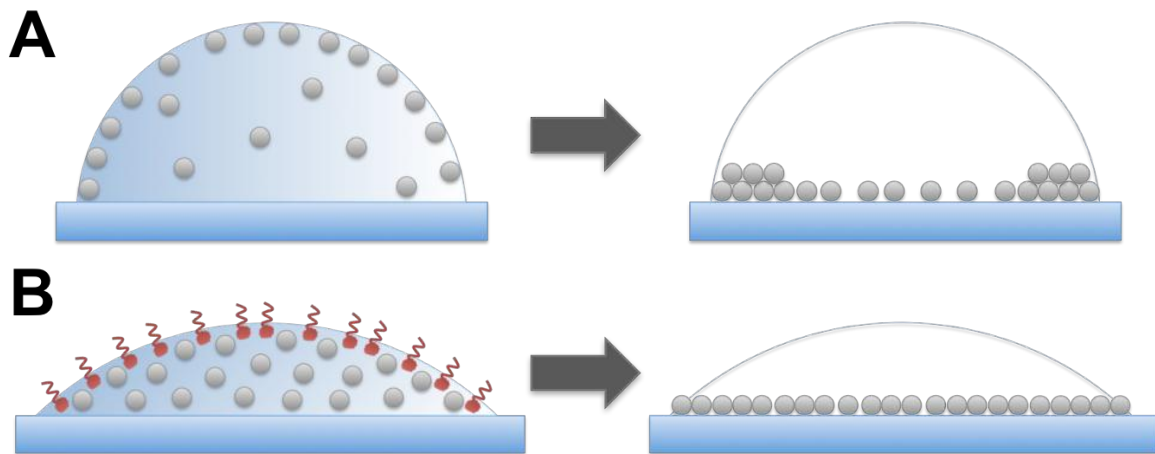
Figure 3.8. Schematic representation of the coverage uniformity improvement upon addition of tween surfactant.
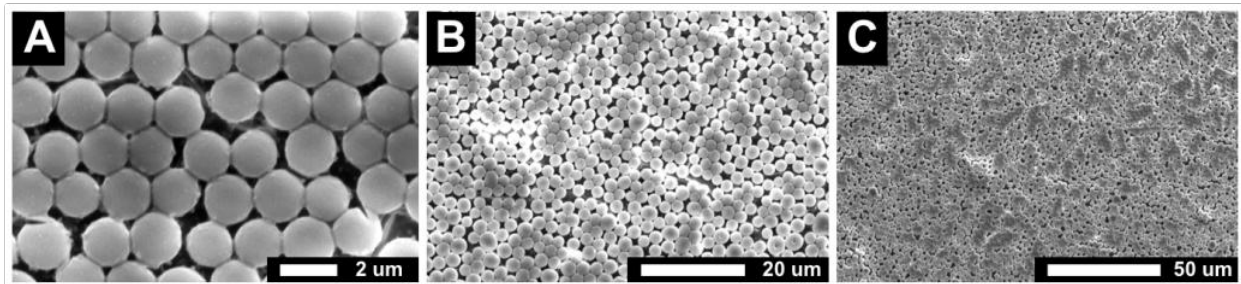
Figure 3.9. Microsphere coating coverage with optimized conditions at 3 different magnifications.

Coating morphology is directly linked to the mode of evaporation. In droplets, it is known that at atmospheric pressure, two main modes of evaporation occur: first, droplets flatten with a constant contact area, to then shrink at a constant contact angle. A constant contact area mode of evaporation is desired in order to obtain uniform coating depositions. In addition, perimetral intensive depositions are often indicative of preferential substrate accumulations at the air/liquid interface. The addition of surfactants can be used to preserve a constant contact area mode of evaporation by decreasing droplet surface tension, lowering the contact angle, and in turn improving the stability of the droplet by reducing the pullback forces at the perimeter during evaporation. In addition, surfactants

can be competitively used to displace substrates at the air/liquid interface, and thus lessen the perimetral deposition on the surface (Figure 3.8.). Results for the addition of Tween surfactant show considerable improvements on the overall uniformity of the coating, lessening perimetral microsphere deposition and allowing for an even distribution of microspheres throughout the entire surface (Figure 3.9.). At higher concentrations (> 0.1%) Tween addition clumped adjacent microspheres to each other, and when added to the solvent prior to the peptoid affected size uniformity in microsphere formation.

In order to increase the inner region coverage, peptoid concentrations and volumes for coverage where optimized. It was possible to increase peptoid concentrations from 3 mg/mL to 5 mg/mL to increase microsphere coverage density without disrupting the morphology and uniformity of either the spheres or coating (Figure 3.10.). Decreases in volume of peptoid solution added greatly affected the coverage density (Figure 3.11.), while increases in volume only further increased the deposition of microspheres towards the perimeter with minimal inner region improvement.
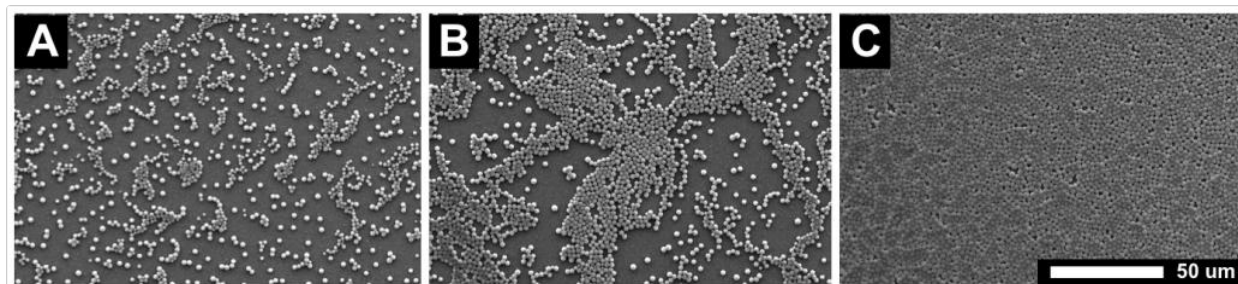
Figure 3.10. SEM images demonstrating the difference in microsphere coverage with peptoid concentration: A) 3 mg/ml, B) 4 mg/ml, and C) 5 mg/ml.
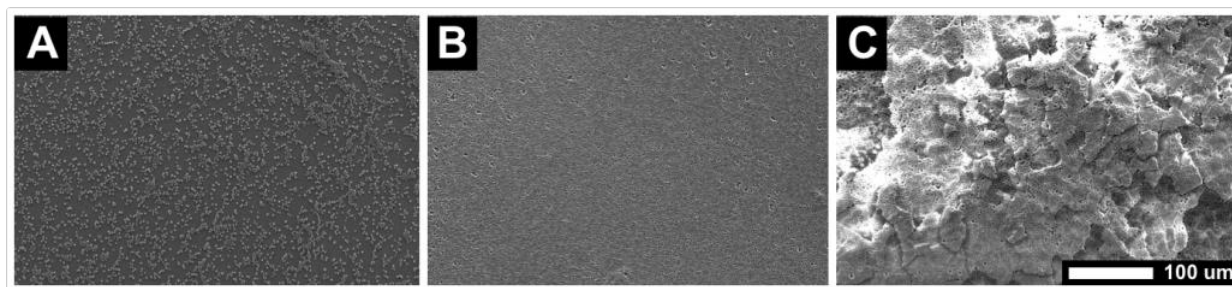
Figure 3.11. SEM images demonstrating the difference in microsphere coverage with volumes: A) 15 ul, B) 30 ul, and C) 45 ul.

ImageJ analysis of the microsphere coatings demonstrate 83.5 ± 3.4 % surface coverage at optimized conditions. Although the peptoid microsph ere coating has similar reactive moieties to poly-L-lysine, the contact angle of the peptoid microsphere coating is considerably more hydrophobic than the poly-L-lysine slides, 53.2 ± 3.9 degrees versus 30.3 ± 2.4 degrees. In general, hydrophobic surfaces limited solvent spreading. The increased roughness of the peptoid microsphere coatings as compared to two dimensional surfaces would similarly disrupt solvent spreading.

4. Detection and Validation of Cancer Biomarkers

4.1 Introduction

Protein microarrays are recognized as one of the most valuable tools in proteomics. In protein microarrays, proteins are immobilized on a solid substrate for the efficient and high-throughput parallel analysis of large population profiles. The technology offers a wide range of applications, including expression profiling, interaction profiling, and functional identification [135]. Protein concentration profiles may depend on age, physicochemical characteristics of the environment, and among those of interest, disease state. The need to study beyond mRNA profiling arises due to post translational modifications and general

protein degradation by proteolysis. Protein screening thus offers a direct way to phenotype cells and diagnose disease state, stage, and response to treatment [135]. This approach has been successfully explored with antibody arrays, where microarray protein chips based on immunological antibody/antigen interaction, offer the necessary high specificity and sensitivity, that have allowed for the development of the broad applications in the technology: proteome analysis, disease diagnostics, identification of biomarkers, and pharmaceuticals response profiling [136] [137].

Among several available immunoassays, ELISA is a popular because of its high specificity, sensitivity, and high throughput [13]. In ELISA, capture antibodies are first immobilized onto a solid support. Those capture antibodies then bind to specific antigen. The chip is then incubated with a detection antibody that binds to the same antigen as the capture antibody, but does so at a different site. Finally, the detection antibodies are tagged with a fluorescent dye, before the slide is scanned for a fluorescent signal with a laser scanner. The intensity of the fluorescence signal is directly related to the concentration of the substrate, and thus allow for the quantitative application of results.

4.2 Materials

Poly-L-lysine and ultra clean glass microarray slides were purchased from Thermo Scientific (Pittsburgh, PA). Disuccinimidyl suberate (DSS) was purchased from Pierce (Rockford, IL, USA). Purified antibodies and antigens were purchased from R&D Systems (Minneapolis, MN, USA). Additional antibodies and glycans were provided by our collaborators at Detroit R&D. Blocking solution containing 10 mg/ml casein in phosphate-buffered saline, pH 7.2 (PBS) was purchased from Bio Rad Laboratories (Hercules, CA,

USA). Tyramide Signal Amplification (TSA) system, including streptavidin-conjugated horseradish peroxidase, amplification diluent, and biotinyl tyramide, was purchased from Perkin Elmer (Wellesley, MA, USA). Alexa647-conjugated streptavidin was purchased from Invitrogen Life Technologies (Gaithersburg, MD). All other reagents were purchased from VWR (Radnor, PA). All chemicals were used without further modifications unless otherwise specified.

4.3. Methods

4.3.1 Microarray Printing

ELISA microarray spotting was performed at room temperature and 60% relative humidity as previously described [138]. A GeSiM NanoPlotter 2.1 (Quantum Analytics, Foster City, CA, USA) non-contact microarray printer with humidity control was utilized to spot the proteins. In some cases, proteins were covalently boud t the slides with a 0.3 mg/ml solution of the homo-bifunctional cross-linker DSS mathanol for 20 minutes. Prior to spotting, the slides were rinsed in nanopure water and dried in a centrifuge. Capture antibodies were suspended in PBS to a concentration of 0.5-1.0 mg/ml and ~400 picoliters per spot were printed at various different layouts. The antibodies were allowed to dry for an additional hour at 60% relative humidity. The slides were blocked with 10 mg/ml casein in PBS, rinsed in nanopure water and dried in a centrifuge. Upon completion, the slides were either stored under vacuum for future use at -20 °**C** or shipped to our collaborators.

4.3.2 ELISA Microarray

ELISA Microarray was performed as previously described [138], with all incubation steps performed at room temperature, in a closed humid chamber with gentle mixing on an orbital shaker (Belly Dancer, Stovall Life Science, Greensboro, NC). A two-step wash procedure between processing steps was performed by submerging the slides twice into PBS containing 0.05% Tween-20 (PBS-T). The slides were incubated with different antigen standards in 1 mg/ml casein in PBS overnight. Standard curves were created using a five-fold dilution series of the antigen mix along with an antigen-free blank for 8 total dilutions. Following a wash cycle, the slides were incubated with biotinylated detection antibody at 25 ng/ml in 1 mg/ml casein in PBS. The signal was amplified using the TSA system following manufacturer instructions, and incubated with 1 μg/ml Alexa647-conjugated streptavidin in PBS-T. Prior to scanning, the slides were rinsed twice in PBS-T and in deionized. A GenePix Autoloader 4200AL (Molecular Devices, CA) laser scanner was used to image the Alexa 647 fluorescence signal on the slides. The spot fluorescence intensity from the scanned slide images was quantified using GenePix Pro 3.0 software. Standard curves were created using ProMAT, a software program specifically developed for the analysis of ELISA microarray data [139].

4.4. ELISA Microarray Marker Assays

4.4.1. Antibody Assays

Initial research was conducted for the development of standard curves on 26 different ELISA microarray antibody assays. Large studies insert greater indices of variation that are

reflected on the quality of standard curves that can be developed. For this reason, significant work was conducted on further optimizing standard curves of all antibodies. In order to do so, special focus was placed on the development of a new antigen mix for the development of the standard curves. The optimized antigen concentration can be seen in Table 1. EGF, GFP, and PSA antigens were excluded from the antigen mix and prepared as separate independent stock solutions from which to be added fresh for each experiment. Additionally, we developed a homemade biotinyltryramide and amplification diluent. These solutions were compared to the TSA amplification kit solutions, obtaining very favorable results with comparable quality. In order to prevent any undesired interactions that might compromise assay specificity and sensitivity, cross-activity studies were first performed on all antibodies. Cross-reactivity studies involve a series careful evaluations [66]. In short, individual antigen and detection antibody pairs are first tested on arrays containing all capture antibodies. Undesired interactions would be detected upon evaluation of signal intensities, no cross-reactivity of either the antigen or the detection antibody with any capture antibody was detected. Nonspecific antigen contamination is then similarly assessed, however this time with all antigens present. A final round of screenings is conducted. These screens consist in preparing separate antigen mixes by removing one of the antigens from the mix, and screening each mix independently using a mixture with all detection antibodies, and then doing the opposite, preparing separate detection antibody mixes, and screening each mix independently using all mixture with all antigens. Cross-reactivity was detected between the TGFalpha and FGFb antibodies. FGFb was removed from future studies for this reason.

4.4.2. Sample Screenings

Serum sample from cancer patients were screened to validate the potential markers. For the initial 9-sample analysis, microarray slides with a 10x12 array layout containing all 26 different antibodies in quadruplicate were first spotted (Table 4.1.). For analysis, three different dilutions of each serum sample in triplicate were utilized. Antigen concentrations can vary by as much as 3 orders of magnitude [66]; for this reason samples are commonly screened at three different dilutions (10-fold, 100-fold, and 1000-fold). The samples were, in addition, arranged at random in order to prevent result bias associated with the placement and processing of samples. Using this ELISA platform, we were able to detect 13 different antigens in the patient samples (CD14, EGF, EGFR, Eselectin, GDF-15, HBEGF, Her2, ICAM, IL18, MMP1, PDGF-AA, PSA, and RANTES), as the other were below detection limits (Amr, FGFb, HGF, IGF, IL1alpha, MMP2, MMP9, TGFalpha, TGFb, TNFalpha, uPAR, and VEGF).

Table 4.1. Summary of the results detailing the maximal concentration for all antigens.

Antigen	Max. Conc.	Antigen	Max. Conc.
Amr	2000	IL18	1000
CD14	5000	IL1alpha	500
EGF	500	MMP1	5000
EGFR	2500	MMP2	5000
Eselectin	2500	MMP9	2000
FGFb	5000	PDGF-AA	1000
GDF-15	250	PSA	5000
GFP	100	RANTES	500
HBEGF	500	TGFalpha	500
Her2	5000	TGF-b	5000
HGF	1000	TNF-alpha	500
ICAM	10000	uPAR	5000
IGF	2000	VEGF	750

The next major undertaking was proceeding with an 82-sample analysis that expanded on

the previous study. For this analysis, only two different dilutions (10 and 100-fold) of each

serum sample in triplicates were used. The analysis was conducted in 3 replicate batches in

random ordering as before. Each batch was conducted using 17 slides, with 3 standard

curves present for each. The data was calibrated to the GFP spot using ProMAT in an effort

to account for any spot, slide, location, and/or batch variations. All standard curves and

predicted concentrations along with data detailing information for each particular sample

as it relates to each antibody and batch, as well as a comparison for averaged block

intensities for A647 and GFP on uncalibrated data to allow for an analysis on block to block variations were sent to Detroit R&D. In general, results for the analysis demonstrated similar trends, with CD14, EGF, EGFR, GDF-15, ICAM, PDGF-AA, and RANTES displaying best results.

4.4.3. Glycan Prints.

Throughout this time, microarray slides most often with the 10x12 array layout containing the 25 different antibodies in quadruplicate were constantly spotted and shipped to our collaborators for further processing. Once the sample analysis concluded, work focused on the printing of different markers of interest, in particular glycans. Glycan microarray slides with a 6x6 array layout containing all 5 different glycans were spotted at a concentration of 0.5 mg/mL in quadruplicate for each block. In order to proceed with the spotting of the glycans, the poly-l-lysine slides were first activated with the DSS. Although full analysis was not performed on the slides, as they were shipped immediately upon printing to Detroit R&D, the quality of the spotting was confirmed with the scanner using the red reflect setting on the microarray scanner. Another frequent glycan print involved a 12x12 array containing 25 different glycans at a concentration of 0.5 mg/mL and 6 different antibody standards at concentrations of of 1000, 100, 10, 1 ug/mL in 0.5 ug/mL BSA in PBS. The print was conducted in quadruplicate for each block for a total of 16 blocks per slide in DSS activated poly-l-lysine slides. Similarly, larger 38x8 arrays containing 74 different antibodies at two different concentrations (0.5 and 0.05mg/ml) in quadruplicate for each block for a total of 4 blocks per slide were spotted and sent to Detroit R&D for analysis.

5. Identification of Tear Cancer Biomarkers

5.1 Introduction

Clinical applications remain limited by the need for more sensitive and reliable methodologies for detection [140]. Tears fluids offer non-invasive insight into a complex biological environment providing valuable information that might help reveal associations between proteins and disease states. Proteomic technologies have currently identified close to 500 different tear proteins [141] [142]. In this study, we develop a ELISA microarray platform for the identification of tear proteins as potential biomarkers for breast cancer.

5.2 Materials

Poly-L-lysine and ultra clean glass microarray slides were purchased from Thermo Scientific (Pittsburgh, PA). Disuccinimidyl suberate (DSS) was purchased from Pierce (Rockford, IL, USA). Purified antibodies and antigens were purchased from R&D Systems (Minneapolis, MN, USA). Proteins were provided by our collaborators at Ascendant Dx. Blocking solution containing 10 mg/ml casein in phosphate-buffered saline, pH 7.2 (PBS) was purchased from Bio Rad Laboratories (Hercules, CA, USA). Tyramide Signal Amplification (TSA) system, including streptavidin-conjugated horseradish peroxidase, amplification diluent, and biotinyl tyramide, was purchased from Perkin Elmer (Wellesley, MA, USA). Alexa647-conjugated streptavidin was purchased from Invitrogen Life Technologies (Gaithersburg, MD). All other reagents were purchased from VWR (Radnor, PA). All chemicals were used without further modifications unless otherwise specified.

5.3. Methods

5.3.1 Microarray Printing

ELISA microarray spotting was performed at room temperature and 60% relative humidity as previously described [138]. A GeSiM NanoPlotter 2.1 (Quantum Analytics, Foster City, CA, USA) non-contact microarray printer with humidity control was utilized to spot the proteins. In some cases, proteins were covalently boud t the slides with a 0.3 mg/ml solution of the homo-bifunctional cross-linker DSS mathanol for 20 minutes. Prior to spotting, the slides were rinsed in nanopure water and dried in a centrifuge. Capture antibodies were suspended in PBS to a concentration of 0.5-1.0 mg/ml and ~400 picoliters per spot were printed at various different layouts. The antibodies were allowed to dry for an additional hour at 60% relative humidity. The slides were blocked with 10 mg/ml casein in PBS, rinsed in nanopure water and dried in a centrifuge. Upon completion, the slides were either stored under vacuum for future use at -20 $°C$ or shipped to our collaborators.

5.3.2 ELISA Microarray

ELISA Microarray was performed as previously described [138], with all incubation steps performed at room temperature, in a closed humid chamber with gentle mixing on an orbital shaker (Belly Dancer, Stovall Life Science, Greensboro, NC). A two-step wash procedure between processing steps was performed by submerging the slides twice into PBS containing 0.05% Tween-20 (PBS-T). The slides were incubated with different antigen standards in 1 mg/ml casein in PBS overnight. Standard curves were created using a five-fold dilution series of the antigen mix along with an antigen-free blank for 8 total dilutions.

Following a wash cycle, the slides were incubated with biotinylated detection antibody at 25 ng/ml in 1 mg/ml casein in PBS. The signal was amplified using the TSA system following manufacturer instructions, and incubated with 1 μg/ml Alexa647-conjugated streptavidin in PBS-T. Prior to scanning, the slides were rinsed twice in PBS-T and in deionized. A GenePix Autoloader 4200AL (Molecular Devices, CA) laser scanner was used to image the Alexa 647 fluorescence signal on the slides. The spot fluorescence intensity from the scanned slide images was quantified using GenePix Pro 3.0 software. Standard curves were created using ProMAT, a software program specifically developed for the analysis of ELISA microarray data [139].

5.4. ELISA Microarray Platform for the Identification of Cancer Biomarkers in Tear Samples

Tear samples were collected from inside the lower eyelid using Schirmer strips, and subsequently reconstituted in PBS for future use. Reverse-phase high-pressure liquid chromatograph was used to fractionate tear proteins for identification. A linear gradient of 20%-30% solvent B (acetonitrile, 5% water, 0.1% TFA) in A (water, 5% acetonitrile, 0.1% TFA) over the first 10 minutes, followed by 30%-70% solvent B in A gradient over the next 60 minutes, and a 70%-90% solvent B in A gradient over the last 10 minutes was used for a total of 80 minutes [143]. Collected proteins were analyzed via electrospray ionization mass spectrometry (ESI-MS).

Preliminary studies with our collaborators at Ascendant Dx helped identify 7 main tears proteins of interest as potential biomarkers for breast cancer. In order to detect and validate these proteins as potential biomarkers, a sandwich ELISA microarray based

platform was developed. Microarray ELISA allows for the parallel screening of multiple proteins (refer to section 1.2.2 for additional details). However, in multiplexed studies there exists the potential for proteins from different assays to interfere with each other. This can happen via direct interactions between capture and detection antibodies, as well as antibodies nonspecifically binding to another antigen or antigens present. In order to prevent any undesired interactions that might compromise assay specificity and sensitivity, cross-activity studies were first performed on all 7 antibodies. No cross-reactivity was detected by the screenings. Standard curves were developed in order to ensure accurate quantification of tear samples (Figure 5.1.). Of the 7 proteins analyzed, 4 proteins were successfully detected in the human tear samples.
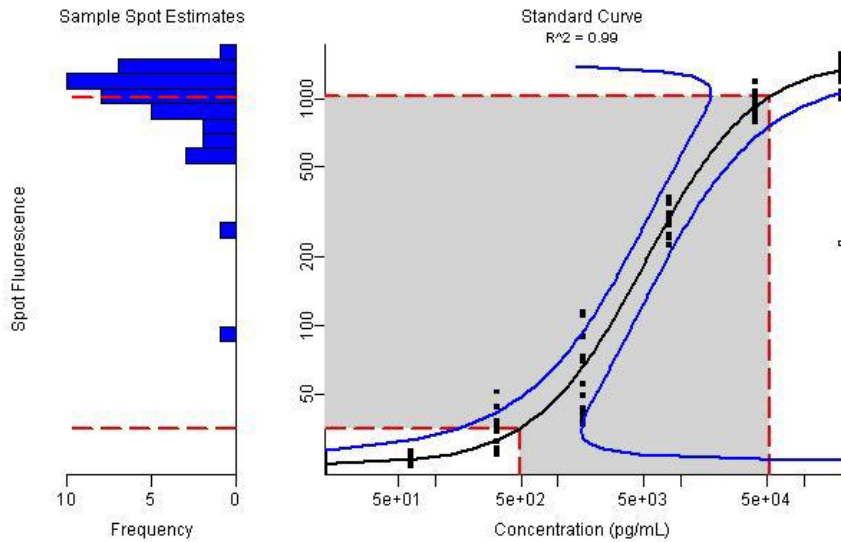

Figure 5.1. Standard curves for representative tear protein assay. Data is representative of the other antibody assays.

6. Biocompatible Interfaces for Neural Differentiation

6.1. Introduction

The use of stem cell regenerative medicine depends on understanding the complex, dynamic interactions that occur in the extracellular matrix (ECM). While differences in the mechanical and chemical interfacial properties of this environment have shown promising effects on diverse cellular functions, the underlying role matrix interfacial properties play on stem cell differentiation is yet to be fully understood. Efforts to mimic the extracellular matrix via surface modifications are an attractive approach to understand the mechanisms by which stem cells respond to inherent interfacial cues that affect cellular behavior. Herein, we report the development of synthetic biocompatible interfaces that allow for the tuning of chemical and mechanical properties of the matrix.

The devastating effects that are commonly associated with traumatic brain injuries and degenerative diseases stem from limited regenerative capabilities of the central nervous system (CNS). Among current tissue engineering strategies, stem cell-based regenerative approaches have demonstrated promising results [144]. Neural stem cells (NSCs) are a self-renewing and multipotent cells that can differentiate into neurons and glia, composed mainly of, astrocytes and oligodendrocytes [145]. The differentiation of NSCs into neurons is crucial for regenerative purposes. Stem cell differentiation is regulated by a combination of complex intrinsic and extrinsic interactions. Intrinsic factors are dependent on cell expression, while extrinsic factors are dependent on environment cues [146]. For this reason, a number of different scaffolds have been studied in an attempt to develop a cellular environment that allows for the selective differentiation of NSCs [147] [148] [149]

[150] [151] [152].

Engineering this artificial extracellular matrices (aECM) allow to elucidate the proud influence a cell's environment has on its progression. These studies, offer valuable mechanistic insights into the complex interactions that occur in the cellular environment. A scaffold's stiffness, for example, elicits different responses. Neural stem cells reach maximal differentiation at a stiffness similar to that of the brain (500 Pascal) [153]. In general, softer substrates tend to preferentially differentiate into neurons, while stiffer substrates tend to preferentially differentiate into glial cells [151]. Studies also demonstrate that topographical cues in the nanometer range elicit different responses, be that in roughness [154] or geometry [155]. Cell behavior can also be influence by the presence of different growth factors [156]. Three-dimensional scaffolds appear to similarly better mimic the physiological environment that two-dimensional variants [157] [158].

6.2. Peptoid Microspheres Interfaces

Initial research was conducted in order to assess the viability of using peptoid based microspheres in the development of an artificial extracellular matrix (aECM) that can be tailored to promote the differentiation of stem cells into neurons. Peptoid microspheres were prepared under sterile conditions. All laboratory equipment and materials were sterilized using a 70% ethanol solution and/or autoclaved. While the microsphere coated slides cannot be sterilized via the same ethanol based sterilization technique as they are formed in a very similar solvents composition, and thus dissolve the peptoid coatings from the surface, different sterilization techniques, such as UV-sterilization and ethylene oxide gas sterilization, have proven to be viable alternatives. Peptoid microspheres were

prepared by dissolving the peptoid in 4:1 (or 80%) ethanol to water solution at a concentration of 3 mg/ml. The addition of 0.01% Tween-20 surfactant onto the peptoid solution improves the overall uniformity of the coatings, allowing for an even distribution of microspheres throughout the entire surface. The peptoid solution was applied to the back (un-etched) face of the coverslips and allowed to dry for 30 minutes in a contained environment under controlled conditions (i.e., 25 °C and 60% humidity). Three different coating densities were prepared by varying the amount of peptoid solution added to each coverslip. This approach has given us in the past control over the coating coverage. A 1X concentration corresponds to 30 uL of the peptoid solution being added onto the surface. A 2X concentration corresponds to a second 30 uL addition of the peptoid solution being added onto the existing 1X microsphere coverage, in essence doubling the concentration. Similarly, a 3X concentration corresponds to a third 30 uL addition of the peptoid solution being added onto the existing 2X microsphere coverage, tripling concentration. The coating morphologies were visually assessed using a 3D Laser Scanning Microscope (Figure 6.1.). SEM images require gold sputtering, and thus, are not a viable imaging technique to assess the morphology of the coatings. The coverslips were prepared for shipped with the help of Josh Goss from Dr. Zou's research group at the University of Arkansas following the exact specification used in the past. In short, the peptoid-coated 12mm cover slips were mounted onto the back of 35mm petri dishes drilled with 9mm holes, sterilized previously via 70% ethanol and plasma treatment, using PDMS. The peptoid cmicropher coated coverslips were sent to Dr. Michael Borrelli's research group for neuronal studies at the University of Arkansas for Medical Sciences as part of the EPSCoR project.
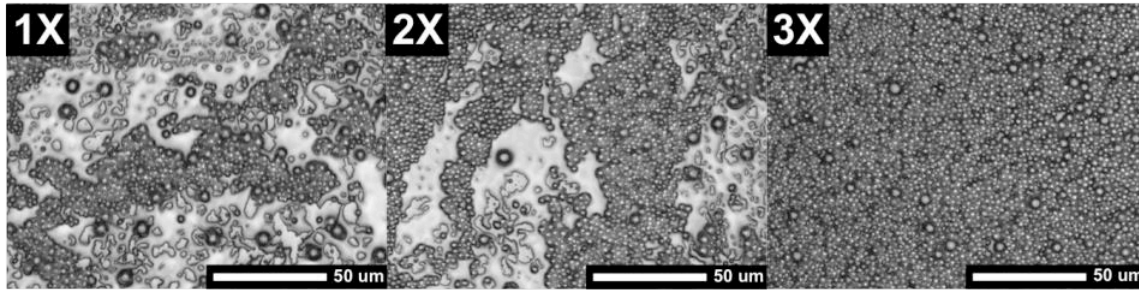
Figure 6.1. 3D laser scanning microscope images of the peptoid-based microsphere coated cover slips for all three concentrations: 1X, 2X, and 3X.

6.3. Nano-Onion Interfaces

In the field of tissue engineering, graphene-based nano-materials, as are nano-onions, have gained interest as biocompatible scaffold due to their unique physical, mechanical, and chemical properties [159]. Carbon nano-onions are multi-shell fullerenes that resemble the structure of onion, hence the origin of their name [160]. Graphene-based nano-materials have been demonstrated to induce stem cell differentiation in neural lineages [161]. They are attractive for neural tissue regeneration because they can incorporate extraordinary topographical, thermal, and electrical properties to scaffolds [162]. They have been demonstrated to be biocompatible and of low cytotoxicity materials [163]. In addition, they can be chemically modified to enable the incorporation of diverse functional features [164].

Nano-onion nano-patterned coverslips were developed in order to asses where their surface incorporation can regulate NSC differentiation. Nano-onion patterned slides were similarly prepared under sterile conditions. Morphology of the patterns was evaluated via SEM. The non-contact nanoplotter was used to spot different patterns across the glass coverslips. The nano-onions dispersions were prepared by dissolving the nano-onions nanoparticles at a 1 mg/mL concentration in a optimized solvent, which consists of a 1%

46

BSA w/w, 0.05% Tween-20 surfactant v/v, and 5% glycerol v/v nano-pure water solution. The nano-onions were initially were thoroughly mixed using a vortexer and then further dispersed using a probe sonicator, and printed immediately using the non-contact nano-plotter Once the printing was complete, the coverslips were allowed to dry at standard conditions (25 C and ~50% humidity) for 24 hours. Results with the optimized conditions considerably improved nano-onion solvent dispersion and deposition uniformity (Figure 6.2.). The addition of glycerol was particularly beneficial when patterning lines over the surface. However, overall spot patterns produced the most uniformly reproducible patterns. In addition, they greatly decrease spotting times considerably. Higher nano-onion concentrations made solvent pick up difficult for the nano-plotter. Based on previous work a higher glycerol content would similarly difficult spotting for the nano-plotter as the solution turns too viscous. The addition of 0.05% Tween-20 surfactant onto the nano-onion solution improves both nano-onion dispersion and the uniformity of the patterns, allowing for an even distribution of nano-onion patterned solutions on the surface. Higher surfactant spread too much and affect reproducibility, in particular when patterning lines instead of spots. Spot patterns with 5 mm margins on 22 x 22 mm on glass coverslips for a patterned coverage of 12 x 12 mm were printed for Dr. Robert Griffin's research group for neuronal studies at the University of Arkansas for Medical Sciences as part of the EPSCoR project.
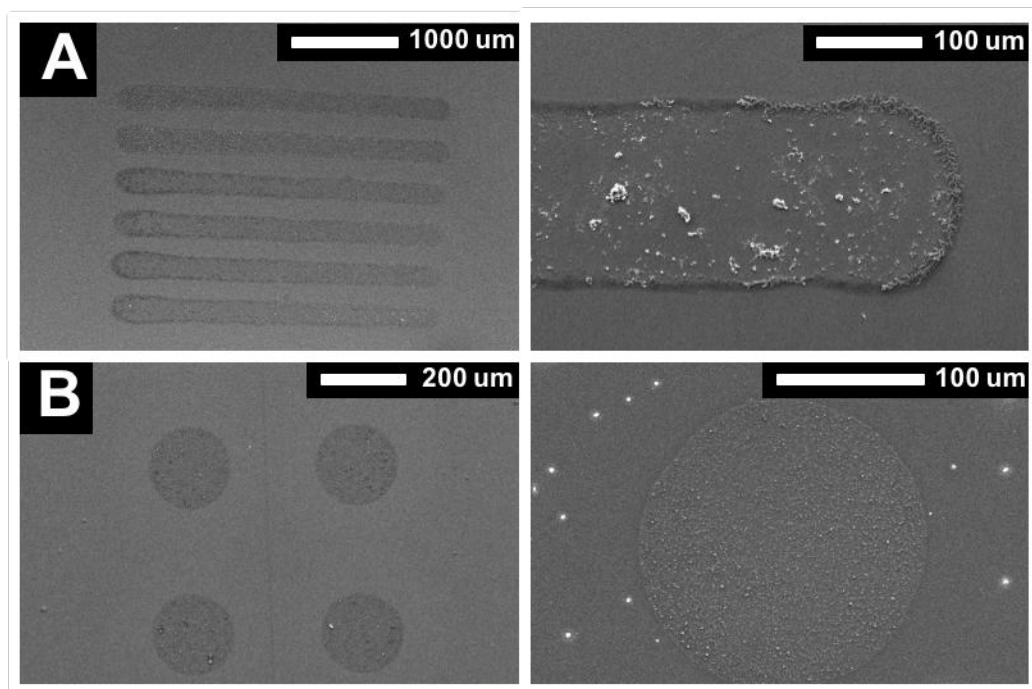
Figure 6.2. SEM images demonstrating the effect of optimized solvent on nano-onion depositions at different magnifications A) line pattern at 1% BSA in water, and B) spot pattern at 1% BSA, 0.05% Tween-20 surfactant in water.

7. Peptoid Microsphere Coatings to Increase the Binding Efficiency in Sandwich ELISA Microarrays

7.1. Introduction

Over the last several decades there has been an enormous effort to develop sensitive, disease-specific assays to assist in therapeutic decisions [1]. Early disease detection decreases economic costs, improves treatment options, and reduces mortality [6]. Biomarker-based technologies, including ELISA microarray and bead-based immunoassay, offer promising platforms for sensitive and specific disease detection [4]. Enzyme-linked immunosorbent assay (ELISA) microarray technology has emerged as a strong platform for the analysis of biomarkers [45] due to its ability to quantify low-abundance proteins in

complex biological fluids over large concentration ranges [65]. The unmatched sensitivity and specificity is associated primarily with the use of matched high-affinity antibody pairs to target a single antigen. The miniature scale of the platform allows for cost-effective and efficient parallel screening of small sample volumes in a high-throughput manner [45].

One of the main challenges in the development of ELISA microarray is the immobilization of antibodies onto a solid support in a manner that maintains their innate binding properties [24]. The surface chemistry of the solid support and the immobilization procedure are crucial for optimal performance of microarray platforms, as is evident by the large number of slide surfaces commercially available [77] [81] [82] [83] [84] [85] [86]. Surfaces for ELISA microarray need to provide strong attachment of the immobilized antibodies while retaining binding activity, high binding capacities, high signal-to-noise ratios, and high reproducibility across all blocks, slides, and experiments. Additionally, the high-throughput nature of the platform requires supports to be robust and retain high levels of specificity and sensitivity through rigorous processing conditions and prolonged storage periods.

Although there are a number of immobilization strategies and solid supports available, microarray surfaces can be broadly categorized as (1) two-dimensional surfaces and (2) three-dimensional surfaces. While two-dimensional surfaces allow for the direct attachment of proteins to the surface (aldehyde [89] [92], aminosilane [77] [93] [94], epoxysilane [93] [94], mercaptosilane [94], polystyrene [77], and poly-L-lysine coated slides [65]), three-dimensional surfaces retain proteins within a matrix (polyacrylamide [89] [95], agarose [90] and nitrocellulose gels [96] [97] [98] [99] [100] [101], as well as

poly(vinylidene fluoride) (PVDF) membranes [102] [103]). In addition, there exist more specialized chemistries that are more difficult to categorize as they combine characteristics of the two; while they do not provide a three-dimensional structure within which proteins are retained, they incorporate some supramolecular assemblies [24]. Some examples include avidin [105], streptavidin [84], nickel [92], dendrimer [106] [107], or polyethylene glycol (PEG) slides [108]. These surfaces immobilize proteins through the covalent attachment of epoxy or specialized affinity groups.

Numerous variables affect antibody microarrays including surface modifications, cross-linking strategies, spotting buffer compositions, blocking reagents, antibody concentrations, and storage conditions [94] [77] [165] [166] [78]. Among two-dimensional surfaces, poly-L-lysine and cross-linked silane slides perform best, displaying good sensitivity and signal-to-noise ratios [94]. Nitrocellulose surfaces, on the other hand, exhibited low signal-to-noise ratios with high signal intensities as well as high background signals [94]. Similar studies, comparing limits of detection, coefficients of variation, and storage characteristics for different commercially available slide chemistries determined that in terms of overall array performance poly-L-lysine and aldehyde slides displayed the best signal uniformity and signal-to-noise ratios [77]. Aldehyde silane, poly-L-lysine, or aminosilane slides were also observed to produce superior result in an independent study [83] . A comprehensive study evaluating 17 commercially available microarray surfaces proposes a rigorous and quantitative system for comparing different surfaces based on spot morphology, background noise, limit of detection, and reproducibility with 23 antibody assays [78].

Microarray surfaces need to provide high surface areas for binding that enable high signal-to-noise ratio and flexible immobilization chemistries. Oligomeric *N*-substituted glycines (peptoids) are promising as biosensor interfaces due to their low immunogenicity, ease of synthesis, highly customizable side chain chemistries, and the ability to form supramolecular structures that can increase surface area [109]. Peptoids are bioinspired, peptidomimetic polymers with a backbone structure closely resembling that of peptides, but with the side chains appended to the amide groups rather than the α-carbons. This structural modification prevents proteolytic degradation, making peptoids attractive as biocompatible materials. However, this modification also removes the presence of backbone amide hydrogens, which are critical for the formation of the hydrogen bond linkages that stabilize beta sheets and helices in peptides. Despite these limitations, secondary structures including turns, loops, and helices, as well as supramolecular assemblies such as superhelices [167], nanosheets [168], nanotubes [169] and microspheres [125] can be induced in peptoids upon the addition of specific side chains. Peptoid helices have been demonstrated to form polyproline type-I-like helices, similar to those of proteins, with a periodicity of three monomers per turn and pitch of approximately 6 Å with as few as five monomer units [120].

In this study, we report the development of peptoid microsphere-coated glass substrates for use in sandwich ELISA microarray. The morphology and uniformity of the coatings was evaluated by SEM and the coating efficacy was analyzed by ELISA microarray with known antibody assays. The peptoid microsphere-coated surfaces were found to exhibit higher signal intensity and dynamic range as compared to commercially available microarray surfaces.

7.2. Materials and Methods

7.2.1. Materials

4-methoxybenzylamine and (S)-methylbenzylamine were purchased from Acros Organics (Pittsburgh, PA). *tert*-butyl N-(4-aminobutyl)carbamate was purchased from CNH Technologies Inc. (Woburn, MA). MBHA rink amide resin was purchased from NovaBiochem (Gibbstown, NJ). Piperidine was purchased from Sigma-Aldrich (St. Louis, MO). Test grade silicon wafers were purchased from University Wafer (South Boston, MA). Poly-L-lysine and ultra clean glass microarray slides were purchased from Thermo Scientific (Pittsburgh, PA). Disuccinimidyl suberate (DSS) and bis[sulfosuccinimidyl] suberate (BS^3) were purchased from Pierce (Rockford, IL, USA). Purified antibodies and antigens were purchased from R&D Systems (Minneapolis, MN, USA). Blocking solution containing 10 mg/ml casein in phosphate-buffered saline, pH 7.2 (PBS) was purchased from Bio Rad Laboratories (Hercules, CA, USA). Tyramide Signal Amplification (TSA) system, including streptavidin-conjugated horseradish peroxidase, amplification diluent, and biotinyl tyramide, was purchased from Perkin Elmer (Wellesley, MA, USA). Alexa647-conjugated streptavidin was purchased from Invitrogen Life Technologies (Gaithersburg, MD). All other reagents were purchased from VWR (Radnor, PA). All chemicals were used without further modifications unless otherwise specified.

7.2.2. Peptoid Synthesis

Peptoids were synthesized via the submonomer solid-phase method on rink amide resin, as previously described [170]. Briefly, the resin was swelled with dimethylformamide (DMF)

52

and the Fmoc protecting group on the resin was removed using a 20% solution of piperidine in DMF. The resin-bound secondary amine was acylated with 0.4 M bromoacetic acid (BAA) in DMF in the presence of N,N'-diisopropyl carbodiimide (DIC). Amine submonomers were incorporated via an S_N2 nucleophilic substitution reaction with primary amine in DMF. The two-step bromoacetylation and nucleophilic substitution cycle was repeated until all desired side chains were incorporated. The peptoid was cleaved from the resin using a mixture of 95% trifluoroacetic acid (TFA), 2.5% water, and 2.5% triisopropylsilane and the acid was removed using a Heidolph Laborota 4001 rotating evaporator (Elk Grove Village, IL). The peptoid was lyophilized to a powder using a Labconco lyophilizer (Kansas City, MO) and diluted to a concentration of ~3 mg/ml in a 50:50 acetonitrile-water solution.

7.2.3. Peptoid Purification

Peptoids were purified using a Waters Delta 600 preparative high-performance liquid chromatography (HPLC) instrument (Milford, MA) with a Duragel G C18 150 × 20 mm column (Peeke Scientific, Novato, CA) and a linear gradient of 35-95% solvent B (acetonitrile, 5% water, 0.1% TFA) in A (water, 5% acetonitrile, 0.1% TFA), over 60 minutes. Peptoids were confirmed to be >98% pure via analytical HPLC (Waters Alliance, Milford, MA) with a Duragel G C18 150 × 2.1 mm column (Peeke Scientific) using a linear gradient of 35 to 95% solvent D (acetonitrile, 0.1% TFA) in C (water, 0.1% TFA), over 30 minutes. Purified peptoid fractions were lyophilized and stored as a powder at -20 °C.

7.2.4. Peptoid Characterization

Synthesis of the desired peptoid sequence was confirmed via matrix assisted laser desorption/ionization time of flight (MALDI-TOF; Bruker, Billerica, MA) mass spectrometry. Secondary structure was confirmed via CD spectrometry using a Jasco J-715 instrument (Easton, MD) at room temperature with a scanning speed of 20 nm/min and a path length of 0.1 mm. The peptoid was dissolved in methanol at a concentration of 120 μM because protic solvents have been demonstrated to help induce helical secondary structure in peptoids. Each spectrum was the average of twenty accumulations.

7.2.5. Peptoid Microsphere Coatings

Peptoid microspheres were prepared by dissolving the peptoid in a 4:1 (v/v) ethanol/water solution at a concentration of 5 mg/ml, as previously described [125]. Glass slides (Erie Scientific, Portsmouth, NH) were outlined with an 8 x 2 array pattern using a Barnstead Thermolyne microarray slide imprinter (Dubuque, IA) to create a hydrophobic barrier for processing 16 wells per slide. The peptoid solution was applied to the glass surfaces and allowed to dry at room temperature and 60% relative humidity. Coating morphologies were visually assessed using a Phillips XL-30 scanning electron microscope (SEM) (FEI, Hillsboro, OR).

7.2.6. Microarray Printing

ELISA microarray printing was performed at room temperature and 60% relative humidity as previously described [138]. A GeSiM NanoPlotter 2.1 (Quantum Analytics, Foster City, CA, USA) non-contact microarray printer with humidity control was used to spot the

antibodies. Prior to spotting, the microsphere coated surfaces, and in some cases the poly-L-lyisne slides, were treated with a 0.3 mg/ml solution of the homo-bifunctional cross-linker BS³ in PBS for 20 minutes to create a reactive site for covalent attachment via the amine groups. After incubation, the slides were rinsed in nanopure water and dried in a centrifuge. Capture antibodies were suspended in PBS to a concentration of 0.8 mg/ml and ~400 picoliters per spot were printed 500 um apart in quintuplicate on each array. Upon completion, the antibodies were allowed to dry for an additional hour at 60% relative humidity. The slides were blocked with 10 mg/ml casein in PBS and processed immediately.

7.2.7. ELISA Microarray

ELISA Microarray was performed as previously described [138], with all incubation steps performed in a closed humid chamber with gentle mixing on an orbital shaker (Belly Dancer, Stovall Life Science, Greensboro, NC), in the dark, at room temperature. A two-step wash procedure between processing steps was performed by submerging the slides twice into PBS containing 0.05% Tween-20 (PBS-T). The slides were incubated with a mixture of antigen standards in 1 mg/ml casein in PBS overnight. Standard curves were created using a three-fold dilution series of the antigen mix along with an antigen-free blank for twelve total dilutions. Following a wash cycle, the slides were incubated with biotinylated detection antibody at 25 ng/ml in 1 mg/ml casein in PBS. The signal was amplified using the TSA system following manufacturer instructions, and incubated with 1 μg/ml Alexa647-conjugated streptavidin in PBS-T. Lastly, the slides were rinsed twice in PBS-T and lastly in deionized prior to scanning.

A GenePix Autoloader 4200AL (Molecular Devices, CA) laser scanner was used to image the Alexa 647 fluorescence signal on the slides. The spot fluorescence intensity from the scanned slide images was quantified using GenePix Pro 3.0 software. Standard curves were created using ProMAT, a software program specifically developed for the analysis of ELISA microarray data based on a four-parameter logistic curves model [139]. The values for the lower limits of detection are calculated as the mean concentration plus three standard deviations of the log-transformed spot intensity for the antigen-free blank. In order to provide a value that is representative of all assays for comparisons, a relative limit of detection value was calculated using the median value for all assay replicates on each surface. Results shown, unless noted otherwise, encompass three replicate experiments performed using slides that were coated, printed, and processed on independent occasions. Statistical significance was assessed using a t-test with a 95% confidence intervals where probabilities of $p < 0.05$ were considered statistically significant.

7.3. Results and Discussion

7.3.1. Peptoid Sequence Rationale

Our lab has previously shown that partially water-soluble, helical peptoids self-assemble into microspheres [125]. The peptoid sequence, referred to as P3 (Figure 7.1.), includes chiral, aromatic side chains on two faces of the helix to induce the formation of helical secondary structure [131]. The third face of the helix, which offers considerable flexibility of design, contains methoxy and amine groups to increase water solubility. The amine groups also enables covalent linkage to and electrostatic interactions with the slide surface. The secondary structure of P3 was determined by circular dichroism, which confirms poly-

proline type-I-like secondary structure (Figure S7.1. in Supplemental Information) [121].
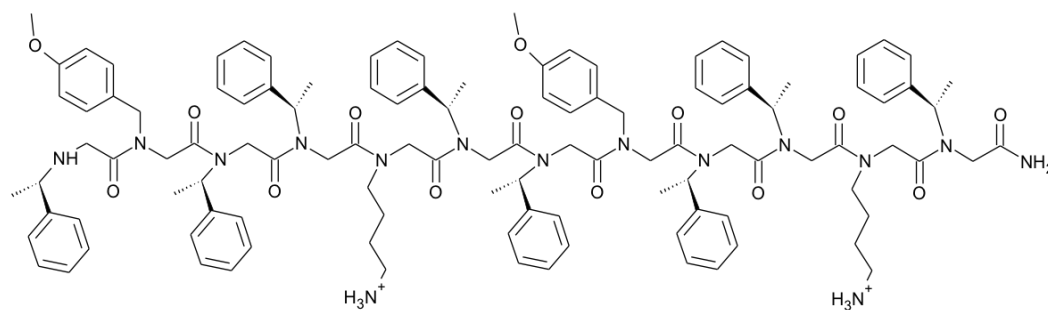

Figure 7.1. Peptoid structure for the P3 sequence.

7.3.2. Coating Characterization

The formation of uniform peptoid microsphere coatings is essential to reduce variability in ELISA microarray assays. Coating morphology is directly linked to evaporation rate, requiring careful monitoring of drying conditions to ensure uniform sphere distribution and reproducible coatings. One issue observed in the formation of peptoid coatings is perimetral intensive deposition, often referred to as the "coffee ring effect", in which denser coverage is observed at the perimeter of the coatings as compared to the center. Previous studies have shown that this effect is reduced when samples are evaporated at a constant contact area, which can be achieved by including surfactant in the microsphere solution [171]. The addition of Tween-20 to the peptoid microsphere solution results in improved coating uniformity, lessening perimetral microsphere deposition and allowing for an even distribution of microspheres on the surface (Figure 7.2.). At concentrations >0.1%, Tween-20 disrupts microspheres formation and alters microspheres size distribution (Figure S7.2. in Supplemental Information).

Microarray results of the microsphere coated slides demonstrated very faint fluorescent signals, indicative of a weak surface attachment of the antibodies. To enhance immobilization, the peptoid microsphere coated surfaces were covalently attached. BS[3] treatment greatly reduced the antibody loss at the surface due to the wash steps necessary for processing the slides. Consistent with findings elsewhere [78], studies for all assays on poly-L-lysine surfaces demonstrate no significant difference when assessing antibodies immobilized on non-covalent surfaces as compared to those attached covalently (Figure S7.3. in Supplemental Information). This supports the notion that the increase in intensities

associated to the microsphere coatings occurs as a result of the increase in surface area available for binding. It is also important to note that although higher backgrounds are observed with the coatings, such background fluorescence was observed independent of covalent treatment.
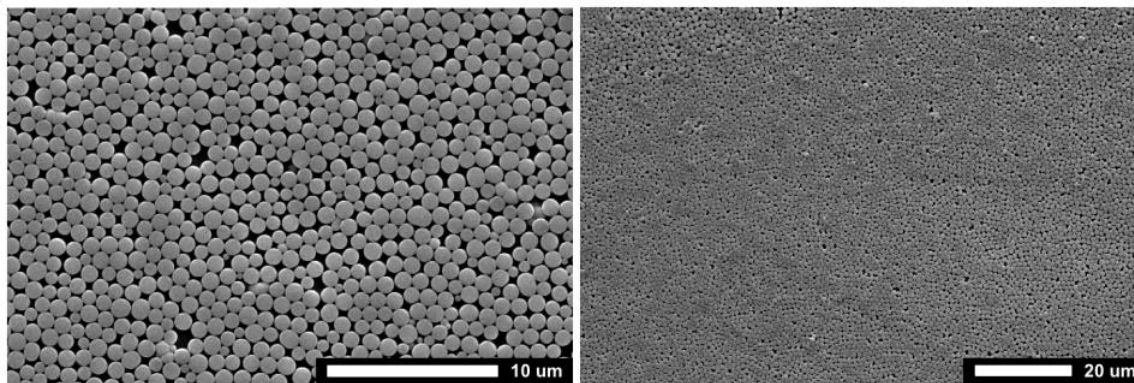

Figure 7.2. Peptoid microsphere coated glass surfaces. Peptoids were dissolved in a 4:1 (v/v) ethanol/water solution at a concentration of 5 mg/ml. The peptoid solution was applied to the glass surfaces and allowed to dry at room temperature and 60% relative humidity.

7.3.3. Coating Efficacy for ELISA Microarray

The efficacy of the peptoid microsphere coatings was evaluated by ELISA microarray with four antibody assays, previously shown to have good assay sensitivity and specificity and low cross-reactivity in multiplexed ELISA microarray (Table 1) [117]. The performance of the surfaces was evaluated based on spot morphology, signal to noise ratio, limit of detection, and concentration dynamic range. Signal intensities were evaluated by comparing single concentration assays on peptoid-based microsphere coated blocks with 'uncoated' poly-L-lysine surfaces. Single point antigen concentrations correspond to the third dilution of the three-fold standard curve dilution series (i.e. approximately 11% of the maximal concentration), previously shown to provide a strong signal intensity near

saturation and in the upper usable range of the standard curve [66].

Spot morphology is dependent on the characteristics of the surface. The increased topographical complexity of three-dimensional surfaces presents its challenges. Although the spot morphology on peptoid microspheres is not as crisp as those on the two-dimensional poly-L-lysine surfaces, they are greatly improved over other three-dimensional surfaces [78]. As is the case with other three-dimensional slide surfaces, the peptoid microsphere coated surface exhibits higher backgrounds of fluorescence as compared to the two-dimensional surface (Figure 7.3.B). Despite the increased background signal, the signal-to-noise ratio for the peptoid microsphere coating is the same as or higher than the poly-L-lysine coating.

Table 7.1. Summary of the results detailing the maximal concentration of antigens, lower, upper bound, dynamic range concentrations, and single point signal intensities (11% of the maximal concentration) for the 'uncoated' poly-L-lysine surfaces and peptoid-based microsphere coated surfaces antigens for all 5 different assays: CD14 (cluster of differentiation 14), GFP (green fluorescent protein), HGF (hepatocyte growth factor), and RANTES (regulated on activation normal T cell expressed and secreted). Statistical significance was assessed using a t-test with a 95% confidence intervals where $*p<0.05$, $**p<0.01$, and $***p<0.001$ for assays on uncoated vs. coated surfaces.

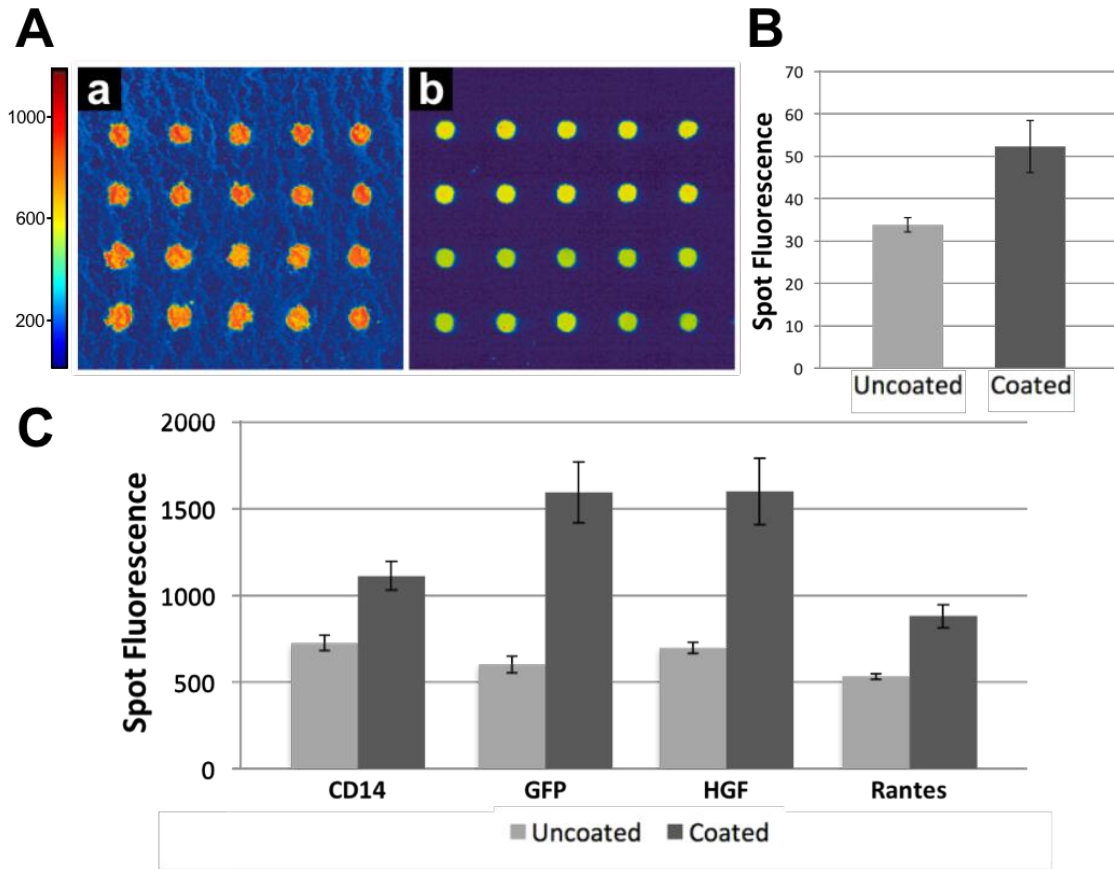| Assay	Max Conc.	Limit of Detection		Dynamic Range		Signal/Noise Ratio	
		Uncoated	Coated	Uncoated	Coated	Uncoated	Coated
CD14 **	2500	1.9	2.0	527.8	530.2	21.4	21.3
GFP ***	500	0.2	0.7	80.0	97.0	17.8	30.5
HGF ***	1000	0.3	2.7	135.3	492.8	20.7	30.6
RANTES ***	500	0.4	0.3	64.6	264.2	15.8	16.8

Figure 7.3. A) Images of fluorescence for GFP and HGF with BS^3 treatment on a) peptoid microsphere coated glass surfaces, b) uncoated poly-L-lysine surfaces. B) Comparison of background fluorescence for the peptoid microsphere coated glass surfaces and 'uncoated' poly-L-lysine surfaces. Columns and cross-bars represent the means and standard deviations, respectively, of the median spot backgrounds on 'uncoated' poly-L-lysine slides and 'coated' peptoid microsphere surfaces across three replicate experiments. C) Comparison of single point signal intensities (11% of the maximal concentration) for all antibody assays (CD14, GFP, HGF, and RANTES) on peptoid microsphere coated glass surfaces with BS^3 treatment and uncoated poly-L-lysine surfaces. Columns and cross-bars represent the means and standard deviations, respectively, of the signal intensities on 'uncoated' poly-L-lysine slides and 'coated' peptoid microsphere surfaces printed and processed at the same time, and representative of additional replicate studies.

The performance of the peptoid microsphere coatings was compared to commercial poly-L-lysine surfaces, which are widely used for antibody assays [126] and provide a similar chemistry for antibody attachment as the peptoid microsphere coatings. As compared to poly-L-lysine slides, peptoid microsphere coated surfaces consistently displayed stronger

signal intensities, averaging a two-fold increase, under identical processing conditions (Figure 7.3.C and Table 7.1.). This observation is clear for all assays and consistent whether the comparisons are based on a single concentration point (Figure 7.3.C) or over the full standard curve (Figure 7.4.).
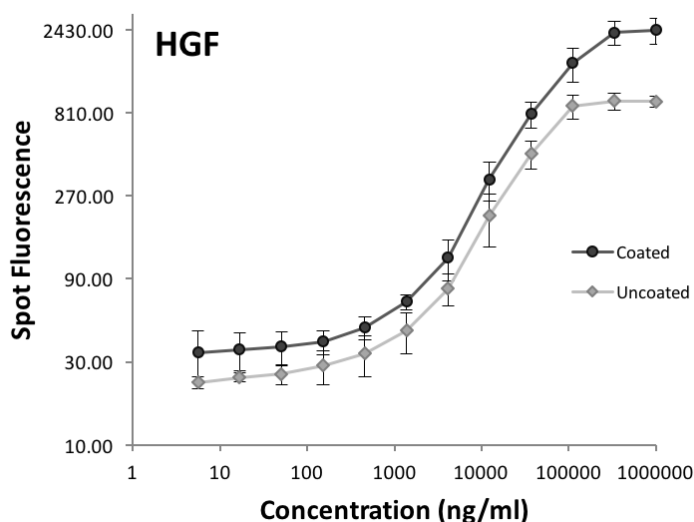

Figure 7.4. Standard curves for HGF on 'uncoated' poly-L-lysine slides and 'coated' peptoid microsphere surfaces on a log 10 vs log 3 plot. Results are representative of the trends observed across all antibody assays (see Figure S7.4. in Supplemental Information). Data points and cross-bars represent the means and standard deviations, respectively. The standard curves encompass data from all three replicate experiments performed using slides that were coated, printed, and processed on independent occasions.

The limit of detection is a direct assessment of assay sensitivity, in other words the lowest concentration that can be reliably detected. Evaluation of surface performance is based on previously published methods, where relative limit of detection below 2 is 'superior', between 2 and 4 is 'normal, and above 4 is 'poor' [78]. Despite the larger standard deviations at low antigen concentration for the peptoid microsphere coatings they are rated in the superior category with a score of 0.9 ± 0.5 as compared to a score of 0.8 ± 0.3

for poly-L-lysine slides in our study. These values are comparable to published values for commercially available slides including poly-L-lysine (0.7 ± 0.1), aminosilane (1.3 ± 0.6), aldehyde silane (1.1 ± 0.4), epoxysilane (1.2 ± 0.6), Slide E (0.8 ± 0.4), and Full Moon (1 ± 0.7) [78].

As hypothesized, the peptoid microsphere coatings have increased dynamic range as compared to poly-L-lysine slides (Table 1). ProMAT outlines the useful range of the standard curves by defining the lower limits of detection and upper concentration bound. As the standard curve for HGF in Figure 7.4. demonstrates, and Table 1 details for all assays, there exists an increase in the concentration dynamic ranges observed for the peptoid microsphere coated surfaces as compared to 'uncoated' poly-L-lysine surfaces. Though the extent of the increase varies (2.4 for CD14, 17 for GFP, 357.5 for HGF, and 199.6 pg/ml for RANTES), this increase is consistently observed for most assays.

Although the performances of the assays are directly associated to the characteristics of the surfaces, it is important to recognize the importance of the protocols by which the assays are spotted, blocked, and processed for fluorescent scanning. It is quite possible that the performance of the microsphere coated surfaces hold ample room for improvement. For instance, adjustments to the spotting protocols, in particular the spotting buffer, offer significant potential. Many of the more complex three-dimensional surfaces often require specialized spotting buffers. We found that the addition of 5% glycerol (Figure S7.5. in Supplementary Information) can improve spot morphology, one of the main detriments the microsphere coatings suffer. Increases in the density of spotting buffers limits spot spreading, decreasing spot diameters, and thus improving the overall spot morphology.

While more densely printed arrays yield high signal intensities, they also complicate surface evaluations as it inserts an additional variable to the comparisons. Results on these coatings are promising because they validate peptoid coatings as viable material for biosensor applications, as well as demonstrate an increase in the dynamic range associated to the increased binding affinity these surfaces offer.

7.4. Conclusion

High-throughput demands in protein detection (including ELISA microarray and biosensors) require the selection and development of optimized support surfaces that allow for more generally applicable and direct immobilization procedures. While high binding affinities are imperative to prevent antibody loss and ensure robust attachment, the challenge lies in designing a microarray support that accommodates proteins of varying characteristics and provides a non-denaturing environment to preserve the active form of the protein. We have evaluated the use of peptoid microsphere coatings as a novel surface for the improvement of sandwich ELISA microarrays. This peptoid-based, three-dimensional coating offers a customizable, water insoluble, biocompatible interface that increases the surface area available for protein binding. The efficacy of the coating was assessed in terms of its overall array performance as compared to commercially available poly-L-lysine coated surfaces [81] [94]. The coatings allowed for strong covalent antibody attachment and performed well in terms of limits of detection. The increase in surface area enables higher protein binding capacities as compared to two-dimensional poly-L-lysine surfaces. Although the peptoid microsphere coatings displayed higher background fluorescence and coefficients of variation, higher signal-to-noise ratios were observed

compared to poly-L-lysine surfaces.

The peptoid microsphere coatings provide an exciting new interface for a wide range of biosensor applications. Results suggest that existing biosensor protocols and procedures (printing, blocking, processing, and storage) can be readily applied to peptoid microsphere coatings and that the coatings outperform state-of-the art surfaces such as poly-L-lysine. The robust peptoid microsphere coated surface provides a versatile platform that can be easily customizable. It offers the benefits that come with an increased surface area for binding, while at the same time allow for use of familiar chemistries that are established for both protein microarray and biosensor applications.
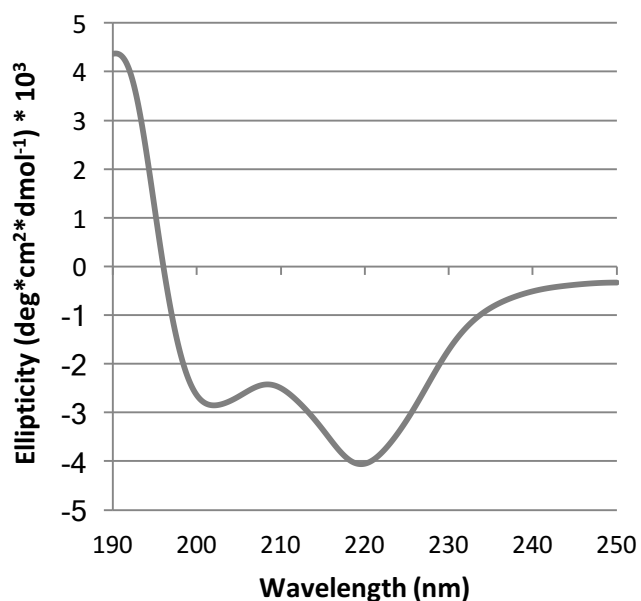
7.6. Supplemental Information

Figure S7.1. Circular dichroism spectra of peptoid showing a poly-proline type-1-like helical secondary structure. CD spectra were taken at room temperature with a scanning speed of 20 nm/min and a path length of 0.1 mm. The peptoid was dissolved in methanol at a concentration of 120 µM.
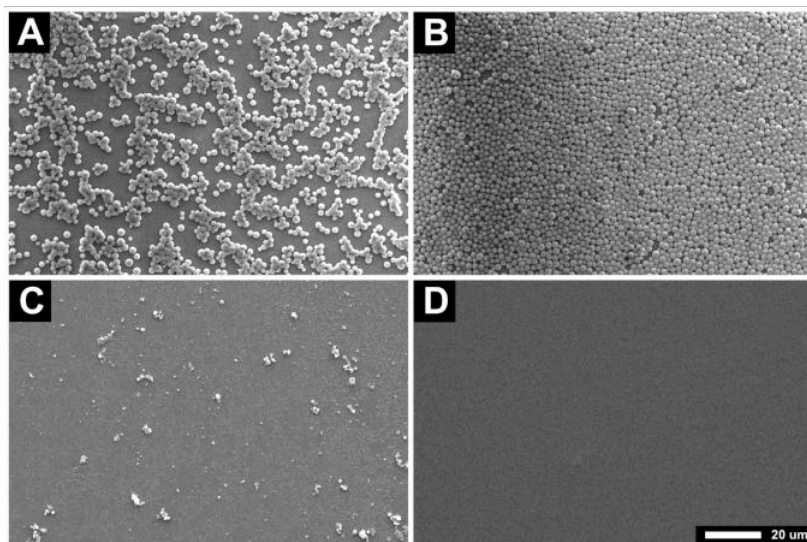

Figure S7.2. Effects of Tween-20 on microsphere coatings: A) 0.001%, B) 0.01%, C) 0.1%, and D) 1% by volume.
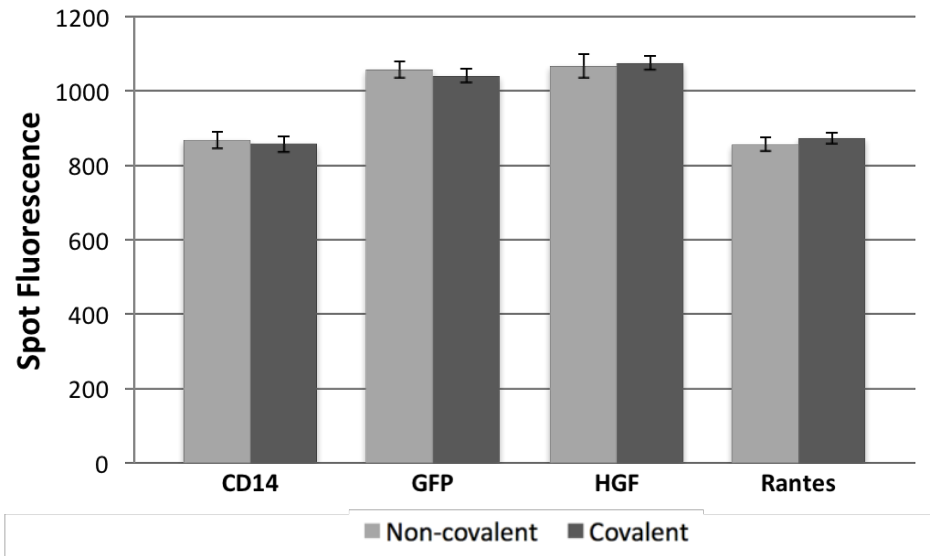
Figure S7.3. Comparison of signal intensities across all antibody assays (CD14, GFP, HGF, ICAM, and Rantes) on uncoated poly-L-lysine surfaces based on non-covalent attachments and covalent attachments via BS^3 treatment.

Figure S7.4. Standard curves for all antibody assays on 'uncoated' poly-L-lysine slides and the peptoid-based microspheres coated glass surfaces on a log 10 vs log 3 plot.

Figure S7.5. Improvement on spot morphology upon the addition of 5% glycerol (bottom) to the GFP 1mg/ml casein in PBS spotting buffer.

8. Peptoid Microsphere Coatings: The Effects of Helicity, pH, and Ionic Strength

8.1. Introduction

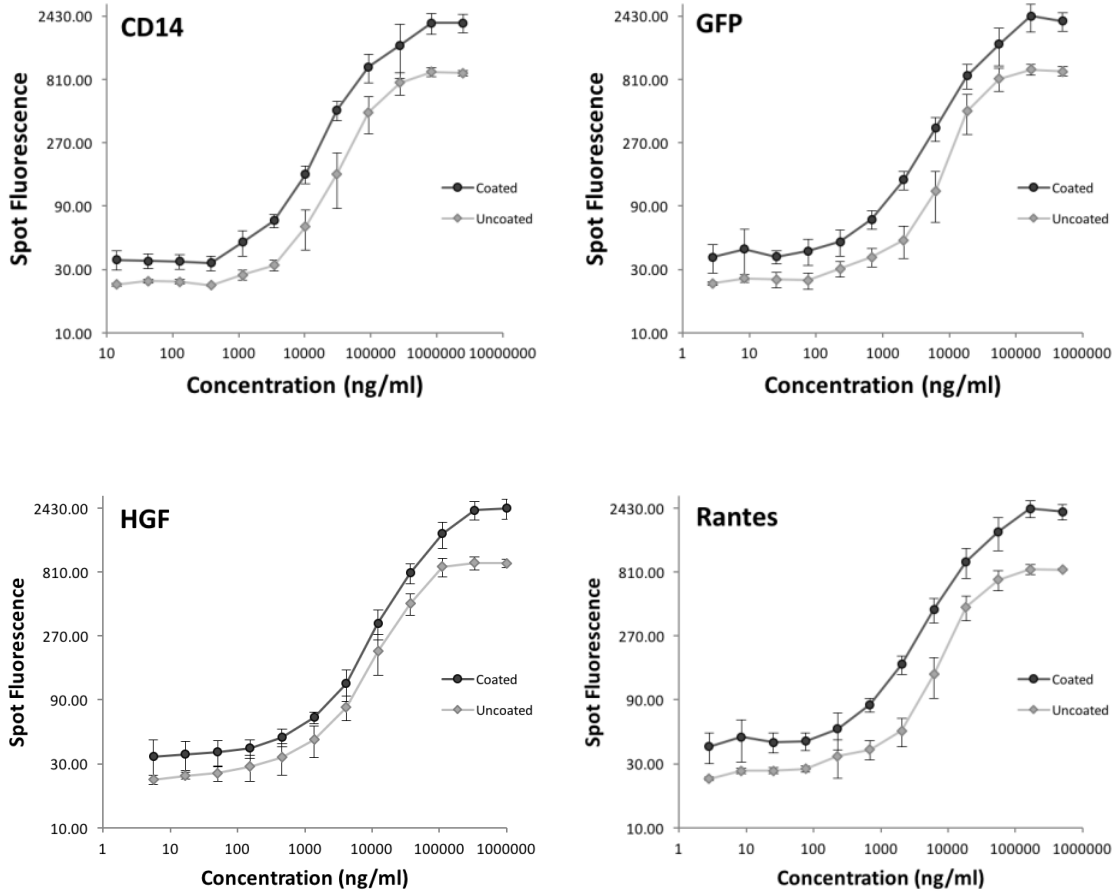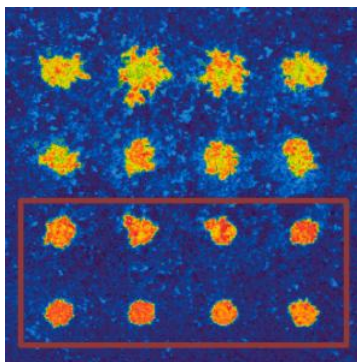Natural polymers have inspired the development of synthetic materials that mimic the fundamental molecular features that allow for the diverse array of functions found in nature [109]. Proteins have a myriad of unique functional properties, providing for example, binding and catalytic sites that together enable molecular recognition. However, as biomaterials peptides present a major drawback due to proteolytic degradation and as a result are limited in their potential for biomedical and therapeutic applications [110]. Efforts to overcome these limitations have led to the design and development of innovative peptidomimetic oligomers [111] [112] [113] [114] [115] [116]. These synthetic polymer analogs predominately exploit structural similarities in order to allow for the mimicry of bioactive functionalities. Bioactive roles however, are often determined by the unique ability of peptides to self-assemble into complex, sequence-specific three-dimensional secondary structures [117]. Specific peptidomimetic oligomers, commonly referred to as foldamers [118], display well-defined secondary structures, are therefore of great interest for use in biomaterials.

Peptoids are a form of bio-mimetic synthetic polymers that closely resemble peptides, but have the side chains attached to the backbone amide nitrogen rather than to the α-carbon as in peptides. Like peptides, peptoids can be constructed via solid-phase synthesis [122] following a submonomer method that provides a robust and highly efficient platform for synthesis, enabling precise sequence control. Synthesis follows a carboxy to amino direction, in which each monomer cycle includes (1) acylation and (2) nucleophilic

substitution [121]. Functional moieties are introduced by the incorporation of commercially available primary amines, enabling access to more than 300 side chain chemistries [109]. Monomer coupling efficiencies of >98% [123] allow for the precise sequence-specific synthesis of polymer chains surpassing over 300 monomeric subunits in length [124].

The seemingly minor modification to the backbone has important implications to peptoid structure and Function. Peptoids are not susceptible to proteolytic degradation, making them a promising alternative to peptides for therapeutic applications where proteolysis is of major concern. However, the backbone modification also prevents backbone hydrogen bonding, which, although critical for the formation of secondary structure in peptides can be overcome by including specific side chains to form secondary structures such as turns [172] [173], loops [174], and helices [175] [123] [120] [132] [133] that in turn allow for the formation of supramolecular assemblies [167] [149] [176] [127] [168] [125]. Stable helices can be formed by peptoids as short as five monomer units with circular dichroism (CD) spectra that strongly resemble those of protein α-helices [117]. NMR studies show that peptoids have a helical structure similar to polyproline type-I helices in proteins, with a periodicity of three residues per turn and a pitch of ~6 Å [120].

Past work in the Servoss lab has focused on the effect of various parameters on the self-assembly of peptoids into microspheres including water solubility, helical content, charge placement, and side chain bulk [125]. It was demonstrated that helicity and partial water solubility are crucial for microsphere formation. Furthermore, peptoid sequences with alternating opposite charges on one face of the helix produce smaller microspheres (~0.3

μm) as compared to those with only positive charges (~1.5 μm). It is believed that the opposite charges interact to form tighter helices, which result in the smaller supramolecular assemblies observed [125]. The microspheres formed are orders of magnitude larger than a single peptoid helix (~24 Å), supporting the theory that larger peptoid groupings are formed by stacking of the chiral aromatic groups [125]. Aromatic stacking has been observed in similar types of supramolecular assemblies in both peptides and peptoids [126] [127] [128] [129] [130]. Further work investigated the factors that affect the reproducible formation microsphere coatings including solvent effects, administration technique, and drying conditions [131].

The present study reports the effect of peptoid chain length (and in turn helicity) as well as pH and ionic strength on the formation and robustness of peptoid microsphere coatings. The morphology of the microsphere coatings was analyzed via SEM. The studies show that variations in chain length lead to changes in microsphere size and size distribution. The morphology of microsphere coatings deteriorated at low ionic strengths and pH, however they are extremely robust at physiological conditions.

8.2. Materials and Methods

8.2.1. Materials

(S)-methylbenzylamine and 4-methoxybenzylamine were purchased from Acros Organics (Pittsburgh, PA). *tert*-butyl N-(4-aminobutyl)carbamate was purchased from CNH Technologies Inc. (Woburn, MA). MBHA rink amide resin was purchased from NovaBiochem (Gibbstown, NJ). Piperidine was purchased from Sigma-Aldrich (St. Louis,

MO). Test grade silicon wafers were purchased from University Wafer (South Boston, MA). Poly-L-lysine, amino silane, and ultra clean glass microarray slides were purchased from Thermo Scientific (Pittsburgh, PA). Disuccinimidyl suberate (DSS) was purchased from Pierce (Rockford, IL, USA). All other reagents were purchased from VWR (Radnor, PA). All chemicals were used without further modifications unless otherwise specified.

8.2.2. Peptoid Synthesis

Peptoids were synthesized via the submonomer solid-phase method on rink amide resin [122]. The resin was initially swelled with dimethylformamide (DMF), and the Fmoc protecting group on the resin was removed using a 20% solution of piperidine in DMF. The resin-bound secondary amine was acylated with 0.4 M bromoacetic acid (BAA) in DMF, in the presence of N,N'-diisopropyl carbodiimide (DIC), mixing for 1 minute. Amine sub-monomers were incorporated via an S_N2 nucleophilic substitution reaction with 0.5M primary amine in DMF, mixing for 2 minutes. The two-step bromoacetylation and nucleophilic substitution cycle were repeated until all desired side chains have been incorporated. The peptoid was cleaved from the resin using a mixture of 95% trifluoroacetic acid (TFA), 2.5% water, and 2.5% triisopropylsilane. The acid was removed using a Heidolph Laborota 4001 rotating evaporator (Elk Grove Village, IL). The peptoid solution was lyophilized to a powder using a Labconco lyophilizer (Kansas City, MO). The peptoid powder was diluted to a concentration of ~3 mg/ml in a 50:50 acetonitrile-water solution.

8.2.3. Purification

Peptoids were purified using a Waters Delta 600 preparative high-performance liquid chromatography (HPLC) instrument (Milford, MA) with a Duragel G C18 150 × 20 mm column (Peeke Scientific, Novato, CA) and a linear gradient of 35-95% solvent B (acetonitrile, 5% water, 0.1% TFA) in A (water, 5% acetonitrile, 0.1% TFA), over 60 minutes. Peptoids were confirmed to be >98% pure via analytical HPLC (Waters Alliance, Milford, MA) with a Duragel G C18 150 × 2.1 mm column (Peeke Scientific, Novato, CA) using a linear gradient of 35 to 95% solvent D (acetonitrile, 0.1% TFA) in C (water, 0.1% TFA), over 30 minutes. Purified peptoid fractions were lyophilized using a and stored as a powder at -20 °C.

8.2.4. Characterization

Synthesis was confirmed via matrix assisted laser desorption/ionization time of flight (MALDI-TOF) mass spectrometry (Bruker, Billerica, MA). Secondary structure was confirmed via CD spectrometry using a Jasco J-715 instrument (Easton, MD) at room temperature with a scanning speed of 20 nm/min and a path length of 0.2 mm. The peptoid was dissolved in methanol at a concentration of 60 μM. Each spectrum was the average of twenty accumulations.

8.2.5. Peptoid Microsphere Coatings

Peptoid microspheres were prepared by dissolving the peptoid in a 4:1 (v/v) ethanol/water solution at a concentration of 5 mg/ml. The peptoid solution was applied using a pipette onto a glass surface and allowed to dry at room temperature and 60%

relative humidity for an hour. Coating morphologies were visually assessed using a Phillips XL-30 environmental scanning electron microscope (SEM; FEI, Hillsboro, OR) at the Material Characterization Facility.

8.2.6. Microsphere Analysis

Particle analysis was performed using ImageJ software (National Institute of Health, MD). Noise reduction through a fast Fourier transform (FFT) band-pass filter normalization. This eliminates low- and high-spatial frequencies and transforms the original SEM images to a two-dimensional representation of its frequencies. The images were converted to an 8-bit grayscale and binarized adjusting the white and black threshold to optimize particle contrast with the background. Lastly, a standard watershed algorithm was used to separate fused markers.

8.3. Results and Discussion

8.3.1. Peptoid Sequence

The peptoid sequence used in this study is based on that previously shown to form microspheres [125] and is referred to as P3 (Figure 8.1.). The addition of chiral aromatic side chains in two faces of the helix sterically induces the formation of a helical secondary peptoid structure (Figure 8.1.). The third face of the peptoid helices allows for the incorporation of more ample chemistries. The P3 sequence, contains side chains with amine and methoxy groups to increase water solubility, as partial water solubility is crucial for microsphere formation. The amine groups facilitate surface attachment, via covalent linkage and electrostatic interactions. To analyze the effects of chain length on microsphere

formation, we prepared four different chain lengths inspired in the P3 sequence (Figure 8.1.) used in previous studies, which essentially repeats a 6-monomer unit sequence twice. For such studies, we synthesized a 6 monomeric unit pepotid sequence (6mer), a 12 monomer sequence (the original P3 12mer), a 18 monomer sequence (18mer), and a 24 monomer peptoid sequence (24mer) all assembled by repeating the 6mer peptoid sequence 2, 3, and 4 times respectively.
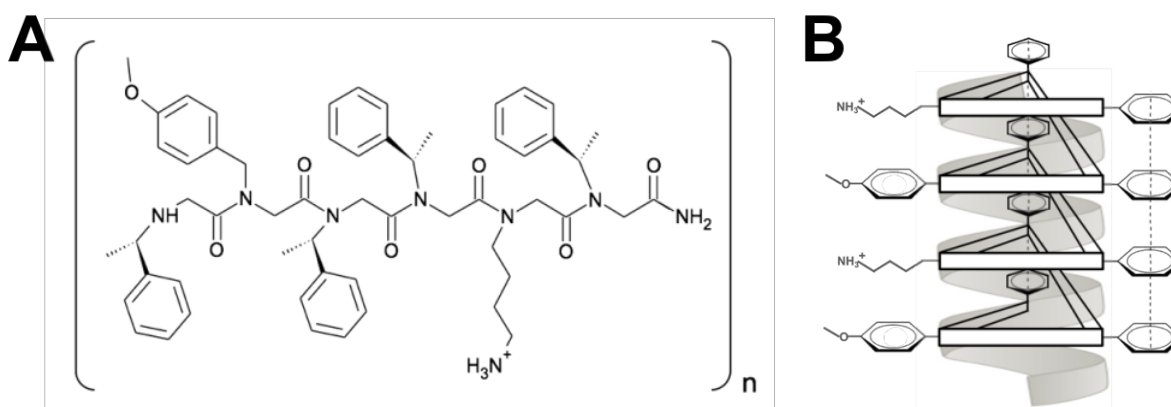

Figure 8.1. (A) Linear peptoid sequence to the n reapeat with n equal to 1 (6mer MW: 968), 2 (12mer MW: 1919), 3 (18mer MW: 2870), and 4 (24mer MW: 3821). (B) Helical representation of the three faces of the 12mer peptoid sequence.

8.3.2. Chain Length Effects

Previous studies have shown that increasing the number of chiral side chains in a peptoid sequence results in a more stable helical secondary structure [117]. In this study, peptoid chain length is varied to alter helicity and ultimately microsphere size. We hypothesize that larger peptoid sequences exhibiting tighter helices will form more closely packed supramolecular assemblies, and thus smaller microspheres, while shorter peptoid sequences exhibiting less structured helices will form less closely packed supramolecular assemblies, and thus larger microspheres. CD spectra (Figure 8.2.) for all of the peptoids

exhibit a maximum near 193 nm and two minima near 208 and 222 nm, commonly indicative of poly-proline type-I-like peptoid helices [121]. We conclude that, analogously, the extent of helicity increases with peptoid length, as evidenced by the increased ratio of the 222 and 208 nm peak intensities [177].
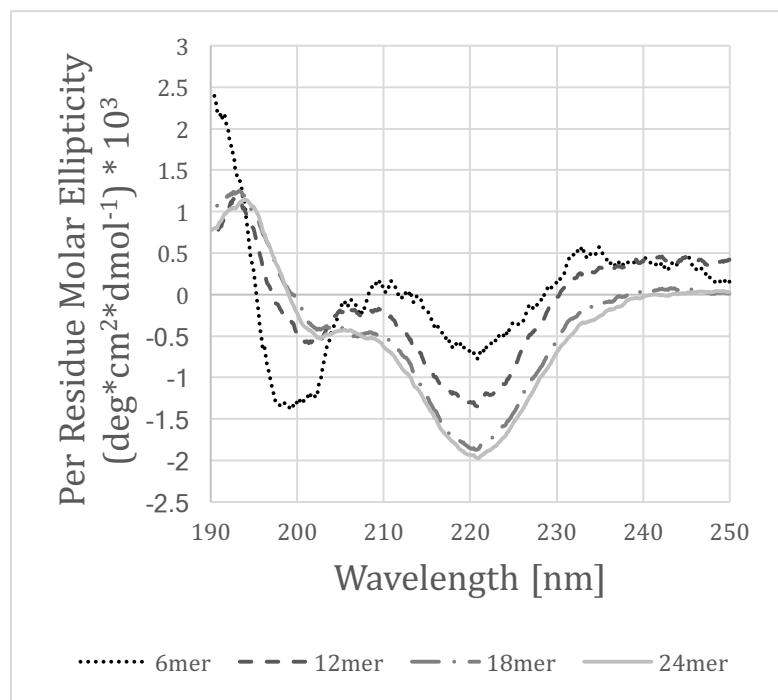

Figure 8.2. Circular dichroism spectra showing a poly-proline type-I-like helical secondary structure for the peptoids in methanol at 60 μM.

SEM analysis of the peptoid coatings formed under standard conditions show that microspheres formed for the 12, 18, and 24mer peptoids and no microspheres were observed for the 6mer peptoid (Figure 8.3.). No differences were observed with changes in these variables, and the 6mer peptoid did not form microspheres under any conditions tested. The average microsphere diameters were 1.59 ± 0.22, 1.19 ± 0.24, and 0.60 ± 0.28 μm for the 12, 18, and 24mer peptoids, respectively, supporting our hypothesis that microsphere size decreases with increasing helicity. While there was a size distribution

present for all of the chain lengths (Figure 8.4.), the larger microspheres formed by the

12mer peptoid were the most uniform.
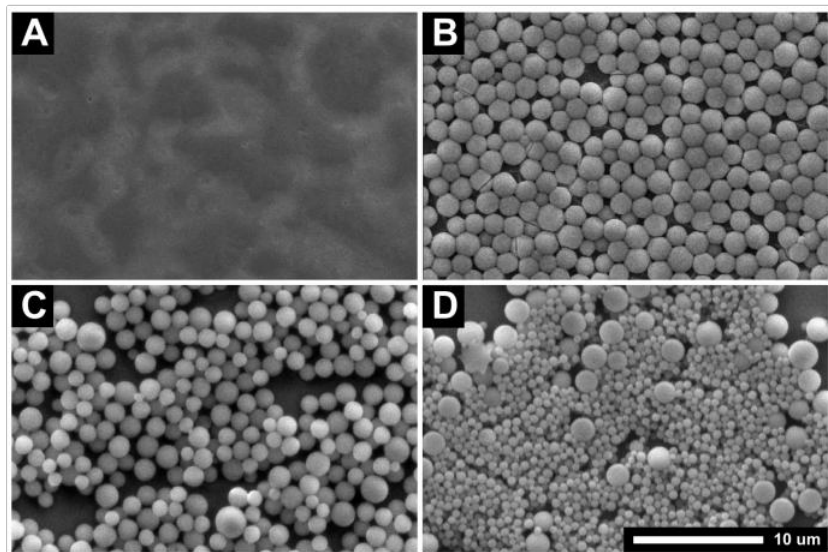
Figure 8.3. Chain length effect on microsphere formation: A) 6mer, B) 12mer, C) 18mer, and D) 24mer. The microspheres were formed by dissolving the peptoid in a 4:1 (v/v) ethanol/water solution at a concentration of 5 mg/ml. The peptoid solution was applied to glass surfaces and allowed to dry at room temperature and 60% relative humidity.
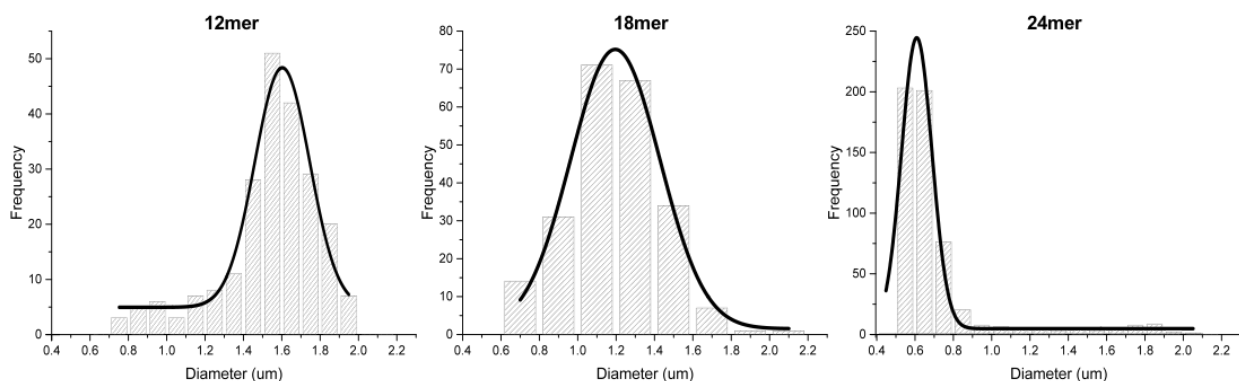
Figure 8.4. Microsphere size distribution present for each peptoid chain length: A) 12mer, B) 18mer, and C) 24mer, and D) 24mer.

8.3.3. Coating Robustness

In order to be practical in biosensor applications, the peptoid microsphere coatings must be robust under various conditions. The robustness of the peptoid microspheres were assessed in conditions common to ELISA microarray including 10 mg/mL casein in phosphate-buffered saline (PBS; pH 7.3, ionic strength 150 mM), 0.05% Tween in PBS (PBS-T; pH 7.3, ionic strength 150 mM), 0.003% hydrogen peroxide in 0.1M sodium borate (pH 8.2, ionic strength 600 mM), and nanopure water (pH ~7, ionic strength ~0 mM). The microspheres were able to withstand all conditions with minimal effect to morphology and total coverage, with the exception of water (Figure 8.5.). After exposure to water for 30 minutes the microspheres appeared to disintegrate and lift from the service. While the peptoid microspheres appear to start to solubilize in water after only 30 minutes, they are robust in PBS for up to 2 months (see Figure S8.1. in Supplemental Information). Based on these preliminary findings, we have investigated the effects of pH and ionic strength on peptoid microsphere coating robustness.
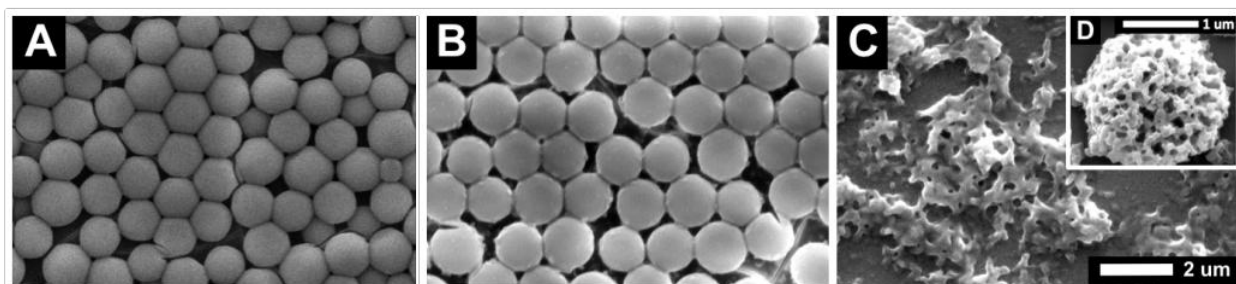
Figure 8.5. SEM images of the peptoid microspheres (A) before incubation, (B) after 24 hour incubation in PBS, (C) after 30 minute incubation in water incubation with inset (D) showing a high magnification peptoid microsphere. The microspheres were formed by dissolving the peptoid in a 4:1 (v/v) ethanol/water solution at a concentration of 5 mg/ml. The peptoid solution was applied to glass surfaces and allowed to dry at room temperature and 60% relative humidity.

pH. In order to determine the effect of solvent pH on peptoid microsphere coating robustness, morphology and coating coverage was assessed by SEM following incubation in PBS and water at different pH values. Coatings exposed to PBS or water with pH of 7 or greater are robust, with no significant differences in microsphere morphology or coating coverage (Figure 8.6. panels A-E). As the solvent approaches acidic conditions (pH less than 7), the microsphere morphology and coating coverage deteriorate (Figure 8.6. panels F-I). This observation was consistent whether the pH effect was analyzed in PBS or water at similar pH values (see Figure S8.2. in Supplemental Information). While we do not anticipate changes in pH of the solvent environment to change the charge state of peptoid. Acidic conditions increase peptoid solubility. Peptoids with ionizable side chains have been demonstrated to destabilize in response to pH-depenent changes in aqueous solvent environment [123] [178]. It would be interesting to complete a more thorough CD studies on the effects of pH on secondary structure for our particular peptoid sequences.
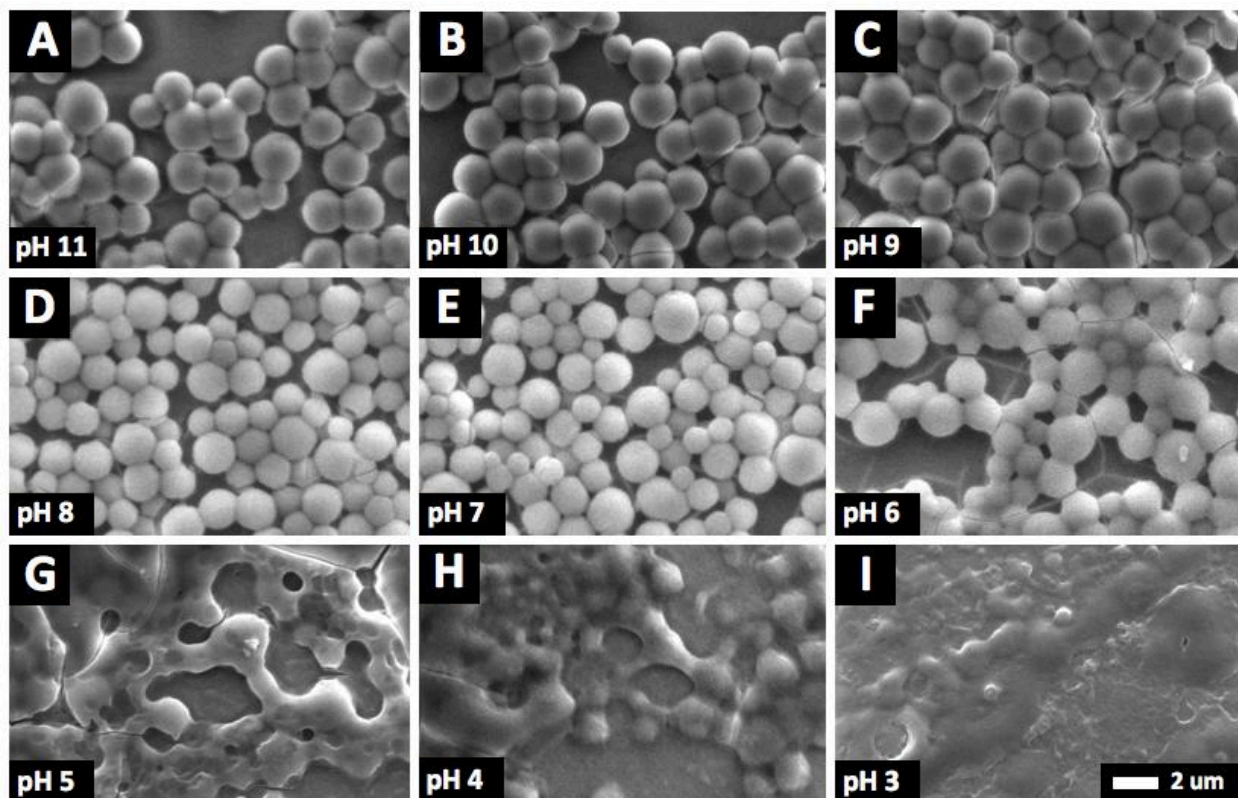
Figure 8.6. SEM images demonstrating the effect of pH on sphere morphology after 30 minutes in PBS, pH values range from: A) pH 11, B) pH 10, C) pH 9, D) pH 8, E) pH 7, F) pH 6, G) pH 5, H) pH 4, and I) pH 11.

Ionic Strength. The effect of ionic strength on peptoid microsphere coating robustness

was assessed via SEM following incubation in various ionic strength solutions (0-500 mM)

at either pH 6.7 (water) or pH 7.3 (PBS). Following incubation in water solutions, SEM

images demonstrate no considerable effect on microsphere morphology at ionic strengths

greater than 150 mM (Figure 8.7. panels A-C). As the ionic strength decreases, microsphere

morphology and coverage begins to deteriorate (Figure 8.7. panels D-F). At ionic strengths

less than 150 mM the microspheres appear to fuse together and as ionic strength decreases

the microspheres detach from the surface. Experiments evaluating the effect of ionic

strength in PBS (pH 7.3) demonstrate similar trends, with the peptoid microspheres

remaining unaffected at ionic strengths above 150 mM (Figure 8.8.).

As compared to peptide helices, peptoid helices have much more stable conformational assemblies. As a result, helical peptiod have been demonstrated to be much less susceptible to their solvent conditions. In peptides, increasing the ionic strength of the solvent has been demonstrated to stabilize secondary structure in a variety of ionic polypeptides by screening the electrostatic repulsion between side chains [179] [180] [181]. Strongly charged helical peptides are completely destabilized in low ionic strength environments [182]. Interestingly, a similar dependence has been observed in high-ionic strength solutions in peptoids [133] [178]. We believe that the screening of charge-charge repulsive interactions at higher ionic strengths preserve the helical secondary that is crucial for microsphere formation.
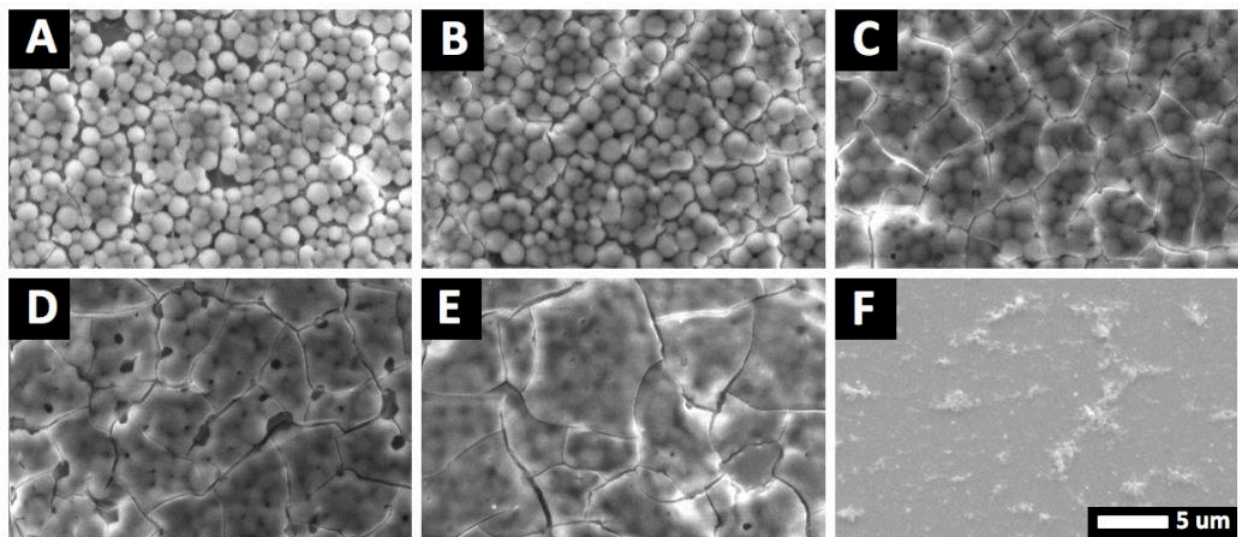

Figure 8.7. SEM images demonstrating the effect of ionic strength on sphere morphology after 30 minutes. A) 500 mM , B) 250 mM, C) 150 mM, D) 100 mM, E) 50 mM, and F) 0 mM ionic strength in water.
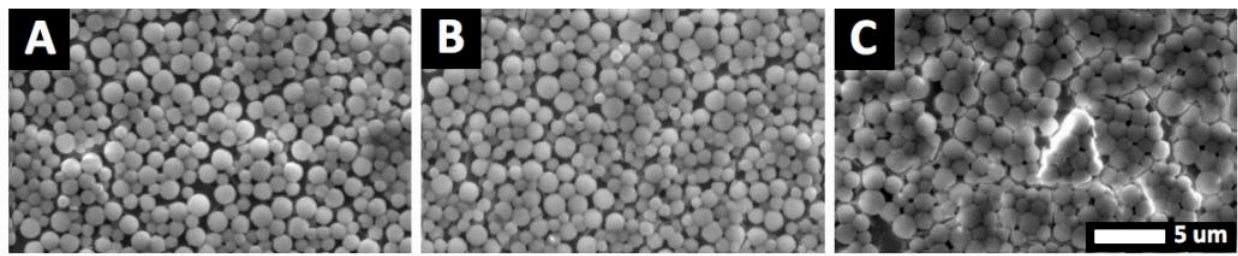
Figure 8.8. SEM images demonstrating the effect of ionic strength on sphere morphology after 30 minutes. A) 500 mM, B) 250 mM, and C) 150 mM ionic strength in PBS.

8.4. Conclusion

We have evaluated the use the effect of peptoid chain length as well as pH and ionic strength on the formation and robustness of peptoid microsphere coatings. We have found that sphere size can be tuned by varying peptoid chain length. CD spectra as a function of peptoid chain length suggests that larger sequence increase the degree of helicity. We believe that larger peptoid sequences form tighter, more stable helices, which enable the formation of smaller supramolecular assemblies. While the microsphere deteriorated at low ionic strengths and pH, the coatings display outstanding robustness at physiological conditions. Acidic conditions increase the peptoid low aqueous solubility. We believe that solvent counterions at higher ionic strengths screen the electrostatic repulsion between side chains and stabilize secondary structure, shielding the micropsheres.

8.6. Supplemental Information
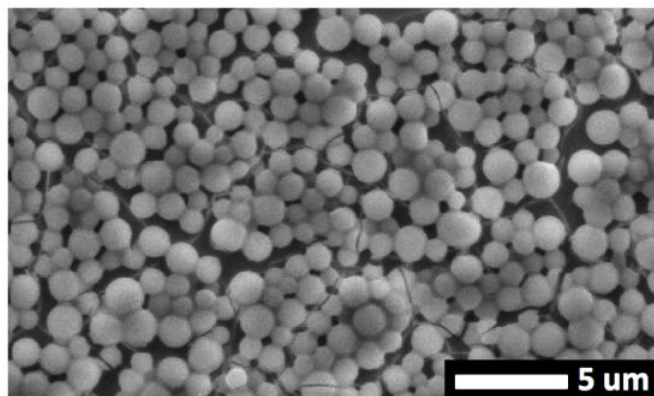

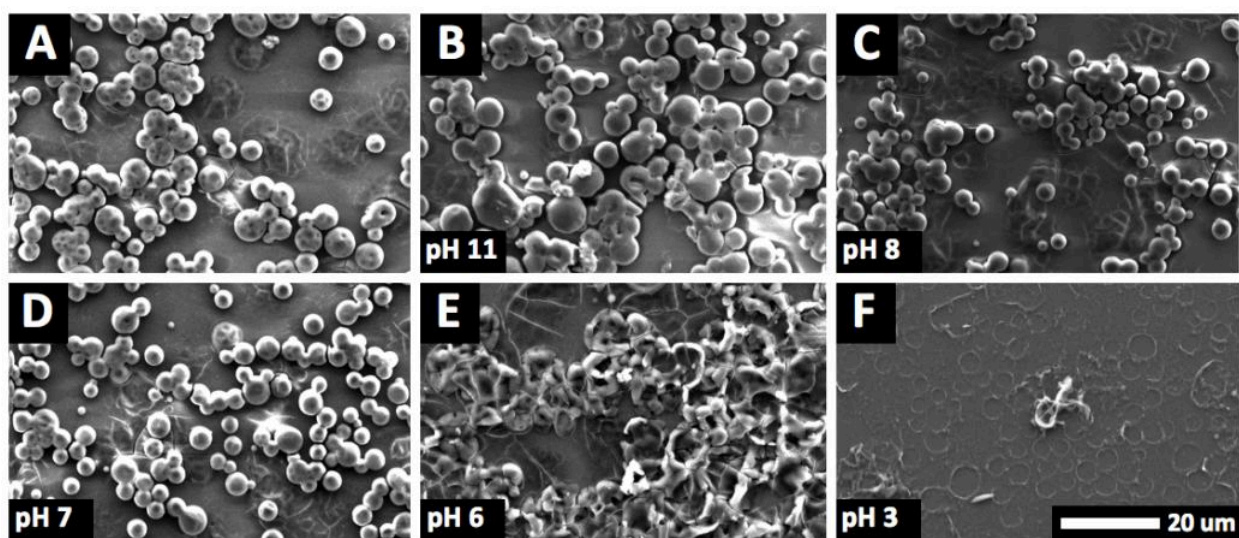Figure S8.1. SEM images demonstrating the robustness of the microsphere in PBS after 2 months.

Figure S8.2. SEM images demonstrating the effect of pH on sphere morphology after 30 minutes in water, pH values range from: A) no incubation, B) pH 11, C) pH 8, D) pH 7, E) pH 6, and F) pH 3.

9. Conclusions

The search for non-invasive, high-throughput, and cost-effective tools for early stage disease detection has led to the development of biosensor technologies of increasing complexity. Advances in biomarker technologies require the development of support surfaces that allow for more versatile immobilization procedures. The challenge lies in designing an interface that accommodates molecules of diverse characteristics in a manner that retains their innate activities. Surfaces need to provide biocompatible and bioresistant interfaces, that offer high surface areas for binding, and enables the incorporation of diverse chemistries. We believe that the use of peptoids as the basis for the deposition of uniform microsphere coatings offers a promising means to the attainment of such interfacial characteristics.

We have studied the variants affecting the formation of the peptoid microspheres, and their deposition into uniform coatings. We have found that varying peptoid chain length allows for the rational tuning of microsphere size. We have demonstrated that the peptoid microsphere coatings are extremely robust for applications at physiological conditions. We have evaluated the use of peptoid microsphere coatings as a novel surface for ELISA microarrays. The peptoid-based coatings increase the surface area for protein binding, and allow for robust chemistries of attachment. While the coatings exhibited higher background fluorescence and coefficients of variation, they performed well in terms of limits of detection and signal-to-noise ratios compared to some of the best microarray surfaces commercially available. We believe that peptoid microsphere coatings provide a robust, biocompatible, versatile new interface that can be easily customized in design and

surface modified for a wide range of biosensor applications.

10. Future Work

It is important to note that these studies were in many cases performed under very particular set of conditions. Valuable insight that could that could elucidate a more complete understating of our peptoid sequence likely lies in the synthesis of a different peptoid sequence. It would be interesting to complete a more thorough study of the effect of pH and ionic strength on secondary structure and its effect of the observed morphological changes. A more hydrophilic variant of our P3 peptoid would likely need to be synthesized for CD studies. Similarly, it would be interesting to assess whether the effects seen would remain for peptoids with non-ionizable side chains. As well as assess whether different acids would result in similar morphological variations. It would be valuable to assess whether differences in osmotic pressure are responsible for the changes seen at different ionic strengths. As well as determine, potentially by measuring the surfaces zeta potential whether the charged sidechains are preferentially facing the outer surface of the microspheres. The covalent immobilization of antibodies on the surface of this microspheres via the amine groups suggests of their surface presence. In regard to the use of the peptoid microsphere coating for microarray applications, I believe there is considerable room for improvement, in particular by further optimizing pre-treatment and blocking buffers in order to reduce background fluorescence, as well as improve spot morphologies and further raise signal intensities upon the addition of different additives, such as glycerol, to the printing buffers.

11. Acknowledgments

First of all, I would like to thank my mentor Dr. Shannon Servoss, who welcomed me into her lab group with the same kindness that she welcomed me into her family's life. I took, and will forever take the outmost pride in having been part of the Servoss lab. To Helya Najafi and Neda Mahmoudi, I thank for their love. I thank you for sharing in my excitement, my happiness, and my accomplishments. You have been unbelievable friends to me. To my buddies Phillip Turner, Dhaval Shah, Alex Lopez, Michael May, Chase Swaffer, John Moore, and Jesse Roberts, I don't know where to start. I have enjoyed every second of our time, and in between conversations about sports, learned from you more about science and engineering than any course so far. You guys made graduate school, quite frankly, an incredible time. I greatly miss our time together. I would like to thank my parents, from the bottom of my heart, for they invested all in providing us with the opportunity of an education. Making you proud is my greatest accomplishment, seeing you smile is my greatest joy. To my brothers I thank for inspiring me to be the very best version of me. You are 'home' to me. I would like to dedicate this thesis in memory of my grandfather, who is everything I aspire to one day be. My best friend, my role model, the single most influential person in everything and anything that is best in me. Finally, I would like to thank the girl that I will one day marry, my girlfriend Daniela. Whose support and belief in me gave me the strength to never falter. Who reminded me in the toughest of days not to forget how to laugh and gave me every day a reason to smile.

I would like to thank the thesis committee members Dr. Kartik Balachandran, Dr. Robert Beitle, Dr. Colin Heyes, and Dr. Ranil Wickramasinghe for their valued input and guidance

12. References

[1]   M. F. Ullah and M. Aatif, "The Footprints of Cancer Development: Cancer Biomarkers," *Cancer Treatment Reviews,* vol. 3, p. 193–200, 2009.

[2]   C. Kosary, L. Ries, B. Miller, B. Hankey, A. Harras and B. Edwards, "SEER Cancer Statistics Review. National Cancer Institute," *National Cancer Institute,* pp. 96-2789, 1995.

[3]   V. Levenson, "Biomarkers For Early Detection of Breast Cancer: What, When, and Where?," *Biochimica et Biophysica Acta,* vol. 1770, no. 6, p. 847–856, 2007.

[4]   N. B. Kiviat and C. W. Critchlow, "Novel Approaches To Identification of Biomarkers for Detection of Early Stage Cancer," *Disease Markers,* vol. 2, p. 73–81, 2002.

[5]   P. R. Srinivas, B. S. Kramer and S. Srivastava, "Trends In Biomarker Research for Cancer Detection," *The Lancet Oncology,* vol. 2, no. 11, pp. 698-704, 2001.

[6]   R. Etzioni, N. Urban, S. Ramsey, M. Mcintosh, S. Schwartz, B. Reid, J. Radich, G. Anderson and L. Hartwell, "Early Detection: The Case for Early Detection," *Nature Reviews Cancer,* vol. 4, p. 243–252., 2003.

[7]   M. A. Tainsky, "Genomic And Proteomic Biomarkers for Cancer: A Multitude of Opportunities.," *Biochimica et Biophysica Acta,* vol. 1796, no. 2, pp. 176-193, 2009.

[8]   U. Manne, R.-G. Srivastava and S. K. Srivastava, "Review: Recent Advances in Biomarkers for Cancer Diagnosis and Treatment," *Drug Discovery Today ,* vol. 10, no. 14, p. 965–976, 2005.

[9]   A. J. Rai and D. W. Chan, "Cancer Proteomics: New Developments In Clinical Chemistry," *Laboratoriums Medizin,* vol. 25, no. 10, p. 399–403, 2001.

[10]   L. Huber, "Is Proteomics Heading in the Wrong Direction?," *Nature Reviews Molecular Cell Biology,* vol. 4, no. 1, pp. 74-80, 2003.

[11]   J. Glökler and P. Angenendt, "Protein And Antibody Microarray Technology," *Journal of Chromatography,* vol. 797, no. 2, pp. 229-240, 2003.

[12]   L. Anderson and J. Seilhamer, "A Comparison of Selected MRNA and Protein Abundances in Human Liver," *Electrophoresis,* vol. 18, no. 3, pp. 533-537, 1997.

[13]   B. B. Haab, "Applications Of Antibody Array Platforms," *Current Opinion in Biotechnology,* vol. 17, no. 4, p. 415–421, 2006.

[14]   D. J. Cahill, "Protein And Antibody Arrays and Their Medical Applications," *Journal of Immunological Methods,* vol. 250, no. 1, pp. 81-91, 2001.

[15]   J. DeRisi, L. Penland, P. Brown, M. Bittner, P. Meltzer, M. Ray, Y. Chen, Y. Su and J. Trent, "Use Of a CDNA Microarray to Analyse Gene Expression Patterns in Human Cancer," *Nature Genetics,* vol. 14, no. 4, pp. 457-460, 1996.

[16]   M. Esteller, P. Corn, S. Baylin and J. Herman, "A Gene Hypermethylation Profile of Human Cancer," *Cancer Research,* vol. 61, no. 8, p. 3225–3229, 2001.

[17]   C. A. Borrebaeck and C. Wingren, "Design Of High-Density Antibody Microarrays for Disease Proteomics: Key Technological Issues," *Journal of Proteomics,* vol. 72, no. 6, pp. 928-935, 2009.

[18]   C. A. Borrebaeck and C. Wingren, "High-Throughput Proteomics Using Antibody Microarrays: an Update," *Expert Review of Molecular Diagnostics,* vol. 7, no. 5, p. 673–686, 2007.

[19]   S. F. Kingsmore, "Multiplexed Protein Measurement: Technologies and Applications of Protein and Antibody Arrays," *Nature Reviews Drug Discovery,* vol. 5, no. 4, p. 310–321, 2006.

[20]   P. Pavlickova, E. Schneider and H. Hug, "Advances In Recombinant Antibody Microarrays," *Clinica Chimica Acta ,* vol. 343, no. 1, p. 17–35. , 2004.

[21]   J. Ingvarsson, A. Larsson, A. G. Sjöholm, L. Truedsson, B. Jansson, C. A. K. Borrebaeck and C. Wingren, "Design Of Recombinant Antibody Microarrays for Serum Protein Profiling: Targeting of Complement Proteins," *Journal of Proteome Research,* vol. 6, no. 9, p. 3527–3536, 2007.

[22]   W. Kusnezow, V. Banzon, C. Schröder, R. Schaal, J. D. Hoheisel, S. Rüffer, P. Luft, A. Duschl and Y. V. Syagailo, "Antibody Microarray-Based Profiling of Complex Specimens: Systematic Evaluation of Labeling Strategies," *Proteomics,* vol. 7, no. 11, pp. 1786-1799, 2007.

[23]   C. Wingren, J. Ingvarsson, L. Dexlin, D. Szul and C. A. Borrebaeck, "Design Of Recombinant Antibody Microarrays for Complex Proteome Analysis: Choice of Sample Labeling-Tag and Solid Support," *Proteomics,* vol. 7, no. 17, p. 3055–3065, 2007.

[24]   P. Angenendt, "Progress In Protein and Antibody Microarray Technology," *Drug Discovery Today,* vol. 10, no. 7, p. 503–511, 2005.

[25] M. Sanchez-Carbayo, "Antibody Arrays: Technical Considerations And Clinical Applications in Cancer," *Clinical Chemistry,* vol. 52, no. 9, p. 1651–1659, 2006.

[26] N. Anderson, "The Human Plasma Proteome: History, Character, And Diagnostic Prospects," *Molecular & Cellular Proteomics,* vol. 1, no. 11, p. 845–867, 2002.

[27] O. Blixt, S. Head, T. Mondala, C. Scanlan, M. E. Huflejt, R. Alvarez, M. C. Bryan, F. Fazio, D. Calarese, J. Stevens, N. Razi, D. J. Stevens, J. J. Skehel, I. V. Die, D. Burton, I. A. Wilson, R. Cummings, N. Bovin, C. Wong and J. Paulson, "Printed Covalent Glycan Array for Ligand Profiling of Diverse Glycan Binding Proteins," *Proceedings of the National Academy of Sciences,* vol. 101, no. 49, p. 17033–17038, 2004.

[28] A. M. Wu, "The Molecular Immunology of Complex Carbohydrates," 2001.

[29] M. E. Taylor and K. Drickamer, "Introduction To Glycobiology," *Oxford University Press,* 2003.

[30] M. M. Fuster and J. D. Esko, "The Sweet and Sour of Cancer: Glycans as Novel Therapeutic Targets," *Nature Reviews Cancer,* vol. 5, no. 7, p. 526–542, 2005.

[31] F. Jacob, D. R. Goldstein, N. V. Bovin, T. Pochechueva, M. Spengler, R. Caduff, D. Fink, M. I. Vuskovic, M. E. Huflejt and V. Heinzelmann-Schwarz, "Serum Antiglycan Antibody Detection of Nonmucinous Ovarian Cancers by Using a Printed Glycan Array," *International Journal of Cancer,* vol. 130, no. 1, p. 138–146, 2011.

[32] M. E. Huflejt, M. Vuskovic, D. Vasiliu, H. Xu, P. Obukhova, N. Shilova, A. Tuzikov, O. Galanina, B. Arun, K. Lu and N. Bovin, "Anti-Carbohydrate Antibodies of Normal Sera: Findings, Surprises and Challenges," *Molecular Immunology,* vol. 46, no. 15, p. 3037–3049, 2009.

[33] N. V. Bovin and M. E. Huflejt, "Unlimited Glycochip," *Trends in Glycoscience and Glycotechnology,* vol. 20, no. 115, p. 245–258, 2008.

[34] O. Oyelaran, L. M. Mcshane, L. Dodd and J. C. Gildersleeve, "Profiling Human Serum Antibodies With a Carbohydrate Antigen Microarray," *Journal of Proteome Research,* vol. 8, no. 9, p. 4301–4310, 2009.

[35] C.-Y. Huang, D. A. Thayer, A. Y. Chang, M. D. Best, J. Hoffmann, S. Head and C.-H. Wong, "Carbohydrate Microarray for Profiling the Antibodies Interacting with Globo H Tumor Antigen," *Proceedings of the National Academy of Sciences,* vol. 103, no. 1, p. 15–20, 2005.

[36] C. H. Lawrie, T. Marafioti, C. S. Hatton, S. Dirnhofer, G. Roncador, P. Went, A. Tzankov, S. A. Pileri, K. Pulford and A. H. Banham, "Cancer-Associated Carbohydrate Identification in Hodgkin's Lymphoma by Carbohydrate Array Profiling," *International Journal of Cancer,* vol. 118, no. 12, p. 3161–3166, 2006.

[37] N. L. Anderson, "The Human Plasma Proteome: History, Character, And Diagnostic Prospects," *Molecular & Cellular Proteomics,* vol. 1, no. 11, p. 845–867, 2002.

[38] R. Wadlow and S. Ramaswamy, "DNA Microarrays In Clinical Cancer Research," *Current Molecular Medicine,* vol. 5, no. 1, p. 111–120, 2005.

[39] R. C. Zangar, S. M. Varnum and N. Bollinger, "Studying Cellular Processes And Detecting Disease with Protein Microarrays," *Drug Metabolism Reviews,* vol. 37, no. 2, p. 473–487, 2005.

[40] N. L. Anderson, "The Roles Of Multiple Proteomic Platforms in a Pipeline for New Diagnostics," *Molecular & Cellular Proteomics,* vol. 4, no. 10, p. 1441–1444, 2005.

[41] K. Powell, "Proteomics Delivers on Promise of Cancer Biomarkers," *Nature Medicine,* vol. 9, no. 8, 2003.

[42] M. Verma and S. Srivastava, "New Cancer Biomarkers Deriving From NCI Early Detection Research," *Tumor Prevention and Genetics Recent Results in Cancer Research,* p. 72–84. , 2003.

[43] R. Ekins and F. W. Chu, "Microarrays: Their Origins and Applications," *Trends in Biotechnology,* vol. 17, no. 6, p. 217–218, 1999.

[44] P. Saviranta, "Evaluating Sandwich Immunoassays In Microarray Format in Terms of the Ambient Analyte Regime.," *Clinical Chemistry,* vol. 50, no. 10, p. 1907–1920, 2004.

[45] R. C. Zangar, D. S. Daly and A. M. White, "ELISA Microarray Technology as a High-Throughput System for Cancer Biomarker Validation," *Expert Review of Proteomics,* vol. 3, no. 1, pp. 37-44, 2006.

[46] D. Stoll, J. Bachmann, M. F. Templin and T. O. Joos, "Microarray Technology: an Increasing Variety of Screening Tools for Proteomic Research," *Drug Discovery Today,* vol. 3, no. 1, pp. 24-31, 2004.

[47] M. Sanchez-Carbayo, N. D. Socci, J. J. Lozano, B. B. Haab and C. Cordon-Cardo, "Profiling Bladder Cancer Using Targeted Antibody Arrays," *The American Journal of Pathology,* vol. 168, no. 1, p. 93–103, 2006.

[48] L. Belov, P. Huang, N. Barber, S. P. Mulligan and R. I. Christopherson, "Identification Of Repertoires of Surface Antigens on Leukemias Using an Antibody Microarray," *Proteomics,* vol. 3, no. 11, p. 2147–2154, 2003.

[49] J. D. Wulfkuhle, K. C. Mclean, C. P. Paweletz, D. C. Sgroi, B. J. Trock, P. S. Steeg and E. Iii, "New Approaches to Proteomic Analysis of Breast Cancer," *Proteomics,* vol. 1, no. 10, p. 1205–1215, 2001.

[50] A. Carlsson, C. Wingren, J. Ingvarsson, P. Ellmark, B. Baldertorp, M. Fernö, H. Olsson and C. A. Borrebaeck, "Serum Proteome Profiling of Metastatic Breast Cancer Using Recombinant Antibody Microarrays," *European Journal of Cancer,* vol. 44, no. 3, p. 472–480, 2008.

[51] G. Hudelist, M. Pacher-Zavisin, C. Singer, T. Holper, E. Kubista, M. Schreiber, M. Manavi, M. Bilban and K. Czerwenka, "Use Of High-Throughput Protein Array for Profiling of Differentially Expressed Proteins in Normal and Malignant Breast Tissue," *Breast Cancer Research and Treatment,* vol. 86, no. 3, p. 283–293, 2004.

[52] A. Vazquez-Martin, R. Colomer and J. A. Menendez, "Protein Array Technology to Detect HER2 (ErbB-2)-Induced 'Cytokine Signature' in Breast Cancer.," *European Journal of Cancer,* vol. 43, no. 7, p. 1117–1124, 2007.

[53] M. W. Shafer, L. Mangold, A. W. Partin and B. B. Haab, "Antibody Array Profiling Reveals Serum TSP-1 as a Marker to Distinguish Benign from Malignant Prostatic Disease," *The Prostate Prostate,* vol. 67, no. 3, p. 255–267, 2007.

[54] J. Ingvarsson, C. Wingren, A. Carlsson, P. Ellmark, B. Wahren, G. Engström, U. Harmenberg, M. Krogh, C. Peterson and C. A. K. Borrebaeck, "Detection Of Pancreatic Cancer Using Antibody Microarray-Based Serum Protein Profiling," *Proteomics,* vol. 8, no. 11, p. 2211–2219, 2008.

[55] R. Orchekowski, "Antibody Microarray Profiling Reveals Individual And Combined Serum Proteins Associated with Pancreatic Cancer," *Cancer Research,* vol. 65, no. 23, p. 11193–11202, 2005.

[56] B. Bartling, H.-S. Hofmann, T. Boettger, G. Hansen, S. Burdach, R.-E. Silber and A. Simm, "Comparative Application of Antibody and Gene Array for Expression Profiling in Human Squamous Cell Lung Carcinoma," *Lung Cancer,* vol. 49, no. 2, pp. 145-154, 2005.

[57] W. Gao, R. Kuick, R. P. Orchekowski, D. E. Misek, J. Qiu, A. K. Greenberg, W. N. Rom, D. E. Brenner, G. S. Omenn, B. B. Haab and S. M. Hanash, "Distinctive Serum Protein

Profiles Involving Abundant Proteins In Lung Cancer Patients Based Upon Antibody Microarray Analysis," *BMC Cancer,* vol. 5, no. 1, p. 110, 2005.

[58] T. Kullmann, I. Barta, E. Csiszér, B. Antus and I. Horváth, "Differential Cytokine Pattern In the Exhaled Breath of Patients with Lung Cancer," *Pathology & Oncology Research,* vol. 14, no. 4, p. 481–483, 2008.

[59] J. Madoz-Gurpide, M. Canamero, L. Sanchez, J. Solano, P. Alfonso and J. I. Casal, "A Proteomics Analysis Of Cell Signaling Alterations in Colorectal Cancer," *Molecular & Cellular Proteomics,* vol. 6, no. 12, p. 2150–2164, 2007.

[60] S. Srivastava, M. Verma and H. D. E., "Biomarkers For Early Detection Of Colon Cancer," *Clinical Cancer Research,* vol. 7, p. 1118–1126, 2007.

[61] M. Srivastava, O. Eidelman, C. Jozwik, C. Paweletz, W. Huang, P. L. Zeitlin and H. B. Pollard, "Serum Proteomic Signature for Cystic Fibrosis Using an Antibody Microarray Platform," *Molecular Genetics and Metabolism,* vol. 87, no. 4, p. 303–310, 2006.

[62] P. Szodoray, P. Alex, J. G. Brun, M. Centola and R. Jonsson, "Circulating Cytokines In Primary Sjogren's Syndrome Determined by a Multiplex Cytokine Array System," *Scandinavian Journal of Immunology ,* vol. 59, no. 6, p. 592–599, 2004.

[63] P. Szodoray, P. Alex, C. M. Chappell-Woodward, T. M. Madland, N. Knowlton, I. Dozmorov, M. Zeher, J. N. Jarvis, B. Nakken, J. G. Brun and M. Centola, "Circulating Cytokines in Norwegian Patients with Psoriatic Arthritis Determined by a Multiplex Cytokine Array System," *Rheumatology,* vol. 46, no. 3, p. 417–425, 2007.

[64] M. Mukoyama, K. Nakao, Y. Saito, Y. Ogawa, K. Hosoda, S. Suga, G. Shirakami, M. Jougasaki and H. Imura, "Increased Human Brain Natriuretic Peptide In Congestive Heart Failure," *New England Journal of Medicine ,* vol. 323, no. 11, p. 757–758, 1990.

[65] B. Haab, M. Dunham and P. Brown, "Protein Microarrays For Highly Parallel Detection And Quantitation Of Specific Proteins And Antibodies In Complex Solutions," *Genome Biology,* vol. 2, 2001.

[66] R. M. Gonzalez, S. L. Seurynck-Servoss, S. A. Crowley, M. Brown, G. S. Omenn, D. F. Hayes and R. C. Zangar, "Development And Validation of Sandwich ELISA Microarrays with Minimal Assay Interference," *Journal of Proteome Research,* vol. 7, no. 6, p. 2406–2414, 2008.

[67] B. B. Haab, "Antibody Arrays In Cancer Research," *Molecular & Cellular Proteomics,* vol. 4, no. 4, p. 377–383, 2005.

93

[68] A. Tannapfel, K. Anhalt, P. Häusermann, F. Sommerer, M. Benicke, D. Uhlmann, H. Witzigmann, J. Hauss and C. Wittekind, "Identification Of Novel Proteins Associated with Hepatocellular Carcinomas Using Protein Microarrays.," *The Journal of Pathology,* vol. 201, no. 2, p. 238–249, 2003.

[69] Y. Lin, R. Huang, X. Cao, S.-M. Wang, Q. Shi and R.-P. Huang, "Detection Of Multiple Cytokines by Protein Arrays from Cell Lysate and Tissue Lysate," *Clinical Chemistry and Laboratory Medicine 2003, 41 (2). ,* vol. 41, no. 2, 2003.

[70] R. Barry, "Competitive Assay Formats For High-Throughput Affinity Arrays," *Journal of Biomolecular Screening,* vol. 8, no. 3, p. 257–263, 2003.

[71] P. D. Wagner, P. Maruvada and S. Srivastava, "Molecular Diagnostics: a New Frontier in Cancer Prevention," *Expert Review of Molecular Diagnostics,* vol. 4, no. 4, p. 503–511, 2004.

[72] C. Bangma, D. Grobbee and F. Schröder, "Volume Adjustment for Intermediate Prostate-Specific Antigen Values in a Screening Population.," *European Journal of Cancer,* vol. 31, no. 1, pp. 12-14, 1995.

[73] P. H. Gann, "A Prospective Evaluation of Plasma Prostate-Specific Antigen for Detection of Prostatic Cancer," *The Journal of the American Medical Association,* vol. 273, no. 4, p. 289–294, 1995.

[74] D. Gillatt and J. Reynard, "What Is the 'Normal Range' for Prostate-Specific Antigen? Use of a Receiver Operating Characteristic Curve to Evaluate a Serum Marker," *British Journal of Urology,* vol. 75, no. 3, p. 341–346, 1995.

[75] H. Lepor, R. S. Owens, V. Rogenes and E. Kuhn, "Detection Of Prostate Cancer in Males with Prostatism," *The Prostate,* vol. 25, no. 3, p. 132–140, 1994.

[76] B. H. Geierstanger, P. Saviranta and A. Brinker, "Antibody Microarrays Using Resonance Light-Scattering Particles For Detection," *New and Emerging Proteomic Techniques,* pp. 31-50, 2006.

[77] P. Angenendt, J. Glökler, D. Murphy, H. Lehrach and D. J. Cahill, "Toward Optimized Antibody Microarrays: a Comparison of Current Microarray Support Materials," *Analytical Biochemistry,* vol. 309, no. 2, p. 253–260, 2002.

[78] S. L. Servoss, A. White, C. Baird, K. Rodland and R. Zangar, "Evaluation Of Surface Chemistries For Antibody Microarrays," *Analytical Biochemistry,* vol. 371, p. 105–115, 2007.

[79] G. Walter, K. Büssow, A. Lueking and J. Glökler, "High-Throughput Protein Arrays: Prospects for Molecular Diagnostics," *Trends in Molecular Medicine,* vol. 8, no. 6, p. 250–253, 2002.

[80] P. Angenendt and J. Glökler, "Evaluation Of Antibodies and Microarray Coatings As a Prerequisite for the Generation of Optimized Antibody Microarrays," *Protein Arrays,* vol. 264, pp. 123-134, 2004.

[81] Q. Xu, S. Miyamoto and K. S. Lam, "A Novel Approach To Chemical Microarray Using Ketone-Modified Macromolecular Scaffolds: Application In Micro Cell-Adhesion Assay," *Molecular Diversity,* vol. 8, p. 301–310, 2004.

[82] M. Lee and I. Shin, "Fabrication of Chemical Microarrays by Efficient Immobilization of Hydrazide-Linked Substances on Epoxide-Coated Glass Surfaces," *Angew. Chem.,* vol. 44, p. 2881–2884, 2005.

[83] W. Kusnezow and J. D. Hoheisel, "Solid Supports for Microarray Immunoassays," *Journal of Molecular Recognition,* vol. 16, no. 4, pp. 165-176, 2003.

[84] P. Peluso, D. S. Wilson, D. Do, H. Tran, M. Venkatasubbaiah, D. Quincy, B. Heidecker, K. Poindexter, N. Tolani, M. Phelan, K. Witte, L. S. Jung, P. Wagner and S. Nock, "Optimizing Antibody Immobilization Strategies for the Construction of Protein Microarrays," *Analytical Biochemistry,* vol. 312, no. 2, p. 113–124, 2003.

[85] J. E. Bradner, O. M. Mcpherson and A. N. Koehler, "A Method for the Covalent Capture and Screening of Diverse Small Molecules in a Microarray Format," vol. 1, no. 5, p. 2344–2352, 2006.

[86] J. E. Bradner, O. M. Mcpherson, R. Mazitschek, D. Barnes-Seeman, J. P. Shen, J. Dhaliwal, K. E. Stevenson, J. L. Duffner, S. B. Park, D. S. Neuberg, P. Nghiem, S. L. Schreiber and A. N. Koehler, "A Robust Small-Molecule Microarray Platform For Screening Cell Lysates," *Chemistry & Biology,* vol. 13, no. 5, p. 493–504, 2006.

[87] R. Wiese, Y. Belosludtsev, T. Powdrill, P. Thompson and M. Hogan, "Simultaneous Multianalyte ELISA Performed On A Microarray Platform," *Clin. Chem.,* vol. 47, no. 8, p. 1451–1457, 2001.

[88] G. MacBeath and S. Schreiber, "Printing Proteins As Microarrays For High-Throughput Function Determination," *Science ,* vol. 289, p. 1760–1763, 2000.

[89] P. Arenkov, A. Kukhtin, A. Gemmell, S. Voloshchuk, V. Chupeeva and A. Mirzabekov, "Protein Microchips: Use For Immunoassay and Enzymatic Reactions," *Analytical Biochemistry,* vol. 278, no. 2, pp. 123-131, 2000.

[90]   V. Afanassiev, "Preparation Of DNA and Protein Micro Arrays on Glass Slides Coated with an Agarose Film," *Nucleic Acids Research,* vol. 28, no. 12, 2000.

[91]   C. A. Rowe, S. B. Scruggs, M. J. Feldstein, J. P. Golden and F. S. Ligler, "An Array Immunosensor For Simultaneous Detection of Clinical Analytes," *Analytical Chemistry,* vol. 75, no. 5, p. 1225–1225, 2003.

[92]   H. Zhu, "Global Analysis Of Protein Activities Using Proteome Chips," *Science,* vol. 293, no. 5537, p. 2101–2105, 2001.

[93]   P. Angenendt, J. Glökler, J. Sobek, H. Lehrach and D. J. Cahill, "Next Generation of Protein Microarray Support Materials," *Journal of Chromatography A,* vol. 1009, no. 1, p. 97–104, 2003.

[94]   W. Kusnezow, A. Jacob, A. Walijew, F. Diehl and J. D. Hoheisel, "Antibody Microarrays: An Evaluation of Production Parameters," *Proteomics,* vol. 3, no. 3, p. 254–264, 2003.

[95]   A. Y. Rubina, E. I. Dementieva, A. A. Stomakhin, E. L. Darii, S. V. Pan'kov, V. E. Barsky, S. M. Ivanov, E. V. Konovalova and A. D. Mirzabekov, "Hydrogel-Based Protein Microchips: Manufacturing, Properties, And Applications," *Biotechniques,* vol. 34, no. 5, p. 1008–1014 , 2003.

[96]   R.-P. Huang, R. Huang, Y. Fan and Y. Lin, "Simultaneous Detection Of Multiple Cytokines from Conditioned Media and Patient's Sera by an Antibody-Based Protein Array System," *Analytical Biochemistry 2001, 294 (1), 55–62. ,* vol. 294, no. 1, pp. 55-62, 2001.

[97]   M. Steinitz and S. Tamir, "An Improved Method to Create Nitrocellulose Particles Suitable for the Immobilization of Antigen and Antibody," *Journal of Immunological Methods,* vol. 187, no. 1, p. 171–177, 1995.

[98]   E. Southern, K. Mir and M. Shchepinov, "Molecular Interactions on Microarrays," *Nature Genetics,* vol. 21, pp. 5-9, 1999.

[99]   H. U. Ge, "A Universal Protein Array System for Quantitative Detection of Protein-Protein, Protein-DNA, Protein-RNA and Protein-Ligand Interactions," *Nucleic Acids Research 2000, 28 (2). ,* vol. 28, no. 2, 2000.

[100] B. Kersten, A. Possling, F. Blaesing, E. Mirgorodskaya, J. Gobom and H. Seitz, "Protein Microarray Technology and Ultraviolet Crosslinking Combined with Mass

Spectrometry for the Analysis of Protein–DNA Interactions," *Analytical Biochemistry,* vol. 331, no. 2, pp. 303-313, 2004.

[101] J. Madoz-Gúrpide, H. Wang, D. E. Misek, F. Brichory and S. M. Hanash, "Protein Based Microarrays: A Tool for Probing the Proteome of Cancer Cells and Tissues," *Proteomics,* vol. 1, no. 10, p. 1279–1287, 2001.

[102] B. Liu, L. Huang, C. Sihlbom, A. Burlingame and J. D. Marks, "Towards Proteome-Wide Production of Monoclonal Antibody by Phage Display," *Journal of Molecular Biology,* vol. 315, no. 5, p. 1063–1073, 2002.

[103] K. Bussow, "A Method for Global Protein Expression and Antibody Screening on High- Density Filters of an Arrayed CDNA Library," *Nucleic Acids Research,* vol. 26, no. 21, p. 5007–5008, 1998.

[104] M. J. Taussig and U. Landegren, "Progress In Antibody Arrays," *Targets,* vol. 2, no. 4, p. 169–176, 2003.

[105] J. B. Delehanty and F. S. Ligler, "A Microarray Immunoassay For Simultaneous Detection of Proteins and Bacteria," *Analytical Chemistry,* vol. 74, no. 21, p. 5681–5687, 2002.

[106] R. Benters, C. M. Niemeyer and D. Wöhrle, "Dendrimer-Activated Solid Supports For Nucleic Acid and Protein Microarrays.," *ChemBioChem,* vol. 2, no. 9, p. 686–694, 2001.

[107] S. Pathak, A. K. Singh, J. R. Mcelhanon and P. M. Dentinger, "Dendrimer-Activated Surfaces For High Density and High Activity Protein Chip Applications," *Langmuir,* vol. 20, no. 15, p. 6075–6079, 2004.

[108] B. A. Stillman and J. L. Tonkinson, "FAST Slides: A Novel Surface For Microarrays," *Biotechniques,* vol. 29, no. 3, p. 630–635, 2000.

[109] T. S. Burkoth, E. Beausoleil, S. Kaur, D. Tang, F. E. Cohen and R. N. Zuckermann, "Toward The Synthesis of Artificial Proteins," *Chemistry & Biology,* vol. 9, no. 5, p. 647–654, 2002.

[110] J. A. Patch and A. E. Barron, "Mimicry Of Bioactive Peptides via Non-Natural, Sequence-Specific Peptidomimetic Oligomers," *Current Opinion in Chemical Biology,* vol. 6, no. 6, p. 872–877, 2002.

[111] R. J. Simon, R. S. Kania, R. N. Zuckermann, V. D. Huebner, D. A. Jewell, S. Banville, S. Ng, L. Wang, S. Rosenberg and C. K. Marlowe, "Peptoids: a Modular Approach to Drug

Discovery," *Proceedings of the National Academy of Sciences,* vol. 89, no. 20, p. 9367–9371 , 1992 .

[112] M. Hagihara, N. J. Anthony, T. J. Stout, J. Clardy and S. L. V. Schreiber, "Polypeptides: an Alternative Peptide Backbone," *Journal of the American Chemical Society,* vol. 114, no. 16, p. 6568–6570, 1992.

[113] K. Burgess, H. Shin and D. S. Linthicum, "Solid-Phase Syntheses Of Unnatural Biopolymers Containing Repeating Urea Units," *Angewandte Chemie International Edition in English Angew,* vol. 34, no. 8, pp. 907-909, 1995.

[114] A. B. Smith, D. A. Favor, P. A. Sprengeler, M. C. Guzman, P. J. Carroll, G. T. Furst and R. Hirschmann, "Molecular Modeling, Synthesis, and Structures of N-Methylated 3,5-Linked Pyrrolin-4-Ones toward the Creation of a Privileged Nonpeptide Scaffold," *Bioorganic & Medicinal Chemistry,* vol. 7, no. 1, pp. 9-22, 1999.

[115] D. H. Appella, L. A. Christianson, I. L. Karle, D. R. Powell and S. H. Gellman, "β-Peptide Foldamers: Robust Helix Formation In a New Family of β-Amino Acid Oligomers," *Journal of the American Chemical Society,* vol. 118, no. 51, p. 13071–13072, 1996.

[116] S. Hanessian, X. Luo and R. Schaum, "Synthesis And Folding Preferences of γ-Amino Acid Oligopeptides: Stereochemical Control in the Formation of a Reverse Turn and a Helix," *Tetrahedron Letters,* vol. 40, no. 27, p. 4925–4929, 1999.

[117] C. W. Wu, T. J. Sanborn, R. N. Zuckermann and A. E. Barron, "Peptoid Oligomers With α-Chiral, Aromatic Side Chains: Effects of Chain Length on Secondary Structure," *Journal of the American Chemical Society,* vol. 123, no. 13, p. 2958–2963, 2001.

[118] S. H. Gellman, "Foldamers: A Manifesto," *Accounts of Chemical Research,* vol. 31, no. 4, p. 173–180, 1998.

[119] D. J. Hill, M. J. Mio, R. B. Prince, T. S. Hughes and J. S. Moore, "A Field Guide To Foldamers," *Chemical Reviews,* vol. 101, no. 12, p. 3893–4012, 2001.

[120] P. Armand, K. Kirshenbaum, R. A. Goldsmith, S. Farr-Jones, A. E. Barron, K. T. V. Truong, K. A. Dill, D. F. Mierke, F. E. Cohen, R. N. Zuckermann and E. K. Bradley, "NMR Determination of the Major Solution Conformation of a Peptoid Pentamer with Chiral Side Chains," *Proceedings of the National Academy of Sciences,* vol. 95, no. 8, p. 4309–4314, 1998.

[121] J. A. Patch, K. Kirshenbaum, S. L. Seurynck, R. N. Zuckermann and A. E. Barron, "Versatile Oligo(N-Substituted) Glycines: The Many Roles Of Peptoids in Drug Discovery," *Pseudo-Peptides in Drug Development,* p. 1–31, 2005.

[122] R. N. Zuckermann, J. M. Kerr, S. B. H. Kent and W. H. Moos, "Efficient Method for the Preparation of Peptoids [Oligo(N-Substituted Glycines)] by Submonomer Solid-Phase Synthesis," *J. Am. Chem. Soc.,* vol. 114, no. 26, p. 10646–10647, 1992.

[123] K. Kirshenbaum, A. E. Barron, R. A. Goldsmith, P. Armand, E. K. Bradley, K. T. V. Truong, K. A. Dill, F. E. Cohen and R. N. Zuckermann, "Sequence-Specific Polypeptoids: A Diverse Family of Heteropolymers with Stable Secondary Structure," *Proceedings of the National Academy of Sciences ,* vol. 95, no. 8, p. 4303–4308, 1998.

[124] D. Y. Dong and M. Wetzler, "Faster And Greener: One Minute Reactions For Synthesis Of Peptoid Oligomers And Polymers," *247th ACS National Meeting and Exposition,* 2014.

[125] M. L. Hebert, D. S. Shah, P. Blake, J. P. Turner and S. L. Servoss, "Tunable Peptoid Microspheres: Effects of Side Chain Chemistry and Sequence," *Organic & Biomolecular Chemistry,* vol. 11, no. 27, p. 4459, 2013.

[126] K. T. Nam, S. A. Shelby, P. H. Choi, A. B. Marciel, R. Chen, L. Tan, T. K. Chu, R. A. Mesch, B.-C. Lee, M. D. Connolly, C. Kisielowski and R. N. Zuckermann, "Free-Floating Ultrathin Two-Dimensional Crystals from Sequence-Specific Peptoid Polymers," *Nature Materials,* vol. 9, no. 5, p. 454–460, 2010.

[127] B. Sanii, R. Kudirka, A. Cho, N. Venkateswaran, G. K. Olivier, A. M. Olson, H. Tran, R. M. Harada, L. Tan and R. N. Zuckermann, "Shaken, Not Stirred: Collapsing a Peptoid Monolayer To Produce Free-Floating, Stable Nanosheets," *Journal of the American Chemical Society,* vol. 133, no. 51, p. 20808–20815, 2011.

[128] M. L. Waters, "Aromatic Interactions in Model Systems," *Current Opinion in Chemical Biology,* vol. 6, no. 6, p. 736–741, 2002.

[129] A. S. Shetty, J. Zhang and J. S. Moore, "Aromatic π-Stacking In Solution as Revealed through the Aggregation of Phenylacetylene Macrocycles," *Journal of the American Chemical Society,* vol. 118, no. 5, p. 1019–1027, 1996.

[130] C. G. Claessens and J. F. Stoddart, "Interactions In Self-Assembly," *Journal of Physical Organic Chemistry,* vol. 10, no. 5, p. 254–272, 1997.

[131] M. Hebert, D. Shah, P. Blake and S. Servoss, "Uniform And Robust Peptoid Microsphere Coatings," *Coatings,* vol. 3, no. 2, p. 98–107, 2013.

[132] C. W. Wu, T. J. Sanborn, K. Huang, R. N. Zuckermann and A. E. Barron, "Peptoid Oligomers With α-Chiral, Aromatic Side Chains: Sequence Requirements for the Formation of Stable Peptoid Helices," *J. Am. Chem. Soc.,* vol. 123, no. 28, p. 6778–6784, 2001.

[133] T. J. Sanborn, C. W. Wu, R. N. Zuckermann and A. E. Barron, "Extreme Stability of Helices Formed by Water-Soluble Poly-N-Substituted Glycines (Polypeptoids) with α -Chiral Side Chains," *Biopolymers,* vol. 63, no. 1, pp. 12-20, 2001.

[134] E. D. Santis, T. Hjelmgaard, C. Caumes, S. Faure, B. D. Alexander, S. J. Holder, G. Siligardi, C. Taillefumier and A. A. Edwards, "Effect Of Capping Groups at the N- and C-Termini on the Conformational Preference of α,β-Peptoids," *Org. Biomol. Chem.,* vol. 10, no. 5, p. 1108–1122, 2012.

[135] X. Zhu and A. Guo, "The Critical Role of Surface Chemistry in Protein Microarrays.," pp. 53-71, 2007.

[136] A. Espejo, "A Protein-Domain Microarray Identifies Novel Protein-Protein Interactions.," *Biochem J.,* vol. 367, pp. 697-702, 2002.

[137] A. Espejo and M. Bedford, "Protein-Domain Microarrays," vol. 264, pp. 173-184 , 2004.

[138] S. L. Seurynck-Servoss, C. Baird, K. Miller, N. Pefaur, R. Gonzalez, D. Apiyo, H. Engelmann, S. Srivastava, J. Kagan, R. K.D. and R. Zangar, "Immobilization Strategies For Single-Chain Antibody Microarrays," *Proteomics,* vol. 8, p. 2199–2210, 2008.

[139] A. White, D. Daly, S. Varnum, K. Anderson, N. Bollinger and R. Zangar, "ProMAT: Protein Microarray Analysis Tool," *Bioinformatics,* vol. 22, p. 1278–1279, 2006.

[140] R. Gonzalez, S. Varnum and R. Zangar, "Sandwich ELISA Microarrays: Generating Reliable And Reproducible Assays For High-Throughput Screening," *Methods for Pharmacology and Toxicology,* pp. 273-290, 2008.

[141] G. Souza, L. de Godoy and M. Mann, "Identification Of 491 Proteins in The Tear Fluid Proteome Reveals A Large Number Of Proteases And Protease Inhibitors," *Genome Biology,* vol. 7, no. 7, 2006.

[142] B. R. Jordan, "DNA Microarrays in The Clinic: How Soon, How Extensively?," *Bioessays,* vol. 29, no. 7, p. 699–705, 2007.

[143] L. Zhou, R. Beuerman, Y. Foo, S. Liu, L. Ang and D. Tan, "Characterisation of Human Tear Proteins Using High-resolution Mass Spectrometry," *Ann Acad Med Singapore,* vol. 35, no. 6, pp. 400-407, 2006.

[144] J. McDonald, X. Liu, Y. Qu, S. Liu, S. Mickey, D. Turetsky, D. Gottlieb and D. Choi, "Transplanted Embryonic Stem Cells Survive, Differentiate And Promote Recovery In Injured Rat Spinal Cord," *Nat. Med,* vol. 5, p. 1410–1412, 1999.

[145] M. K.B., C. Carromeu, K. Griesi-Oliveira and A. Muotri, "Maintenance And Differentiation of Neural Stem Cells," *Wiley Interdiscip Rev Syst Biol Med.,* vol. 3, no. 1, pp. 107-114, 2011.

[146] F. Watt and T. S. Wilhelm, "Role of The Extracellular Matrix in Regulating Stem Cell Fate," *Nat. Rev.,* vol. 14, pp. 467-473, 2013.

[147] E. Hadjipanayi, R. A. Brown and V. Mudera, "Interface Integration Of Layered Collagen Scaffolds With Defined Matrix Stiffness: Implications For Sheet-Based Tissue Engineering," *J. Tissue Eng. Regen. Med. ,* vol. 3, p. 230–241, 2009.

[148] A. Jha, X. Xu, R. L. Duncan and X. Jia, "Controlling The Adhesion And Differentiation Of Mesenchymal Stem Cells Using Hyaluronic Acid-Based, Doubly Crosslinked Networks," *Biomaterials,* vol. 32, p. 2466–2478, 2011.

[149] J. Nam, J. Johnson and J. A. S. Lannutti, "Modulation Of Embryonic Mesenchymal Progenitor Cell Differentiation Via Control Over Pure Mechanical Modulus In Electrospun Nanofibers," *Acta Biomater.,* vol. 7, p. 1516–1524, 2001.

[150] L. Binan, C. Tendey, G. D. Crescenzo, R. E. Ayoubi, A. Ajji and M. Jolicoeur, "Differentiation Of Neuronal Stem Cells Into Motor Neurons Using Electrospun Poly-L-Lactic Acid/Gelatin Scaffold," *Biomaterials,* vol. 35, no. 2, pp. 664-674, 2014.

[151] N. Evans, C. Minelli, E. Gentleman, V. LaPointe, S. Patankar, M. Kallivretaki, X. Chen, C. Roberts and M. Stevens, "Substrate Stiffness Affects Early Differentiation Events In Embryonic Stem Cells," *Eur. Cell Mater.,* vol. 18, pp. 1-13, 2009.

[152] P. Y. Wang, W. Tsai and N. Voelcker, "Screening Of Rat Mesenchymal Stem Cell Behavior On Polydimethylsiloxane Stiffness Gradients," *Acta Biomater.,* vol. 8, p. 519–530, 2012.

[153] K. Saha, A. Keung, E. Irwin, Y. L. L. Li and D. H. K. Schaffer, "Substrate Modulus Directs Neural Stem Cell Behavior," *Biophys. J.,* vol. 95, p. 4426–443, 2008.

[154] A. Engler, L. Bacakova, C. Newman, A. Hategan, M. Griffin and D. Discher, "Substrate Compliance Versus Ligand Density In Cell On Gel Responses.," *Biophys. J.,* vol. 96, p. 617–628, 2004.

[155] H. Unadkat, M. Hulsman, K. Cornelissen, B. Papenburg, R. Truckenmüller, A. Carpenter, M. Wessling, G. Post, M. Uetz, M. Reinders, D. Stamatialis, C. van Blitterswijk and J. de Boer, "An Algorithm-Based Topographical Biomaterials Library To Instruct Cell Fate," *Proc. Natl Acad. Sci.,* vol. 108, p. 16565–16570, 2011.

[156] M. F. Brizzi, G. Tarone and P. Defilippi, "Extracellular Matrix, Integrins, And Growth Factors As Tailors Of The Stem Cell Niche," *Curr. Opin. Cell Biol.,* vol. 24, p. 645–651, 2012.

[157] R. McBeath, D. Pirone, C. Nelson, K. Bhadriraju and C. Chen, "Cell Shape, Cytoskeletal Tension, And Rhoa Regulate Stem Cell Lineage Commitment," *Dev. Cell,* vol. 6, p. 483–495, 2004.

[158] K. Kilian, B. Bugarija, B. Lahn and M. Mrksich, "Geometric Cues For Directing The Differentiation Of Mesenchymal Stem Cells," *Proc. Natl Acad. Sci.,* vol. 107, p. 4872–4877, 2010.

[159] Y. Zhu, S. Murali, W. Cai, X. Li, J. Suk and J. R. R. Potts, "Graphene and Graphene Oxide: Synthesis, Properties, And Applications," *Adv. Mater.,* vol. 22, no. 35, pp. 3906-3924, 2010.

[160] J. K. Mcdonough and Y. Gogotsi, "Carbon Onions: Synthesis and Electrochemical Applications," *Interface Magazine,* vol. 22, no. 3, pp. 61-66, 2013.

[161] W. Lee, C. Lim, H. Shi, L. Tang, Y. Wang, C. Lim and K. Loh, "Origin of Enhanced Stem Cell Growth And Differentiation On Graphene And Graphene Oxide," *ACS Nano,* vol. 5, no. 9, p. 7334–7341, 2011.

[162] N. Li, Q. Zhang, S. Gao, Q. Song, R. Huang, L. Wang, L. Liu, J. Dai, M. Tang and G. Cheng, "Three-Dimensional Graphene Foam As A Biocompatible And Conductive Scaffold For Neural Stem Cells," *Scientific Reports,* vol. 3, p. 1604, 2013.

[163] W. La, S. Park, H. Yoon, G. Jeong, T. Lee, S. Bhang, J. Han, K. Char and B. Kim, "Delivery Of A Therapeutic Protein For Bone Regeneration From A Substrate Coated With Grapheneoxide," *Small,* vol. 9, no. 23, p. 405–406, 2013.

[164] E. Bressan, L. Ferroni, C. Gardin, L. Sbricoli, L. Gobbato, F. Ludovichetti, I. Tocco, A. Carraro, A. Piattelli and B. Zavan, "Graphene Based Scaffolds Effects On Stem Cells Commitment," *J. Trans. Med.,* vol. 12, p. 296, 2014.

[165] B. Guilleaume, A. Buness, C. Schmidt, F. Klimek, G. Moldenhauer, W. Huber, D. Arlt, U. Korf, S. Wiemann and A. Poustka, "Systematic Comparison of Surface Coatings For Protein Microarrays," *Proteomics,* vol. 5, no. 18, pp. 4705-4712, 2005.

[166] I. Balboni, C. Limb, J. Tenenbaum and P. Utz, "Evaluation of Microarray Surfaces And Arraying Parameters For Autoantibody Profiling," *Proteomics,* vol. 8, no. 17, pp. 3443-3449, 2008.

[167] H. Murnen, A. Rosales, J. Jaworski, R. Segalman and R. Zuckermann, "Hierarchical self-assembly of a biomimetic diblock copolypeptoid into homochiral superhelices," *J. Am. Chem. Soc.,* vol. 132, p. 16112–16119, 2010.

[168] E. Robertson, A. P. C. Battigelli, R. Mannige, T. Haxton, L. Yun, S. Whitelam and R. Zuckermann, "Design, Synthesis, Assembly, and Engineering of Peptoid Nanosheets," *Acc. Chem. Res.,* vol. 49, no. 3, p. 379–389, 2016.

[169] J. Sun, X. Jiang, R. Lund, K. Downing, N. Balsara and R. Zuckermann, "Self-Assembly Of Crystalline Nanotubes From Monodisperse Amphiphilic Diblock Copolypeptoid Tiles," *PNAS,* vol. 113, no. 15, pp. 3954-3959, 2016.

[170] H. Tran, S. L. Gael, M. D. Connolly and R. N. Zuckermann, "Solid-phase Submonomer Synthesis of Peptoid Polymers and their Self-Assembly into Highly-Ordered Nanosheets," *Journal of Visualized Experiments,* vol. 57, 2011.

[171] Y. D. a. X.-Y. Zhu., "Transport at the Air/Water Interface is the Reason for Rings in Protein Microarrays," *J. Am. Chem. Soc.,* vol. 128, no. 9, p. 2768–2769, 2006.

[172] J. R. Stringer, J. A. Crapster, I. A. Guzei and B. H. E., "Construction of Peptoids with All Trans-Amide Backbones and Peptoid Reverse Turns via the Tactical Incorporation of N-Aryl Side Chains Capable of Hydrogen Bonding," *J. Org. Chem.,* vol. 75, p. 6068–6078, 2010.

[173] S. B. Shin, B. Yoo, L. J. Todaro and K. Kirshenbaum, "Cyclic Peptoids," *J. Am. Chem. Soc.,* vol. 129, p. 3218–3225, 2007.

[174] K. Huang, C. W. Wu, T. J. Sanborn, J. A. Patch, K. Kirshenbaum, R. N. Zuckermann, A. E. Barron and I. Radhakrishnan, "A Threaded Loop Conformation Adopted by a Family of Peptoid Nonamers," *J. Am. Chem. Soc.,* vol. 128, p. 1733–1738, 2006.

[175] P. Armand, K. Kirshenbaum, A. Falicov, R. L. Dunbrack Jr, K. A. Dill, R. N. Zuckermann and F. E. Cohen, "Chiral N-Substituted Glycines Can Form Stable Helical Conformations," *Fold. Des. ,* vol. 2, p. 369–375, 1997.
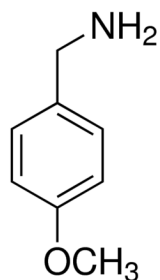
[176] X. Chen, K. Ding and N. Ayres, "Investigation Into Fiber Formation In N-Alkyl Urea Peptoid Oligomers And The Synthesis Of A Water-Soluble PEG/N-Alkyl Urea Peptoid Oligomer Conjugate," *Polym. Chem.*, vol. 2, p. 2635–2642, 2011.

[177] Y. Wei, A. Thyparambil and R. Latour, "Protein Helical Structure Determination Using CD Spectroscopy for Solutions with Strong Background Absorbance from 190-230 nm," *Biochim Biophys Acta,* vol. 1844, no. 12, p. 2331–2337, 2014.

[178] S. Shin and K. Kirshenbaum, "Conformational Rearrangements by Water-Soluble Peptoid Foldamers," *Organic Letters,* vol. 9, no. 24, pp. 5003-5006, 2007.

[179] M. van der Graaf and M. Hemminga, "Conformational Studies on a Peptide Fragment Representing the RNA-Binding N-terminus of a Viral Coat Protein Using Circular Dichroism and NMR Spectroscopy," *The FEBS Journal,* vol. 201, no. 2, pp. 489-494, 1991.

[180] W. Kohn, C. Kay and R. Hodges, "Protein Destabilization by Electrostatic Repulsions in the Two-Stranded α-Helical Coiled-Coil/Leucine Zipper," *Protein Sci ,* vol. 4, p. 237–250., 1995.

[181] I. Jelesarov, E. Durr, R. Thoma and H. Bosshard, "Salt Effects on Hydrophobic Interaction and Charge Screening in the Folding of a Negatively Charged Peptide to a Coiled Coil (Leucine Zipper)," *Biochemistry,* vol. 37, p. 7539 –7550, 1998.

[182] M. Hoshino, N. Yumoto, S. Yoshikawa and Y. Goto, "Design And Characterization f the Anion-Sensitive Coiled-Coil Peptide.," *Protein Sci.,* vol. 6, no. 7, p. 1396–1404, 1997.

[183] R. P. Ekins and F. W. Chu, "Multianalyte Immunoassay.," *Fresenius Journal of Analytical Chemistry 1992, 343 (1), 23–23. ,* vol. 343, no. 1, p. 23, 1992.

13. Appendix: Submonomer Structures

(S)-Methylbenzylamine
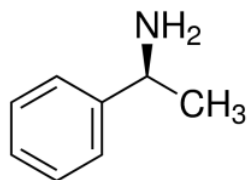
4-Methoxybenzylamine

Tert-butyl N-(4-aminobutyl)carbamate